Functional characterization of a hypothetical protein, Sll1252 in *Synechocystis* sp. PCC 6803

Thesis submitted to the University of Hyderabad for the award of

Doctor of Philosophy

By

Radha Rani Balaga

(Regd. No. 09LPPH15)

Department of Plant Sciences

School of Life Sciences

University of Hyderabad

Hyderabad - 500046

India

Dec, 2020

University of Hyderabad

(A Central University established in 1974 by act of parliament)
HYDERABAD – 500 046, INDIA

CERTIFICATE

This is to certify that this thesis entitled **"Functional characterization of a hypothetical protein Sll1252 in *Synechocystis* sp. PCC 6803"** is a record of bonafide work done by **Mrs. Radha Rani Balaga,** a research scholar for Ph.D. programme in Department of Plant Sciences, School of Life Sciences, University of Hyderabad under my guidance and supervision. The thesis has not been submitted previously in part or in full to this or any other University or Institution for the award of any degree or diploma

Dr. J. S. S. Prakash
(Supervisor)

Head,
31/12/2020
Department of Plant Sciences.

Dean,
School of Life Sciences.

DEAN
School of Life Sciences
University of Hyderabad
Hyderabad - 500 046.

अध्यक्ष / HEAD
वनस्पति विज्ञान विभाग / Dept. of Plant Sciences
जैविक विज्ञान संकाय / School of Life Sciences
हैदराबाद विश्वविद्यालय / University of Hyderabad
हैदराबाद / Hyderabad-500 046, भारत / INDIA

University of Hyderabad

(A Central University established in 1974 by act of parliament)

HYDERABAD - 500 046, INDIA

DECLARATION

I, Radha Rani. Balaga hereby declare that this thesis entitled **"Functional characterization of a hypothetical protein S111252 in *Synechocystis* sp.** PCC 6803" submitted by me under the guidance and supervision of **Dr. Jogadhenu S. S. Prakash, Head of the Department, Department of Biotechnology,** is a bonafide research work which is also free from plagiarism. I also **declare** that it has not been submitted previously in part or in full to this University or any other University or Institution for the award of any degree or diploma. I hereby agree that my thesis can be deposited in Shodhganga/INFLIBNET. **A report on plagiarism statistics from the university Librarian is enclosed.**

Radha

Dr. J.S.S.Prakash
(Supervisor)

Radha Rani Balaga
(09LPPH15)

DEDICATED TO MY BELOVED

ANGELS (SMILY DOLLY)

HUBBY (SRIKANTH) &

PARENTS

CONTENTS

Page No.

Acknowledgements (i-ii)

Abbreviations (iii-iv)

List of figures (v-vi)

List of tables (vii)

Chapter 1. Introduction 1 – 23

Chapter 2. Objectives 24 – 25

Chapter 3. Materials and Methods 26 – 43

Chapter 4. Results 44-73

Chapter 5. Discussion & conclusions 74 – 80

Primer sequences 81 – 83

References 84- 91

List of publications & presentations 92-95

Plagiarism Report 96

Acknowledgements

This Report would not have been possible without the essential and gracious support of many individuals.

I take immense pleasure in thanking **Dr. Jogadhenu S. S. Prakash**, Head, ***Laboratory of microbial genes to functions*** group, for providing me with an opportunity to work in his lab and had been a source of inspiration and role model in any given way, for his constant moral and personal support and guidance throughout my doctoral research. The leadership and critical assessment capabilities of **Dr. Jogadhenu S. S. Prakash**, allowed me to mobilize my collective knowledge and capacity in the best way possible and created an enabling environment to complete my research work.

I thank Dean, School of Life Sciences, Prof. Dayananda Siddavattam and Head, Department of Plant Sciences Prof. G.Padmaja mam for allowing me to use the facilities of the School and the Department. I sincerely acknowledge the infrastructural support provided by UGC-SAP, DST-FIST, DBT-CREBB, to the Dept. of Plant Sciences and the CSIR, Govt. of India for the research fellowship.

I thank my Doctoral Committee members Prof. P.B.Kirthi and Prof. P. Appa Rao for their valuable suggestions.

This work was supported by grants from the CSIR project (Project Nos: 38 (1249) / 10 / EMR-II (grant to J.S.S.P.). J. S. S. P and I.S acknowledge the support from DST-JSPS Project. No: DST/INT/JSPS/P-125/2011. This work was also partly supported by a Grant-in-Aid for Scientific Research(C) (23570046) (IS) from Japanese Society for the Promotion of Science.

We thank Prof. Ken-Ichiro Ishida for allowing us to use the transmission electron microscopic facility at University of Tsukuba.

I wish to express my deep sense of gratitude to Dr. Iwane Suzuki, who graciously extended his laboratory facilities during initial microarray experiments.

I would thank Itoh for generating truncated mutants and his help in performing few experiments.

This thesis is not only the result of my scientific works but the outcome of a long road and I am glad to acknowledge everyone who has contributed to the build-up of my scientific personality and therefore, to the completion of this thesis.

My heartfelt thanks are also due to my colleague scholars of Microbial genes to functions group Dr. K. Sirisha, Dr. P.Bhavani devi, Dr M. Karthik Mohan, Dr. M. Subhashini, Dr. P.V.P. Sai Arun, Dr.Deepak Kumar Singh, Dr.Reetika Chaurasia, Dr.Linga Swamy Bantu and Dr.Afshan Sri Kumar , Dr. Shalu for their timely help and constant encouragement.

I would like now to mention "some" of Project students who have helped me, while learning B. Yesu Nadha Rao, D. SomaSekhar, Dr.Surjeet Kumar Arya, Dr.A. Venkateswara Rao, Santosh and Dr.B. Ranjith .

This dissertation work at Laboratory of Microbial genes to functions (MGF) group could never run smoothly without all the help I got from lab helpers. I wish to thank G. Ramesh, Ch. Sridhar Yadav for their assistance in the lab.

I am thankful to all my batch mates and other research scholars of the School of Life Sciences for their timely help.

I highly acknowledge the efforts of Ramesh, Mohan Rao, Sudarshanam and other non-teaching staff.

Saving the most important for the last, I would like to express my heartfelt thanks to my guide, Dr. J. S. S. Prakash and his family for their blessings, wishes, support and constant encouragement throughout my Ph. D tenure.

I acknowledge CSIR for financial aid (fellowship in the form of JRF and SRF and DSRF.

I would like to thank my husband, who cooperated me and encouraged me to do Ph.D or else I would have been left as a Masters instead of becoming a DOCTORATE.

I would say that without my angelic daughters Smily n Dolly 's cooperation this piece of work wouldn't had been possible, especially for their love n care n maturity not to disturb me while writing my thesis.

Last but not least I would like to thank my parents for their love and constant support and their encouragement for my higher studies , I am grateful to my Chinna mamu who gifted me laptop for my research work.

I am very much thankful to my Lord, without his blessings , I would have never completed my Ph.D.

Radha Rani Balaga

ABBREVIATIONS

µg : microgram
µM : micromolar
°C : degree centigrade/degree Celsius
Abs : absorption
ALP : alkaline phosphatase
ATP : adenosine tri phosphate
BCIP : 5-bromo-4-chloro-3-indolyl phosphate
BLAST : basic local alignment search tool
Bp : base pair (bp)
BSA : bovine serum albumin
cDNA : complementary DNA
Chl : Chlorophyll
C-terminal : carboxy terminal
Cyt C : cytochrome C
DBMIB : 2,5-dibromo-3-methyl-6-isopropyl-*p*-benzoquinone
DCMU : 3-(3, 4,-dichlorophenyl)-1,1-dimethylurea
DNA : deoxy ribonucleic acid,
dNTPs : deoxy nucleotide triphosphates
ds : double stranded
EDTA : ethylene diamine tetra acetic acid
ET : electron transport
Gm : gram
GOLD : gold online database
h : hour(s)
Hepes : 4-(2-Hydroxyethyl)piperazine-1-ethanesulfonic acid sodium salt, N-(2- Hydroxyethyl) piperazine-N′-(2-ethanesulfonic acid) sodium salt
HPs : hypothetical species
IgG : immunoglobulin G
IPTG : isopropyl β-D-thiogalactoside
Kb : kilobase pair
kDa : kilodalton
L : litre
LB : Luria-Bertani
M : molar
Mb : mega base pair
mg : milligram
Min : minute
ml : milliliter
mM : Sodium bicarbonate
$NaHCO_3$: millimolar
NBT : nitroblue tetrozolium
Ni-NTA : nickel-nitroacetic acid agarose

nm	:	nanometers
N-terminal	:	amino terminal
OD	:	optical density
ORF	:	open reading frame
PAGE	:	polyacrylamide gel electrophoresis
PBS	:	phosphate buffered saline
PCR	:	polymerase chain reaction
PET	:	photosynthetic electron transport
PFAM	:	protein family database
PPBQ	:	para phenyl benzoquinone
PSI	:	photosystem - I
PSII	:	photosystem - II
PSI BLAST	:	position specific interface
PQ		plastoquinone
RNA	:	ribonucleic acid
rpm	:	revolutions per minute
SDS	:	sodium dodecyl sulphate
Sec(s)	:	seconds
SEM	:	scanning electron microscopy
Ss	:	single stranded
TE	:	Tris-EDTA
TEM	:	transmission electron microscopy
Tris	:	tris-(Hydroxymethyl) aminoethane
V	:	volts
WCE	:	whole chain electron transport
WT	:	wild type

List of figures

Figure No.		Title of the figure	Page No
1.1	:	Progress of genome sequencing and total projects in Gold by Domain group.	**3**
1.2	:	Percentage of known and unknown proteins and relation between number of sequenced genomes and protein families.	**4**
1.3	:	Cyanobacterial species.	**12**
1.4	:	Cyanobacterial photosynthetic apparatus.	**13**
1.5	:	Genome map of *Synechocystis* sp. PCC 6803 and it's known versus unknown function proteins.	**15**
1.6	:	*sll1252* in genome context (gene map) and location of its S4 Domain.	**17**
1.7	:	Polypeptide profile of purified His-tagged PSII complex of *Synechocystis*.	**18**
1.8	:	Organization of PSII biogenesis model in *Synechocystis*.	**20**
1.9	:	Site of DCMU and DBMIB inhibition in electron flow.	**23**
4.1	:	*In silico* analysis of the Sll1252 protein.	**45**
4.2	:	Mutation of *sll1252* and PCR based confirmation of mutation	**47**
4.3	:	Growth profile of wild type *Synechocystis* cells and Δ*sll1252*^{ins} mutant.	**49**
4.4	:	Measurement of PSII and WCE activity in wild type and Δ*sll1252*^{ins}	**50**
4.5	:	Genome wide expression of the genes due to mutation in sll1252 gene.	**52**
4.6	:	Venn diagram showing, common genes induced by *sll1252* mutation, DCMU and DBMIB.	**57**
4.7	:	Effect of inhibitors DCMU and DBMIB on PSII and WCE activities.	**59**
4.8	:	Rate of reduction of PQ pool in wild type, *sll1252* mutant and wild type+DBMIB.	**60**
4.9	:	Schematic representation of the complementation of Δ*sll1252*^{ins} and PCR based confirmation.	**62**
4.1	:	Growth profile of wild type *Synechocystis,* Δ*sll1252*^{ins} mutant and *sll1252*$^{+}$ complement.	**63**
4.11	:	PCR based amplification and confirmation of cloned gene in Pet28(+) vector.	**64**
4.12	:	SDS PAGE analysis of the over expressed and purified Sll1252 protein.	**65**
4.13	:	Localization of Sll1252 by western blot experiment	**66**

4.14 : Schematic representation of the genotype of suppressor mutant and PCR based confirmation of Δ*sll1252*^{del,} Δ*sll1252*N^{ter} and Δ*sll1252*C^{ter} truncated mutants. **69**
4.15 : TEM images of thylakoid membrane of wild type Δ*sll1252*N^{ter} and Δ*sll1252*C^{ter} truncated mutants. **73**
4.16 : Proposed model to explain the function of Sll1252 protein **79**

List of tables

Table No.		Title of the table	Page No.
1.1	:	Genome milestones during genome sequencing	**2**
3.1	:	Preparation of BG-11 from stocks	**27**
4.1	:	Effect of *sll1252* mutation on genome-wide expression of genes	**54**
4.2	:	Comparision of PSII activity, WCE activity and growth of Δ*sll1252* mutant strains and wild type cells	**71**

INTRODUCTION

A revolution started in the field of molecular biology in the last two decades: The major challenge of modern biology is genome sequencing. Genome sequencing provides the information of every single gene in the genome (1). Genome contains the genetic material DNA (deoxyribonucleic acid) which is hereditary in nature. Hence it is important to sequence a genome to understand the architecture of life. An amazing and exciting breakthrough in sequencing began with the introduction of the dideoxy chain termination (2) and chemical degradation (3) techniques in 1977, followed by the invention of PCR (1985) and automated, fluorescence-based Sanger sequencing machines in 1986 (4). The first genome of a prokaryote, *Haemophillus Influenz*a (5) was sequenced completely and published in 1995. In 2000 the human genome sequence was published as a draft (6) and complete sequence in 2003 (7). Due to the invention of more advanced technologies like HT-NGS developed by (http://www.454.com/) (8) resulted in the sequencing of genome of organisms from all domains of life (Table 1). By the end of 2010 it became possible to sequence 28 GB genome in a single sequencing run with (Heliscope Sequencer), the third generation HT-NGS technique (9). Sequence data grew exponentially and today genomes of ~158,121 bacterial, 1519 archaeal, 13,028 eukaryotic and many of the organisms genome used in research (molecular biology and genetics) are available in the GOLD database (www.genomesonline.org) (Figure 1.1).

Table1. Genome milestones during genome sequencing

Group	Organism	Genome size	Year
Ss DNA	Bacteriophage PhiX174	5386bp	1976
Ds DNA	Bacteriophage lambda 13	48502bp	1976
Bacteria	*Haemophilus Influenza*	1.8 Million	1995
Archaeon	*Methanococcus Jannaschii*	1.7 Million	1996
Yeast	*Saccharomyces Cerevisiae*	12.1 Million	1996
Nematode	*Caenorabhditis elegans*	100 Million	1998
Insect	*Drosophila melanogaster*	165 Million	2000
Plant	*Arabidopsis Thaliana*	119 Million	2000
Human	*Homo sapiens*	3.2 Billion	2001
Mouse	*Mus musculus*	2.6 Billion	2002
Rat	*Rattus norvegicus*	2.75 gigabases	2004
Rice	*Oryza sativa*	389 Mb	2005
Red alga	*Cyanidioschyzon,merolae*	16.5Mb	2007
Maize	*Zea mays*	2.3 gigabases	2009
Hominids	*Neandertha*	4 billion	2010
African Frog	*Xenopus laevis*	3.1 billion	2017

Table1.1: Genome of organisms sequenced from all domains of life. Genome sequencing started in 1976 with the sequencing of Ss DNA of bacteriophage containing 5386 bp, due to development in sequencing technologies, year by year more complex genomes including human genome (3.2 billion) were sequenced, the genomes in the table represent genome milestones during genome sequencing.

Figure 1.1: Progress of Genome Sequencing and total projects in GOLD by Domain group

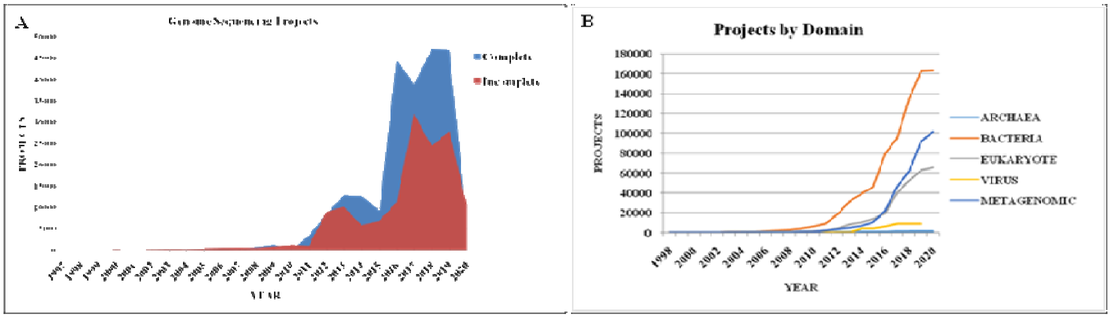

Figure 1.1: Genome sequencing data from GOLD Database. (A). Progress in genome sequencing since 1997 till 2020.The inset plots the number of complete and incompletely sequenced genome projects against time (year); By the end of 2019, 47,006 projects have been completed and 38,754 projects are still incomplete. (B) Project totals in GOLD by year and Domain group, Bacteria 163,672, Metagenomic 101,794, Eukaryote 65,431, Virus 9,218, Archea 1760 till April 2020.

It was realized soon that after sequencing a genome, extracting and interpreting that data is laborious. The main subject in genome era was genome annotation. With the increase in number of sequenced genomes, the number of protein families also increases (Figure 1.2) but only 60-70% of the proteins functions have been predicted in well studied organisms. Functionally unknown protein is a protein whose existence has been proven but with no clear idea about its function. Hypothetical protein is a protein whose existence has been predicted but for which there is no experimental evidence (10). Therefore genome annotation is the central goal after sequencing the genome of a species (11). Well established bioinformatics tools and pipelines are being used for the assembly and annotation of the genomes. Different search tools are integrated to predict the function of proteins (12). There are evidences from the past where gene and protein functions have been predicted using bioinformatics (13) and data of most of the genes for which reliable predictions should be made grows constantly (14). Even though the functions of many proteins are known, in model organisms like *Escherichia coli*, for only 57% of the proteins experimental proof is available (15). As the complexity of genome increases from bacteria to higher plants the number of unknown proteins also increases. The percentage of unknown proteins in bacteria, *archaea* and eukaryotes is 30%, 40%, 60% respectively (16) (Figure 1.2). Proteins are responsible for complex cellular process in organisms. There is a huge gap between sequence deposition and protein’s function. Therefore protein functional characterization is required to fill this gap.

Figure1.2: Percentage of known and unknown proteins and relation between number of analyzed genomes and protein families

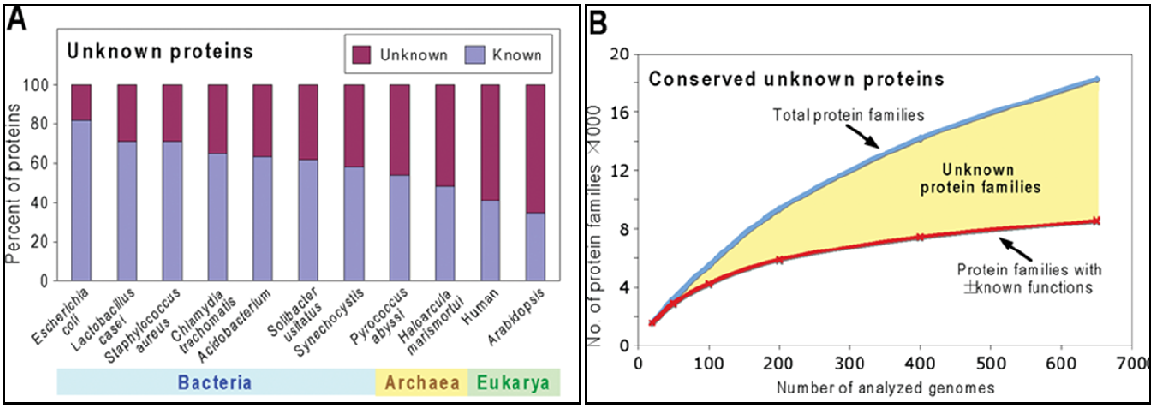

Figure 1.2: (**A**) The percentage of known and unknown proteins, encoded by bacterial, *archaeal* and eukaryotic genomes. (**B**). Relationship between the number of protein families (SEED Database) and the number of sequenced genomes. Red curve shows protein families with at least some elements of assigned function. Yellow area indicates the number of unknown protein families. Blue curve indicates total protein families. This figure was taken from (16).

In this thesis, I will give a general overview on hypothetical proteins, and explain the computational approaches for getting clues on their function and existing strategies for the characterization of protein function and finally focus on characterization of a novel hypothetical protein Sll1252 in cyanobacterium *Synechocystis* sp. PCC 6803.

Hypothetical proteins:

Protein in an organism which is thought to be expressed from predicted genes but there is no experimental proof of its translation, is known as Hypothetical protein (10). Computationally their existence can be predicted. Microbial genome sequence data has revealed that on average ~30–40% of the proteins encoded by typical bacterial genome are not functionally characterized and are annotated as either hypothetical proteins which are very much important to complete proteomic and genomic information (17,18,19).

Functional characterization of hypothetical proteins:

Presence of hypothetical proteins probably indicates presence of yet to be identified metabolic pathways. Hence it is important to characterize the function of HPs to fill the gaps in the metabolic pathways by discovering new functions. Hypothetical proteins play an important role in metabolic processes, as enzymes, transporters, regulators etc and are used in the development of vaccines for pathogenic microorganisms, development of resistance and treatment of diseases (20,21,22,).

Conserved HPs are the priority targets for characterization:

The genes coding for hypothetical proteins that have been retained in at least several distantly related organisms are known as 'conserved hypothetical's' (23) they may have important physiological function and majority of these conserved hypotheticals are expected to be essential for survival of the cell. Even though the metabolic pathways are well known in model organisms like *E.coli*, *S. cerevisae* and *Bacillus subtilis,* they contain so many conserved HPs which indicate that there are still important functions to be discovered among these conserved HPs (24).

For example the 3D structure of an *archaeal* conserved HP (MJ0226) (25) perfectly fits the structure of ITPase (ITP pyrophosphatase) from human RBC, thus the function of this protein was characterized. In humans this protein was proved to account for ITPase acitivity to study human physiology.

Protein function prediction by *insilico* methods:

In order to prove the function of a protein it is essential to get clues from *insilico* analysis and then prove its function experimentally. Insilico analysis includes several approaches like homology, phylogenetic profiles, comparative genomics, 3D structures, protein-protein interactions, presence of common regulatory sites, gene clustering and gene expression profiles. Several papers have been published revealing function of genes, coding for hypothetical proteins using one or the other above mentioned strategies (26).

Homology detection – The first and foremost step in predicting a protein’s function is searching for its homologs. Homology search is done with the help of bioinformatic tools, FASTA (27), and PSI-BLAST (28) and multiple sequence alignments can be done using tools like CLUSTALW (29) or T-COFFEE (30). Databases such as SMART (31), PFAM (32), CDD (33), and PROSITE (34), or combined resources such as Interpro (35) are frequently used to identify the structural and functional domains in query proteins.

Function based on Comparative genomics:

Comparision of complete genomic sequences of different species to understand evolutionary relationships is termed as comparative genomics. Many genomes can be compared in a single study. It identifies the DNA sequences that are preserved over millions of years in many different organisms. As proteins are translated from DNA, proteins with similar function evolve together during course of evolution and they are either preserved in a new species or eliminated. Such proteins are called as functionally linked and have similar homologs in a group of organisms and they can be detected by phylogenetic profiling

(36). Hence clues obtained from comparative genomics plays a vital role in characterization of a hypothetical protein.

Function prediction based on 3D structure:

Hypothetical proteins 3D structure may provide clues of their biochemical or biophysical functions. The protein folding patterns are preserved during evolution, and hence homologs can be identified based on structure comparisons. Proteins sharing the same fold carry similar function (37). Furthermore, catalytic sites and function can be predicted by carefully analyzing the residue positions (38), Protein-protein interactions can also be analyzed using 3D structures (39).

Computationally tertiary structure of proteins can be compared (e.g. using DALI, VAST or STAMP (40), which shows the probability to what extent the two 3D structures are evolutionarily related. 3D models can also be obtained by homology-modelling for unknown proteins with the structure of its related homologs (41). Threading provides clues about the 3D structure in the absence of close homologs (42).

Strategies for the characterization of the hypothetical proteins:

There are several approaches for the characterization of hypothetical proteins. The most widely used methods of functional characterization are genetic approaches (mutagenesis and phenotypic characterization), functional complementation, heterologous expression, gene expression profiling (DNA microarrays) reverse genetics, localization assays. Functional characterization of hypothetical proteins in a model cyanobacterium *Synechocystis*, using one or the other methods mentioned above are described below.

Mutagenesis and Phenotypic Characterization:

The widely used experimental strategy for unraveling the function of a hypothetical protein is by generating knockout mutant of the hypothetical gene by targeted mutagenesis, and subsequent characterization of the mutant by physiological, biochemical and biophysical methods. Several papers have been published from different laboratories using above strategy and reported the function of various hypothetical proteins in *Synechocystis.* The function of the Hypothetical proteins Sll1495, Sll0804, Sll1306, Sll1125 encoded by the genes *sll1495, sll0804, sll1306, sll1125* was proved by transposon mutagenesis. These four proteins are required for optimal photoautotrophy (43). Hypothetical protein, Sll0088 was identified as a regulator of photosystem I biogenesis (44) by transposon mutagenesis of *sll0088*, and subsequent physiological characterization. Putative ATP/GTP binding protein, Sll1717 was reported to affect the redox state of PQ pool by modifying the quinol oxidase activity (45). By generation and characterization of *Δssr2998,* and analysis of co-purification of protein complex it is associated with, Ssr2998 was reported as a regulator of PET chain (46). Together with targeted mutagenesis and, recombinant expression and biochemical characterization of the expressed protein, Sll1575 was reported as a protein required for motility of the cyanobacterium *Synechocystis* (47). By deletional inactivation and subsequent DNA microarray analysis of a gene coding for putative RNA helicase protein, CrhR*,* it was reported that it regulates the translation of the heat shock genes under low temperature stress (48). Bacterial knockout collections and knockout phenotype databases provide information about the essentiality of a gene and its particular phenotype it is associated with. One such database is SEED database which contains data of bacterial genes which are essential for cell survival (49, 50) Details of cyanobacterial mutants and their corresponding phenotypes are available in (http://genome.microbedb.jp/cyanobase/).

Complementation as an alternative strategy:

A second strategy for characterization of a hypothetical protein is by functional complementation with autonomously replicating plasmid pVZ321 in model organism like *E. coli,* by triparental mating. When the wild type gene is reintroduced into the mutant, the ability of the gene to restore the mutant phenotype with that of wild type phenotype is functional complementation. In *Synechocystis,* the ORF, *sll1468* was identified as a gene for β-carotene hydroxylase by functional complementation in a β-carotene producing *E. coli* in which its homologue has been mutated (51).

Heterologous expression:

A third strategy for characterization of hypothetical proteins is heterologous expression. Introducing the gene of interest in a host organism preferably *E.coli,* by rDNA technology is heterologous expression. The expressed protein is purified and *in vitro* biochemical and biophysical analysis of the purified protein is carried out. Four ADP-ribose pyrophosphatases Sll1054, Slr0920, Slr1134, and Slr1690 have been characterized in the cyanobacterium *Synechocystis*. These proteins were characterized by recombinant expression and biochemical characterization (52). Sll1575 was reported as a protein required for motility of the cyanobacterium *Synechocystis* (47) by recombinant expression and biochemical characterization.

Protein-Protein interactions:

Another strategy for getting clues on hypothetical proteins function is by identification of proteins, the hypothetical protein in question, is associated with. If the functions of interacting protein partners are already known, it is possible to predict the function of hypothetical protein in question. Kashino and coworkers reported the association of five novel proteins, Sll1252, Sll1130, Sll1390, Sll1414 and Sll1638 with PSII core complexes from *Synechocystis* (53). Kashino *et al*., proposed a functional role for one of these five proteins, Sll1252, as a protein that appears to be in the downstream of the sensory signal transduction pathway of PQ pool to balance in PET (54). Sll1638 protein homologous with the plant PsbQ protein was reported to be involved in water oxidation process in the luminal side of PSII (55). Auxiliary functions have been reported for Sll1414 and a homologue of Sll1390 (TLP18.3 protein in *Arabidopsis thaliana*), in the assembly and repair of PS II (56,57).

Gene expression profile for the characterization of hypothetical proteins:

Determination of the expression of genes, in a cell, at the transcription level to understand cellular function globally is termed gene expression profiling. DNA microarrays (58) or the SAGE techniques are generally used in gene expression profiling (59). Regulation of spatial and temporal expression of genes in higher organisms is very important for the development of the organism. So in plants and animals the spatial or the temporal stage in which a gene is expressed provides us essential clues about its function (60). If a gene is specifically expressed in a tissue it is highly possible, that it has role only in that particular tissue's function. Functional associations of a protein can be derived from its expression profile and co-expression data from (microarrays, iTRAQ2D and electrophoresis)

(61,62,63). Microarray databases include GenExpDB for bacteria and Microbes Online (http://genexpdb.ou.edu/main/), and a web server exclusively for cyanobacteria named Cyanoexpress (http://cyanoexpress.sysbiolab.eu/) has the data of gene expression profiles.

From these databases its expression profile and co-expression datasets for gene in question can be derived. *Synechocystis* microarray chip used to study gene expressions contains 95 % of its genes. Investigations on DNA microarrarys in *Synechocystis* include, the response to salt and osmotic stress (64), acclimation to high light (65) the response to cold stress (66) phosphate sensing etc (67). Therefore DNA microarray analysis would provide clues on the function of hypothetical proteins.

There are several other examples revealing functions of genes coding for hypothetical proteins using above mentioned strategies along with new strategies.

Cyanobacteria:

Cyanobacteria are the first organisms to carry out oxygenic photosynthesis, over 3 billion years ago (68). They have played a special role in earth's history, by being the producers of the oxygen that we all breathe today. They are important for the earth's ecosystem as primary producers in the oceans, responsible for 20-30% of overall photosynthetic production today (69). One of the major contributions to the development of life, is the endosymbiotic relationship they formed with eukaryotic organisms, creating a partnership that transcended the ages. (70) Inside the slightly bigger cells, the cyanobacteria would morph into what is today the chloroplast, thereby creating the origin of all plants, and made life on land possible (71).

Morphologically, they comprise a diverse group of unicellular (*Synechocystis sp.,*) multicellular (*spirulina*) and many with heterocyst's (*Nostoc* and *Anabaena*) (Figure 1.3) and can inhabit most ecological niches, like oceans, freshwater, soils from the frozen tundra to the scorching desert (72). Thus they occur in all habitats differing in levels of desiccation, pH, temperature, salinity, humidity, light, O_2 and CO_2 concentrations (73). Hence they are used to investigate stress responses and adaptive strategies of photosynthetic organisms on osmotic and salt stress (74), oxidative stress (75), chilling stress (76,77), heat shock (78), photo-inhibition (79), nitrogen and sulphur starvation (80) acclimatization to high light (81) and high temperature (82) adaptation to light-dark transitions (83,84) phosphate ion sensing (85,86) manganese ion sensing (87,88) and photoinhibition (89).

Figure 1.3: Cyanobacterial species

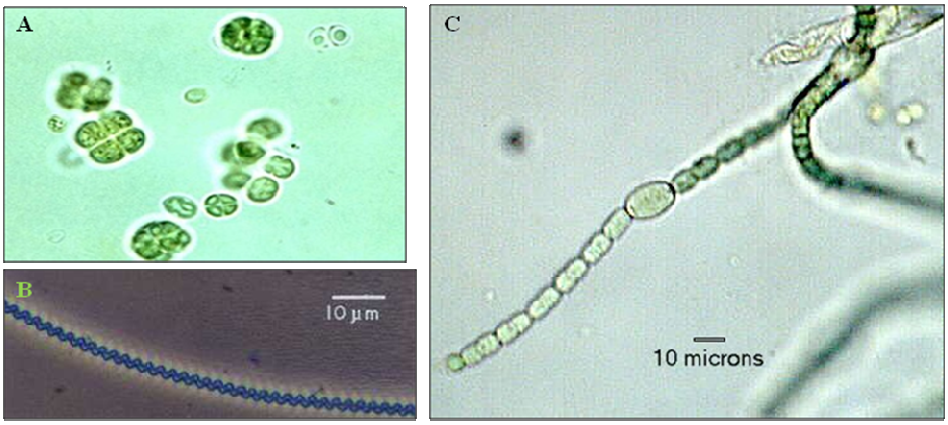

Figure1.3. Species of Cyanobacteria: A. *Synechocystis* sp. B. *Spirulina.* C.*Nostoc*. Images were taken from Cyanosite (http://www-cyanosite.bio.purdue.edu).

Cyanobacteria versus plants:

Using Cyanobacteria instead of plants to study photosynthesis is beneficial for several reasons. Photosynthesis in Cyanobacteria is several times more efficient than in plants, they do not spend energy making non-fermentable parts such as stems and roots, they grow year round, are easy to genetically engineer and they enable a minimum amount of steps from CO_2 fixation to end product, thereby reducing energy waste. Another key benefit of Cyanobacterial based production is that they do not need to be grown on arable lands and thereby compete with our food production. In fact, many species naturally grow in salt water, allowing for large scale cultivations in desert regions or along the coast in seawater, thereby decreasing our use of fresh water and the competition between food productions.

Photosynthesis in Cyanobacteria:

Much of the electron transport pathways work was performed in *Synechocystis* sp. PCC 6803 (here after *Synechocystis*) (Figure1.4).

Figure 1.4: Cyanobacterial Photosynthetic Apparatus

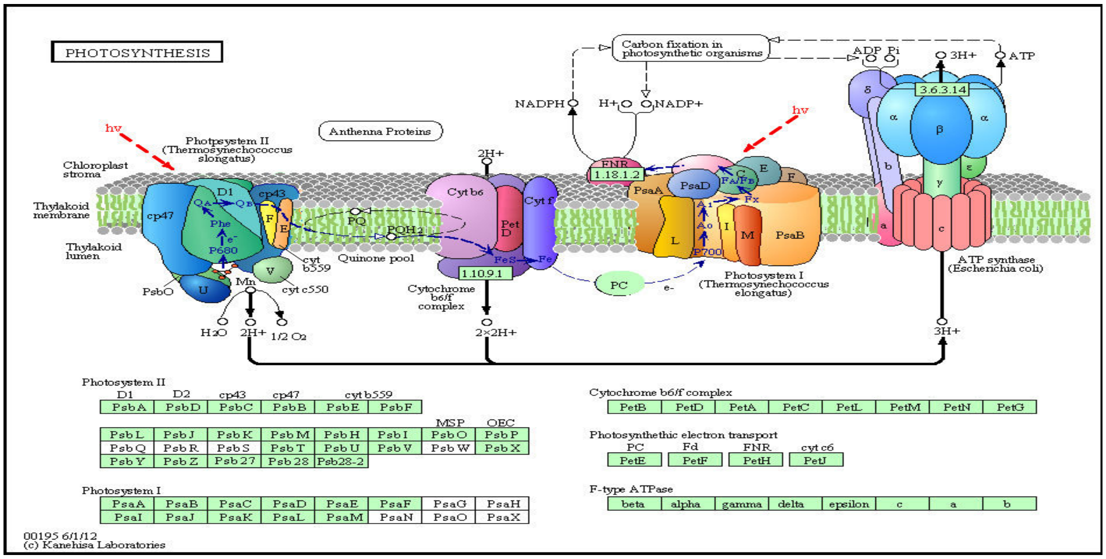

Figure 1.4: Components in the thylakoid membrane and the process of photosynthetic electron transport. Photosystem II (PSII), PQ-plastoquinone, PQH2-plastoquinol, cyt b_6-cytochrome b_6 complex, cytf-cytochrome f complex, Flv2/4-Flavodiiron 2/4, Pc-plastocyanin, PSI- Photosystem I, Fd- ferredoxin, FNR- ferredoxin-NADP+ reductase, NAD(P)H- dehydrogenase1, SDH- succinate dehydrogenase, phycocyanin (PC), phycoerythrin (PE), allophycocyanin (AP). Figure obtained from Kanehasi laboratories.

Cyanobacterium *Synechocystis* sp. P.C.C 6803 as - model research organism: One of the most well studied cyanobacterium and the one that has lent its name to the title of this thesis is *Synechocystis*. It is a unicellular bacterium that was first isolated from a freshwater pond in Oakland, California and has since then become a model organism for cyanobacteria and for photosynthetic research. *Synechocystis* can grow autotrophically, heterotrophically or mixotrophically (90). The first photosynthetic Cyanobacterial genome to be sequenced was that of *Synechocystis* (91). Due to being highly amendable for genetic modification, naturally taking up exogenous DNA and incorporating it into its chromosome by homologous recombination, the popularity and wealth of knowledge about it continues to expand (92). Cyanobacterial vectors for complementation of the mutants and protein expression were developed and successfully used in *Synechocystis* for complementation (93). Minimal requirements for growth, easy maintenance, natural competency, and availability of genome sequence, methods of mutagenesis and microarray chips attracted the research groups to work with *Synechocystis*. Due to availability of DNA microarray chips this model was extensively studied in terms of responses to different stress conditions at the level of gene expression.

Genome of *Synechocystis*:

Synechocystis contains 7-10 copies of circular chromosomes and seven plasmids of different sizes (pSYSM:120 kb, pSYSA:103 kb, pSYSX:106 kb, , pSYSG:44 kb, pCA2.4: 2.4 kb, pCC5.2: 5.2 kb, and pCB2.4:2.3 kb). *Synechocystis* genome is 3,956,957 bp including all native plasmids. It contains total 3725 genes involved in various cellular processes and genes for functionally uncharacterized proteins) (Figure 1.6). Data of all 3725 genes is available in KEGG and Cyanobase (94). Functional annotation of the genome, has identified (46.3%) functionally unknown proteins (hypothetical proteins) (95), suggesting a number of unknown molecular events occurring in the cell. Under one or more abiotic stress conditions, the expression of several hypothetical genes has been up-regulated in this organism (96-100). Induced expressions of hypothetical genes under abiotic stress conditions indicate execution of several unidentified short term adaptive molecular mechanisms by the cell to cope up with the stress. Elucidating the functional role of stress regulated hypothetical proteins is a matter of utmost importance to decode the role played by them under various stresses.

Figure1.5: Genome map of *Synechocystis* and known versus unknown proteins

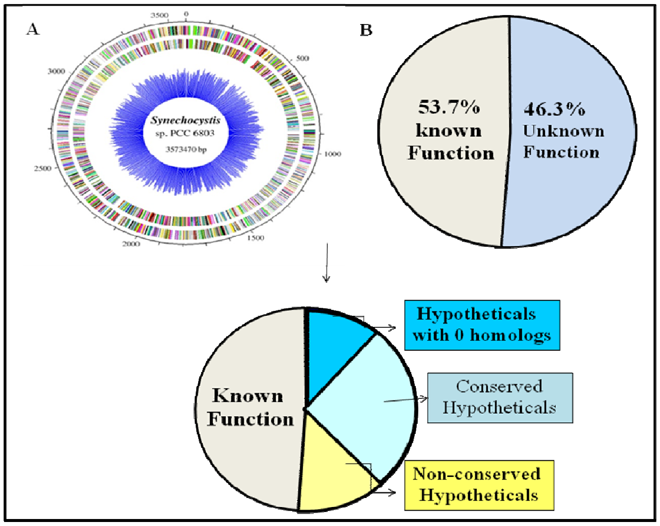

Figure 1.5: (A). 3.5 Mb genome map of *Synechocystis* sp. PCC 6803 (chromosome), with 3573470 bp. (B). Known versus unknown proteins. *Synechocystis* genome contains 46.3% hypothetical proteins of unknown function. The percentage of hypotheticals with 0 homologs and non conserved hypotheticals is almost same but conserved hypotheticals occupy major portion.

Sll1252, a hypothetical protein in *Synechocystis*:

In this study, we focused on a hypothetical protein Sll1252 in the genome of *Synechocystis* (Figure 1.6). Sll1252 is a hypothetical protein of unknown function, containing 259 amino acids with a calculated mass of 28.4 KDa. It has a unique characteristic. Smart domain analysis indicated that it contains a S4 domain at its C terminal. The S4 domain consists of 60-65 amino acids (Figure 1.6) that was detected in the bacterial ribosomal protein S4, and a number of uncharacterized, small proteins (101). The S4 domain probably mediates binding to RNA (102). However physiological function of S4-domain is yet to be elucidated (101). Homology detection of Sll1252 showed that it was highly homologous to YlmH (103), a protein of *Streptococcus pneumoniae* that acts in cell division. Orthologs of Sll1252 are present in *Arabidopsis thaliana* (At1g53120) and *O. sativa* (Os01g0747700) (104). In chloroplasts in *O. sativa* its corresponding gene product was detected (105). As the corresponding protein of Sll1252 is present in higher plant chloroplasts, it might not be involved in cell division. This protein is assumed to have important physiological function, since it is conserved in Cyanobacteria and also in higher plants.

Figure 1.6: *sll1252* in genome context (gene map) and S4 domain of Sll1252

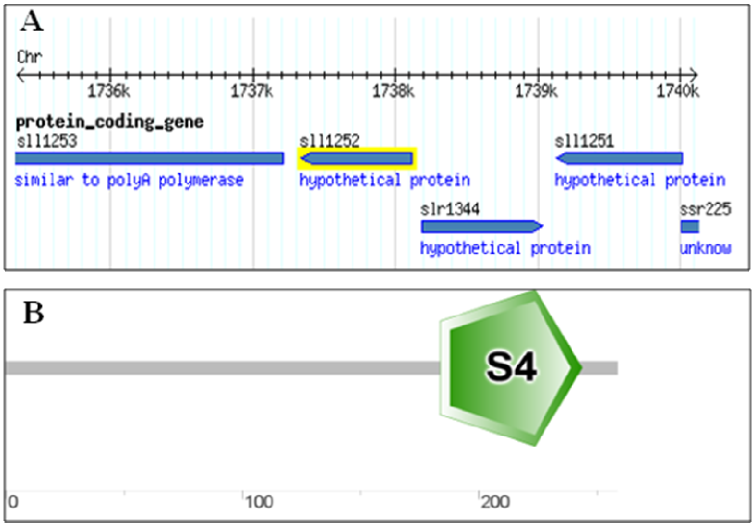

Figure 1.6: (A). *sll1252* gene location in the genome of *Synechocystis* and location of its S4 Domain. *Synechocystis* has a 780bp chromosome in which *sll1252* is located between 1738120 and 1737350. *sll1252* is annotated as hypothetical protein in the genome map. This gene is oriented in the reverse orientation (in the *sll1252* annotation's' stands for *Synechocystis,* 'l' stands for long and second 'l' stands for left orientation). (B). Location of S4 domain of Sll1252: (http://genome.microbedb.jp/cyanobase/Synechocystis/genes/sll1252). Sll1252 protein consists of 259 amino acids in which S4 domain is present in the C terminal i.e, in between 184 to 244 amino acids.

Sll1252 was co-eluted with the PSII complex

Kashino *et al.,* reported that, Sll1252 is associated with photosystem II. Proteomic analysis of PSII preparation from *Synechocystis* revealed the presence of novel polypeptides (106). The PSII complex was purified from the HT-3 strain of *Synechocystis*, in which the CP47 polypeptide contained a poly His tag which was genetically engineered at its C-terminus. Out of the total 31 polypeptides identified in PS II of *Synechocystis*, 26 polypeptides are functionally well characterized while 5 polypeptides are not characterized. The five novel polypeptide encoding genes are *sll1414, sll1252, sll1390, sll1638*, and *sll1130* (Figure 1.7). Kashino *et al.,* proposed a functional role for one of these five proteins, Sll1252, as a protein that appears to be in the downstream of the sensory signal transduction pathway of redox sensing of the plastoquinone pool to balance the photosynthetic electron flow (107). Since Sll1252 protein is associated with PS II core complexes and the presence of the homologous protein in higher plant chloroplasts, Sll1252 may not act in cell division. Since it is a probable member of PSII protein complex, we assumed that this protein may have vital role in structure and function of PSII. Hence elucidating the functional role of Sll1252 is a major addition to the current understanding of the process of photosynthesis in both Cyanobacteria and higher plants.

Figure 1.7: Polypeptide profile of purified His-tagged PSII complex of *Synechocystis*

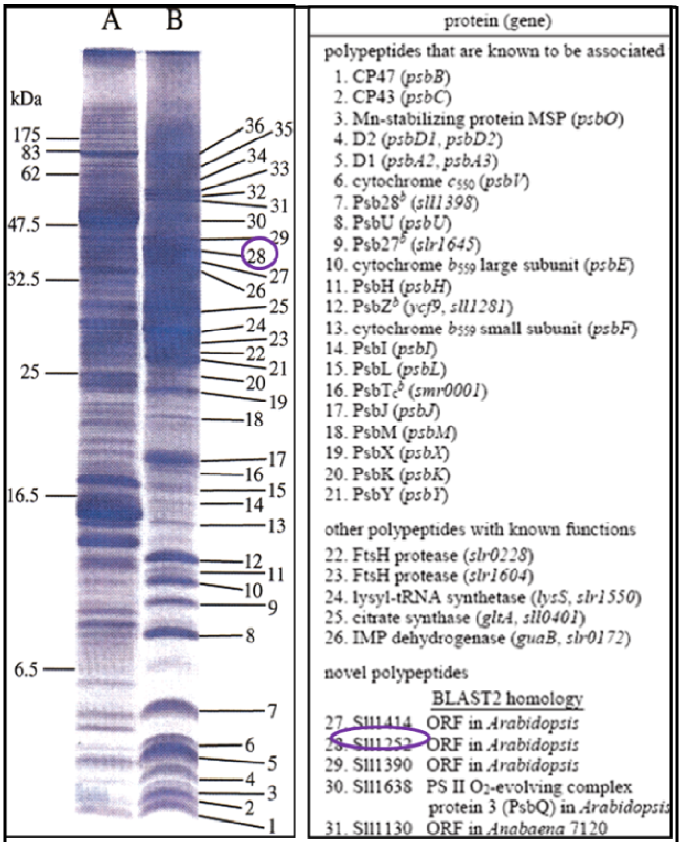

protein (gene)

polypeptides that are known to be associated

1. CP47 (*psbB*)
2. CP43 (*psbC*)
3. Mn-stabilizing protein MSP (*psbO*)
4. D2 (*psbD1*, *psbD2*)
5. D1 (*psbA2*, *psbA3*)
6. cytochrome c_{550} (*psbV*)
7. Psb28^b (*sll1398*)
8. PsbU (*psbU*)
9. Psb27^b (*slr1645*)
10. cytochrome b_{559} large subunit (*psbE*)
11. PsbH (*psbH*)
12. PsbZ^b (*ycf9*, *sll1281*)
13. cytochrome b_{559} small subunit (*psbF*)
14. PsbI (*psbI*)
15. PsbL (*psbL*)
16. PsbTc^b (*smr0001*)
17. PsbJ (*psbJ*)
18. PsbM (*psbM*)
19. PsbX (*psbX*)
20. PsbK (*psbK*)
21. PsbY (*psbY*)

other polypeptides with known functions

22. FtsH protease (*slr0228*)
23. FtsH protease (*slr1604*)
24. lysyl-tRNA synthetase (*lysS*, *slr1550*)
25. citrate synthase (*gltA*, *sll0401*)
26. IMP dehydrogenase (*guaB*, *slr0172*)

novel polypeptides

	BLAST2 homology
27. Sll1414	ORF in *Arabidopsis*
28. Sll1252	ORF in *Arabidopsis*
29. Sll1390	ORF in *Arabidopsis*
30. Sll1638	PS II O_2-evolving complex protein 3 (PsbQ) in *Arabidopsis*
31. Sll1130	ORF in *Anabaena* 7120

A- membrane, B- Purified PSII

FIGURE 1.7: Polypeptide profiles of membrane and purified PSII complex from *Synechocystis*. (A) Membrane (detergent-solubilized) (B) Purified His-tagged PSII complex. On the left side, molecular-weight standards are shown. Numbers on the right correspond to those in Table. Gene names are taken from the Cyanobase. To each lane10µg Chl containing sample was loaded, fractionated by SDSPAGE, and polypeptides were finally stained with Coomassie blue. This figure was adapted from (106).

Photosystem II is an important protein complex of *Synechocystis*

The most important protein complex of the thylakoid membrane is Photosystem II (108). PSII utilizes energy from the sunlight to carry out the initial processes of photosynthesis, like separation of charges, reduction of quinones and splitting of H_2O molecule to molecular O_2. Each monomer of the PSII complex consists of up to twenty protein subunits [(D1, D2 Reaction centre proteins, CP43, CP47 antennae proteins, 13 extrinsic proteins (PsbH, PsbJ, PsbI, PsbK, PsbX, PsbY, PsbZ, Psb30 PsbF, PsbE PsbL, PsbT, PsbM), 3 intrinsic proteins (PsbO, PsbU and PsbV))] (Figure:1.8), 35 chlorophyll a molecules, 12 β-carotenes, 20–25 lipids, 2–3 plastoquinones, two pheophytins, two hemes, one bicarbonate, the water oxidizing complex (Mn_4O_5Ca), four Ca_2 + ions, three Cl− ions and a non-heme iron (109). D1 and D2 proteins form the reaction center of the PSII complex. The Reaction centre is surrounded by the lipid belt formed by eleven lipids. This lipid belt separates reaction centre from the antenna proteins CP43, CP47 (PsbB, PsbC) and small protein subunits. Lipid molecules assist in the assembly and function of PSII. Chlorophyll a molecules bound to the antennae proteins CP43 and CP47 mediate the light harvesting reactions. These antennae proteins accept excitation energy from LHC and transfer it to PSII reaction centre (D1, D2) (110). Mn_4O_5Ca cluster catalyses the oxidation of water, that is coordinated by amino acid residues in D1, D2 and CP43 (111). The large number of 13 small (< 10 kDa) and hydrophobic subunits is quite remarkable. Cyt b_{559}, PsbE, PsbF helps in protection, PsbL, PsbM, PsbT proteins precise functions remain elusive. Under high light conditions, D1 protein is degraded (112) and a loss in photosynthetic activity is observed. CP43 and CP47 are also impaired resulting in the photoinhibition of photosynthesis with PSII as the main target (113). Hence detailed understanding of the structure and function of PSII is important.

Figure 1.8: Organization of PSII biogenesis model in *Synechocystis*

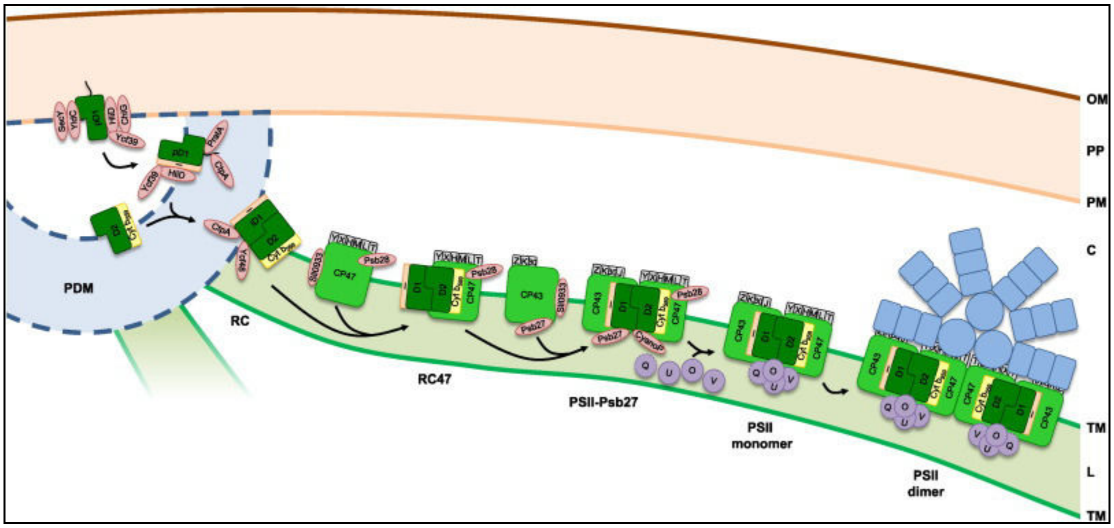

Figure 1.8: **Assembly of PSII subunits to form PSII dimer**: OM – Outer membrane, PP-periplasmic space, PM-Plasma membrane, C-cytoplasm, TM-Thylakoid membrane, RC-Reaction centre (D1&D2 proteins, $Cytb_{559}$), RC47- RC with CP47 antenna protein, PSII-Psb27- RC with CP43 and CP47. This figure was adapted from (114).

Effect of light on photosystems and state transitions:

In oxygen-producing photosynthetic organisms, functional coordination between photosystem II (PSII) and photosystem I (PSI) complexes is regulated to achieve optimal performance. Such functional coordination between the two photosystems is affected by dynamic changes in the environmental conditions (115). For instance, it has been demonstrated that high light intensity, affects the structure and function of photosystem II thereby leading to functional imbalance between photosystems (116–118). However, this imbalance in the relative activities of PSII and PSI in response to dynamic changes in the environment is overcome by employing various strategies (119-120). For instance, one of the strategies, common to higher plants and cyanobacteria, employed for maintaining functional balance between the photosystems is by a mechanism called state transitions (121) involving distribution of absorbed light energy between photosystems (122–124). Under state 1, the captured excitation energy is directed largely to PSII, but under state 2, most of the energy is redirected to PSI (125–127). In cyanobacteria it has been demonstrated that the balanced distribution of excitation energy was mainly regulated by the mobility of phycobilisomes (128,129). Adjustment of PSI to PSII stoichiometry is yet another mechanism by which functional coordination of photosystems is achieved (130–132). In cyanobacteria the trimeric form of PSI is relatively more abundant as compared to monomeric form (133).

Regulation of redox state of PQ pool:

When an imbalance occurs between the action of PSI and PSII, cells adjust the stoichiometry between PSI and PSII in the thylakoid membrane, so as to balance their actions (129). Studies in higher plants have indicated that energy redistribution between PSII and PSI, and changes in stoichiometry of photosystems are regulated by the redox state of plastoquinone (PQ) pool (119,133). At the molecular level, PQ pool exerts redox regulatory control over transcription. PQ in the reduced state causes an increase in the transcription of PSI reaction center genes whereas PQ in the oxidized state causes a decrease in PSI, providing a compensatory self-adjusting response in higher plants (134). However, in cyanobacteria, PQ redox state is not involved in transcriptional regulation of PSI reaction-center genes. It has been reported that the PSII-light activates and PSI-light represses the *psaAB* transcription in *Synechocystis* (135). Addition of glucose, which enhances the PQ reduction, also triggers *psaAB* gene expression (136). In addition, both inhibitors, DCMU and DBMIB repress the *psaAB* genes under moderate light conditions (137). These observations suggest that the oxidation of downstream components of PQ represses and reduction of the same upregulates the *psaAB* gene expression. On the other hand, under high light conditions PSI genes are largely down-regulated and this down-regulation is suppressed by addition of either DCMU or DBMIB (138) showing that the reduction of downstream components of PQ causes down regulation of PSI genes under high light conditions. Although the mechanism of transcriptional regulation of PSI genes seems different under different light conditions, the PQ redox is not the primary signal in both cases. Unlike in higher plants, the signal for PSI gene expression seems to reside at or after cytochrome b_6f complex in cyanobacteria. Strategies mentioned above are meant for regulating the functional balance and coordination between the photosystems in order to maintain optimal photosynthetic performance and thereby acclimation to changed environmental condition in photosynthetic organisms

DCMU and DBMIB Inhibitors to study photosynthesis:

To understand the process of photosynthesis, inhibitors are used to measure the rate of electron transport. Two inhibitors, DCMU and DBMIB, are generally used as they modulate the redox state of the PET chain. DCMU inhibits electron transfer between the (Q_A) to (Q_B) quinones by binding to the Q_B site of PSII, This interrupts the PET chain and reduces the production of O_2 from water molecules by PSII. DBMIB inhibits cytochrome b_6/f complex activity by attaching to the Q_0 site (the PQH_2 binding site, and prevents reoxidation of the PQ pool (139) (Figure 1.10). Thus both inhibitors show antagonistic effects on the redox state of PQ pool.

Figure 1.9: Site of DCMU and DBMIB inhibition in electron flow

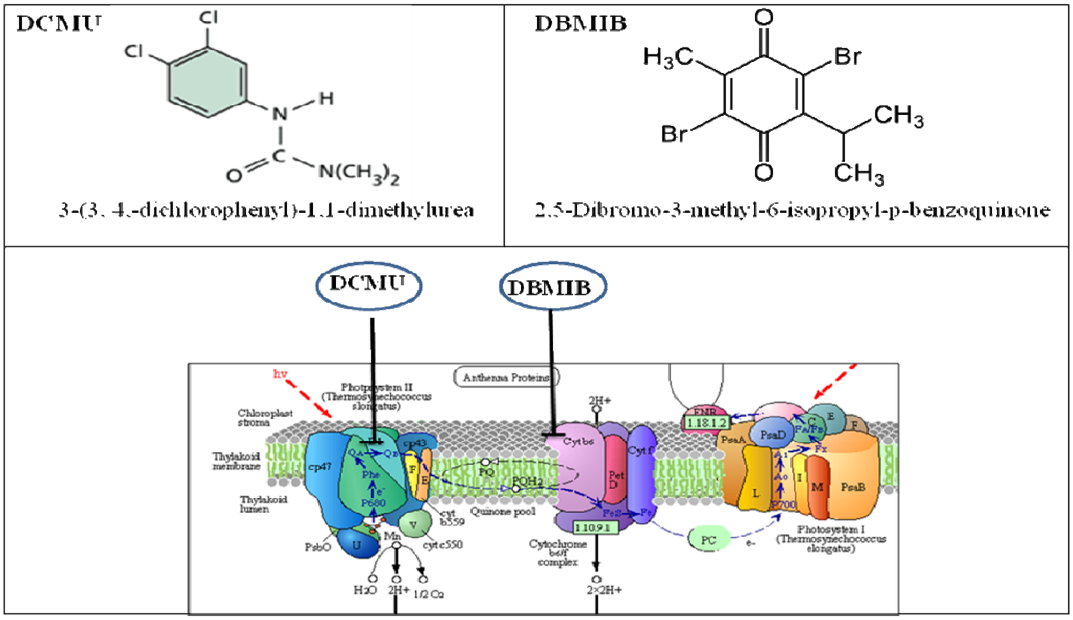

Figure 1.9: Structure and sites of DCMU and DBMIB inhibitors: PSII- photosystem II, Cyt b_6f-cytochrome b_6f complex, PSI- photosystem I, PQ- plastoquinone, cytochrome b_6f complex, PC-Plastocyanin. DCPIP, is an artificial electron donor of PSI that can be used to allow electron transport through PSI under conditions of inhibited PSII to I electron transport. This figure was taken from (140).

Based on the available literature of *sll1252* gene, its conservation in higher plants, its association with the PSII complex and the presence of S4 domain in Sll1252 protein. I have chosen this hypothetical protein to characterize its function in *Synechocystis* s.

2. OBJECTIVES

In *Synechocystis* about 46.3% ORFs code for proteins with unknown function and several of these functionally uncharacterized proteins are conserved among cyanobacteria. Sll1252 is one of them coding for a protein of unknown function and is assumed to have important physiological function, since it is conserved in cyanobacteria, and also in higher plants. It was also reported to be associated with highly purified PSII core complexes by (53) which might be involved in structural and functional integrity of PS II complex. Present work was designed to identify the function of Sll1252 in *Synechocystis* by mutation, phenotypic characterization, microarray analysis and by physiological and biochemical experiments.

Proposed objectives

1. Targeted mutagenesis of *sll1252* gene in *Synechocystis* to analyze the effect of mutation on function of PSII by growth analysis of the wild type and mutant cells.
2. DNA Microarray analysis of wild type/Δ*sll1252*$^{\text{ins}}$ to find the role of Sll1252 in gene regulation, in order to get clues on its function.
3. DCMU and DBMIM inhibitor studies to find the site of action of Sll1252 protein.
4. Expression and purification of Sll1252 in *E.coli* and generate its antibody to find whether Sll1252 protein is present in soluble or insoluble fraction of *Synechocystis* cells.

5. Functional Complementation of Δ*sll1252*^{ins} using a cyanobacterial expression vector to check if the phenotypical outcomes of Δ*sll1252*^{ins} mutation are due to polar effects or due to mutation itself.
6. Generation of N-terminal, C-terminal and deletional mutants of *sll1252* gene to determine which domain of the protein is involved in PSII regulation.
7. Determination of rate of PQ pool reduction in order to confirm the site of action.
8. Transmission electron microscopy to check the organization of the thylakoid membrane in wild type and mutant cells.

In the present study we elucidated the function of Sll1252 by targeted insertional inactivation of *sll1252* and comparative transcriptomic analysis of the mutant. Based on comparative transcriptomics, suitable physiological and biochemical experiments were performed to completely reveal the function of Sll1252. As will be presented, Sll1252 is essentially required for regulation of electron transfer between plastoquinone pool to Cytochrome b_6/f complex in the linear photosynthetic electron transport.

3. MATERIALS AND METHODS

Culture conditions:

Synechocystis, a glucose-tolerant strain, was originally obtained from Dr J.G. K. Williams (Dupont de Nemours, Wilmington, DE, U.S.A.) (141) served as the wild-type. Wild type cells were grown photoautotrophically at 34°C in BG-11 medium (142) buffered with 20 mM Hepes/NaOH (pH 7.5) aerated with 1.5% CO_2, Light intensities used for growth were 70 µmol photons/m2 per sec (optimal light) (143) or 5 µmol photons m^{-2} s^{-1} (low light) light. For photoheterotrophic growth, we cultured the cells in the BG-11 medium additionally containing 10 µM DCMU and 5 mM glucose. For photomixotrophic growth the BG-11 medium contained 5 mM glucose. For both photohetertrophic and photomixotrophic conditions, cells were cultured with continuous light illumination of 5 µmol photons m^{-2} s^{-1}. The *sll1252* culture (Δ*sll1252*^{ins} cells) in which the *sll1252* gene was disrupted by inserting a Kan^R (kanamycin-resistance gene) cassette, was grown under the same conditions as described above with the exception that the culture medium contained kanamycin at 25 µg/ml in pre cultures. Growth of the culture was monitored by measuring absorbance at 730 nm using a spectrophotometer (Shimadzu UV-160A).

Preparation of BG-11 for *Synechocystis* sp PCC6803 culture:

Stock 1: Citric acid $C_6H_8O_7$-0.3g, Ferric ammonium citrate-0.3g and EDTA-0.05g weighed and adjusted to 100 ml with milliQ water, filter sterilized it separately and stored in dark and low temperature. **Stock 2:** $NaNO_3$-30g, K_2HPO_4-0.7g and $MgSO_4.7H_2O$-1.5g weighed and adjusted to 1litre with milliQ water. **Stock 3:** $CaCl_2.2H_2O$ -1.9g weighed and adjusted to 100ml with milliQ water. **Stock 4:** Na_2CO_3-2g weighed and adjust to 100ml with milliQ water. **Stock 5:** $MnCl_2.4H_2O$-1.81g, H_3BO_3-2.86g, $ZnSO_4.7H_2O$-0.222g, $Na_2Mo_4.2H_2O$-0.391g, $Co(NO_3)_2.6H_2O$-0.049g, $CuSO_4.5H_2O$-0.079g and weighed and

adjusted to 1 litre with milliQ water. **Stock 6:** HEPES-119.15g weighed and dissolved in milliQ water (750ml), pH adjusted to 7.5 with 2M NaOH and volume made up to 1 litre. All stocks are kept at cool temperature.

Table 3.1: Preparation of BG-11 from stocks

Stock solution	**1X - 1000ml**	**2X - 500ml**
Stock 2	50ml	50ml
Stock 3	2ml	2ml
Stock 4	1ml	1ml
Stock 5	1ml	1ml
Stock 6	40ml	40ml
Milli Q water	Up to 1000ml	Up to 500ml

Table 3.1: Preparation of BG-11 nutrient medium from the stocks

Stock 1 is added just prior to inoculation, 2ml in 1000ml of 1X BG-11solution after Autoclaving.

Preparation of BG-11 Agar plates:

For preparation of agar plates 2X BG-11 and 2X agar agar (3% agar agar) were autoclaved separately and mixed in 1:1 ratio after autoclaving, poured in sterile petri plates after addition of stock-1 and100 mM $Na_2S_2O_3$ (10ml for 1 lit).

Preparation of BG-11 antibiotic medium:

To give a selection pressure suitable antibiotics were added just prior to inoculation to the above mentioned Bg-11 medium. 25 μg/ml filter sterilized Kanamycin and 20 μg/ml Chloramphenicol were added to a final concentration of the media.

Escherichia coli:

Escherichia coli (DH5α) was used for cloning and DNA modification experiments while *E. coli* BL21 (DE3) pLysS was used for expressing His tagged recombinant proteins. Bacterial cultures were grown/maintained in LB broth or LB plates, respectively, with appropriate antibiotic(s) at 37 °C.

Luria and Bertani medium (L.B. MEDIUM):

Tryptone (10gm), Yeast extract (5gm), NaCl (10gm) and pH adjusted to 7-7.2 (For LB agar 1.5% agar agar to the above mentioned components). All these ingredients were added to 950ml of double distilled water (DDW). The pH was adjusted to 7.2 with 1N HCl/1N NaOH and DDW was added to make up to 1 liter. In order to prepare LB Agar, 1.5% of agar agar (w/v) was added to the LB solution. This is then sterilized by autoclaving at 15 psi pressure for 15-20 minutes. In case of LB Agar the media was allowed to cool to 50°C before adding appropriate antibiotics. About 25 ml of media was poured in 90mm Petri plate and allowed it to solidify. These solidified LB plates were stored at 4°C.

Preparation of antibiotic LB medium:

To give selection pressure selective antibiotics were added just prior to inoculation to the above mentioned LB medium. 25 μg/ml, filter sterilized Kanamycin, and 20 μg/ml Chloramphenicol were added to a final concentration of the media.

Kits, enzymes, chemicals and reagents:

Molecular biology kits and enzymes were procured from Simga Aldrich (USA), Qiagen (Germany), MBI Fermentas (Germany) and Takara bio (Japan). Precautions were taken as per manufacturers' instructions. The chemicals and reagents were of analytical grade and obtained from Sigma Aldrich (USA), GE health care (USA), Fermentas (Germany), Agilent technologies (USA) Himedia (India), SRL (India) and Qualigens fine chemicals (India).

Molecular biology protocols:

Plasmid DNA isolation, genomic DNA isolation, competent cell preparation and transformation, restriction digestion, ligation, agarose gel electrophoresis, were according to (144) and/or as per manufacturers' protocol.

Plasmid DNA vectors:

Commercially available T-vector of fermentas/Bangalore genei was used for simple TA-cloning experiments and blue white screening. pVZ321 a cyanobacterial vector was used to express the *sll1252* with its native promoter in *Synechocystis*. pET28a(+) a high copy number prokaryotic expression vector was used for the cloning and expression of Sll1252.

Quantification of DNA and RNA:

RNA and DNA concentration was examined by spectrophotometric analysis (Nanodrop ND-1000). The concentration of DNA and RNA was measured at 260 nm and 280nm and RNA using spectrophotometry. A value of OD_{260} =1 corresponds to 50 µg/ml for DNA, while OD_{260} =1 corresponds to 40 µg/ml for RNA. A value of OD_{260}/OD_{280} between 1.8 and 2.0 and between 1.9 and 2.1 was considered as pure form of DNA and RNA, respectively.

Oligonucleotides and sequencing:

All DNA oligonucleotides were synthesized by either Sigma Aldrich or MWG Biotech (Eurofins). Nucleic acid sequencing was carried out by Eurofins as per requirement. All the expression clones used for purification were prior confirmed at sequence level.

DNA microarray chip:

We used a *Synechocystis* DNA Microarray, (Cyano CHIP, Takara Co. Ltd.) which covers 3079 (97%) of the 3168 genes on the chromosome of *Synechocystis* (99 genes for transposases are excluded from this calculation). Sequences of the four plasmids of *Synechocystis* [pSYSM, pSYSX, pSYSA and pSYSG] and a number of putative genes are present in them, a total of 397 genes were reported (145). However, these genes are not included in the DNA microarray from Takara Bio Co.

Extraction of total RNA:

RNA from the *Synechocystis* cells was isolated essentially by the method of Los *et al*., (146). Actively growing *Synechocystis* cells (treated or untreated (or) mutant/WT) in bubbling culture (O.D-0.4-0.6) were immediately killed by addition of equal volume of ice cold 5% (w/v) phenol in ethanol, cells were harvested at 4^oC and cell pellet is stored in -80^oC. Cells were lysed by heating the cells in presence of 1% SDS and using acid phenol method. To the obtained nucleic acids DNase I treatment was given, to remove the contamination of genomic and plasmid DNA and the obtained RNA pellet was dissolved in 30 µl of DEPC water and stored in -80^oC.

Expression and purification of recombinant proteins (His-tag):

E. coli BL21 DE3 competent cells were transformed with recombinant plasmids and plated on LB kanamycin (25 µg/ml) plate and incubated overnight. Single colony was picked up from plate and inoculated in 5 ml LB broth with antibiotics and incubated over night with continuous shaking. Overnight 5 ml culture was inoculated in 500 ml of fresh LB broth with antibiotics and incubated in shaker till OD_{600} reached 0.5, and then cells were induced with 0.4M IPTG to express its peptides. Cells were harvested after 4 h of induction and washed with 100 mM Tris.Cl pH 8.0 and 300 mM NaCl and resuspended in same buffer. Cells were disrupted by sonication and insoluble debris was removed by centrifugation. Protein preparations were compared with un-induced controls to check the expression of peptides by SDS PAGE. Five ml of Ni-NTAgarose (Sigma-Aldrich) was packed in a polypropylene column and equilibrated with 25 ml of Tris-NaCl buffer with 5 mM imidazole. Sonicated supernatant was added to the column and flow through was collected and stored at -20°C. The column was washed with 20 ml of washing buffer (Tris-NaCl buffer with 25 mM imidazole) and wash through was collected. Finally the protein was eluted with 15 ml of elution buffer (Tris-NaCl buffer with 200 mM imidazole) and elutes were collected. Purity of the protein was analyzed by SDS-PAGE, and visualized after Coomassie blue staining. Fractions containing pure protein were pooled and stored at -20°C after addition of glycerol to final concentration of 10% (v/v).

Generation of *sll1252 insertional* mutant: (Δ*sll1252*^{ins}):

We generated a Δ*sll1252*^{ins} mutant of *Synechocystis* by insertional inactivation of the *sll1252* gene. A DNA fragment containing the *sll1252* ORF (open reading frame) with 80-bp upstream and 97-bp downstream flanking regions was amplified using PCR with the following primers: *sll1252*-F, 5'-AAC CAT AGG CGC ATT GTA GCT CCT TG-3'; and *sll1252*-R 5'-GAT ATC AAC ATT ATC CTT TGC CTC GAA CG-3'. The PCR amplified 957 bp fragment was ligated to the pT7 Blue T-A cloning vector using GeNei™ instant cloning kit (Cat No: 107416, Bangalore Genie) and the resultant plasmid *pT-sll1252* was used to inactivate the *sll1252* ORF by performing *in vitro* transposon reaction according to the protocol provided by the manufacturer (EZ::Tn5™ <KAN-2> Insertion kit, Cat No: EZ1982K, Epicentre). The plasmid DNA construct in which the *sll1252* ORF was disrupted by the kanamycin resistance gene cassette was designated as *psll1252::km*. This construct was used to transform *Synechocystis* cells. The site of insertion of kanamycin gene cassette was located by sequencing the *psll1252::km* DNA construct using kan-FP1 primer.

For transformation, wild-type *Synechocystis* cells that have been grown photoautotrophically to an OD_{730} of about 0.6 were adjusted to OD_{730} of 2, by centrifuging cell culture at 3,000 x g for 5 min and resuspending the resulted cell pellet in 200 µl of fresh BG-11 medium. About 5 µg of *psll1252::Km* was mixed with 150 µl of cell suspension and incubated for 16 h in a sterile microfuge tube at 30 °C in light at 50 µmol photons m^{-2} s^{-1} without shaking. The cells were then placed on BG11 agar plates that contained a concentration gradient of kanamycin. Single colonies, which had developed on the BG11-containing agar in the region where kanamycin was present at a low concentration, were placed on the BG11- agar plates supplemented with 10 µg/ml kanamycin. Cells that had been grown actively were subsequently transferred to BG11 agar plates, containing increasing concentrations of kanamycin. The maximum concentration used was 25 µg/ml. As *Synechocystis* contains multiple identical copies of the genome, increasing antibiotic pressure is necessary to completely replace all the wild-type copies of the *sll1252* gene, with the *in* *vitro* disrupted copy of the gene, *sll1252::Km* by homologous recombination. Genomic DNA of the *Δsll1252* mutant cells grown for several rounds in BG11 medium was prepared and extent of the replacement of wild-type copies of *sll1252* with the *sll1252::km* was checked by primers *sll1252* –F and *sll1252*-R. The mutant thus generated was named Δ*sll1252*^{ins}.

Preparation of cDNA for DNA microarray analysis:

Wild-type *Synechocystis* cells and Δ*sll1252*^{ins} mutant cells that were grown at 70 µmol photons m^{-2} s^{-1} (50 mL) were killed instantaneously by the addition of 50 mL of ice cold 5%-phenol in ethanol (w/v) and then total RNA was extracted as described previously (145). The RNA was treated with DNase I (Nippon Gene, Tokyo, Japan) to remove contaminating DNA. cDNAs, labeled with fluorescent dyes [Cy3 and Cy5 (indodicarbocyanine); Amersham Pharmacia Biotech] were prepared from 10 µg total RNA with an RNA fluorescence labeling core kit [M-MLV (Moloney murine leukaemia virus), version 2.0 Takara Co. Ltd., Kyoto, Japan] according to the manufacturer's instructions.

DNA microarray analysis of Δ*sll1252*/WT:

Genome-wide analysis of transcript levels was performed with DNA microarrays (64, 48) for finding genes with altered expression due to mutation in *sll1252*. Labelled cDNAs were hybridized to the DNA microarray allowed for 16 h at 65°C. Then the hybridized microarrays were rinsed with 2x SSC (1x SSC is 15 mM sodium citrate and 150 mM NaCl) at 30°C, and then washed with 2x SSC for 10 min at 60°C and with 0.2x SSC, 0.1% SDS for 10 min at 60°C and rinsed with distilled water for 2 min at room temperature. An air spray was used to remove the moisture from the microarray chip before analyzing with the array scanner (GMS418; Affimetrix, Woburn, MA, USA). Each signal was quantified with the

ImaGene ver. 4.0 program (BioDiscovery, Los Angeles, CA, USA). The signal from each gene was normalized by reference to the total intensity of signals from all genes, (except genes for r RNAs). Then the change in the level of the transcript of each gene relative to the total amount of mRNA was calculated.

Measurement of photosynthetic evolution of oxygen:

Photosynthetic oxygen evolution was measured in 1ml of cell suspension (OD_{730} of ~ 1, about 5 µg/ml chlorophyll), using an oxygen electrode (Oxygraph plus, Hansatech Instruments Ltd., Norfolk, England). Cells were cultivated photoautotrophically under aeration in light at 70 µmol photons m^{-2} s^{-1} or 5 µmol photons m^{-2} s^{-1}. PSII activity was determined in the presence of 1.0 mM p-benzoquinone (PBQ) or 2 mM Methyl viologen. Photosynthetic oxygen evolution was recorded at 1000 µmol photons m–2 s–1. PSII activity was determined as a difference of net oxygen evolution in light and oxygen consumption in the dark. Effects of varying concentrations (0 to 800 nM) of DBMIB were analyzed by measuring the oxygen-evolving activity in presence of 2 mM MV (Methyl viologen or $NaHCO_3$). The rate of PSII-catalyzed electron transport was measured in the presence of various concentrations (0 to 600 nM) of DCMU. Three independent cultures of wild type and Δ*sll1252* cells were measured with technical triplicates. The chlorophyll concentration of cultures was determined using 80% acetone as a solvent for extraction.

Estimation of chlorophyll:

Chlorophyll was estimated by a modified method from (147). 1 ml of cells, of density 0.4 (O.D 730 nm) was centrifuged at a speed of 15k rpm and supernatant was discarded to the maximum extent possible. Cell pellet was suspended in 200 µL of water and added 800 µl of acetone (to final 80% (v/v) conc. Acetone) kept on shaking for 15 min and centrifuged at high speed (15k rpm) for 15 min pellet containing phycobilisomes is deep blue. Absorbance of the supernatant was measured at 663 nm taking 80% acetone as the blank. The amount of chlorophyll was calculated using the formula; [Chl μg / ml = abs at 663 nm X 12.189]. Equations were used to calculate the chlorophyll content from the peaks (heights) of absorption spectra (live cells) (147).

Determination of rate of PQ pool reduction:

The reduction rate of PQ pool in the intact cells was determined by changes in absorption of a measuring light at 260 nm upon the initiation of irradiation of the actinic light at 600 nm at 70 μmole photons m^{-2} s^{-1}, following the method reported previously (148). Briefly, the cells were cultivated at 30˚C for some days under the constant illumination with incandescent lamps at 7 μmol photons m^{-2} s^{-1} with aeration of 2% CO_2-enriched air. The cells were suspended with fresh BG-11 medium at O.D. 730 nm 1.5 and put into a spectrophotometer cuvette. The cell suspension was put in a spectrophotometer, UVIDEC-4 (JUSCO, Tokyo, Japan), installed in dark room at 25˚C and aerated for more than 5 min with air in order to maintain redox state of the PQ pool at a certain level by the respiration under the O_2-sufficient conditions. During the period of pre incubation, absorption of 260 nm by the cell suspension became constant. To measure the reduction rate of the PQ pool under the illumination, we halted the aeration and immediately initiated the illumination of the actinic light and monitored the initial rate of the change in the absorption at 260 nm.

Overexpression and purification of Sll1252 protein:

The *sll1252* ORF was PCR amplified with the following primers: *sll1252*-ExF (5'- ACT CAT ATG TTA CCA AGA GAA GCT TTG TTA AAG -3') and *sll1252* ExR (5'- CCC GGA TCC TTA AAG ATA TCG GGT TAA TTG GAT GC-3') and purified by agarose gel electrophoresis. The NdeI and BamHI restriction sites are underlined. The amplified ORF of *sll1252* was inserted into pET-28a(+) at the NdeI and BamHI sites to generate pET-Sll1252. The N-terminally His-tagged Sll1252 protein was expressed in BL21 (DE3) pLysS cells harboring pGKJE8 plasmid vector, which had been transformed with pET-Sll1252. and was purified using HIS-Select TM Nickel-Affinity gel (catalogue number P6611, Sigma) according to the manufacturer's instructions. The Sll1252 protein expression was induced by the addition of IPTG at a final concentration of 400 µM. To induce expression of chaperons for proteins folding, host cells were grown at 37°C in presence of arabinose and tetracycline at a final concentration of 2 mg / ml and 5 ng / ml until the OD_{600} of the cells reaches to 0.6. Bacterial cells were centrifuged at 10,000 g for a period of 10 min, supernatant was discarded and cells in the pellet were disrupted in 100 mM Tris-HCl (pH 8.0) and 200 mM NaCl with the help of a sonic oscillator (Model, UV2070; Probe, MS-72; Bandelin Electronic) operated for at 50% power, for 10 min with 1 min pulse interval. Sonicated cells were centrifuged at 20,000 x *g* at 4°C for 20 min to remove insoluble materials. Then the supernatant was loaded onto a HIS-Select Nickel Affinity column. Then the column was washed with 100 mM Tris-HCl (pH 8.0), 200 mM NaCl and 10 mM imidazole and sequentially with 100 mM Tris-HCl (pH 8.0), 200 mM NaCl and 40 mM imidazole. Again using the same buffer with increase in imidazole concentration to 200 mM, His-Sll1252 protein was eluted. Each eluted fraction was loaded onto SDS-gel electrophoresis to check purity. The purified Sll1252 protein was examined under denaturing (the protein was mixed with loading dye containing 2-

mercaptoethanol and SDS and was boiled before electrophoresis) conditions. Elutes which gave a single band on the gel at the expected region, were combined and dialyzed against 5 mM Tris-HCl (pH 8.0). The purified protein was used to generate anti-Sll1252 antibody.

Generation of anti-Sll1252 antibody:

Antibody against Sll1252 protein was raised in New Zealand white rabbit with His-Sll1252 (48). Primary induction was done by injecting 250 µg of purified protein with equal amount of Freund's complete adjuvant. Secondary induction was done using 150 µg of pure protein and equal volume of the Freund's incomplete adjuvant (booster). Serum was collected after the second booster, diluted 3000 fold in 3% BSA and used for the detection of Sll1252 protein by western blot analysis. Animal experiments were carried out under the appropriate institutional guidelines.

Western blotting analysis of Sll1252 protein:

In order to extract soluble proteins from *Synechocystis* cells, the wild type, *sll1252*$^{+}$, Δ*sll1252*^{ins} were grown to a O.D of 0.6 and centrifuged at 8k, for 4 min at 4°C. The pellet containing the cells was suspended in 200 µl of 50 mM Tris-HCl (pH 8.0) and 1mM EDTA buffer in a thick walled glass tube along with 330 mg glass beads and subjected to disruption by vigorous mixing in a vortexer for 10 times with intervals of vortexing for 1 min and cooling for 2 min on ice. After disruption, the cells were centrifuged for 20 min at 25k at 4°C. The supernatant of wild type, mutant and complement cells containing the soluble proteins were loaded (25 µg of protein) on to SDS-PAGE gel, on equal protein basis. After SDS/PAGE separation, proteins were blotted on to PVDF membrane (Immobilon-P; Millipore) in a semi-dry transfer apparatus (TE77-PWR semi-dry transfer unit, GE Healthcare). Levels of Sll1252 were determined immunologically with the NBT (Nitro Blue

Tetrazolium)/BCIP (5-bromo-4-chloroindol-3-yl phosphate) chromogenic detection system aaccording to the manufacturer's instructions (Sigma fast BCIP/NBT; catalogue number B5655, Sigma–Aldrich). Polyclonal antibodies raised in Rabbit against His–Sll1252 protein

were used as the primary antibody, and alkaline-phosphatase-linked antibody raised in goat against Rabbit IgG was used as the secondary antibody.

Denaturing and semi-denaturing SDS gels:

Proteins were separated on SDS-PAGE, 12% or15% as per the requirement. The over-expressed and purified Sll1252 protein was examined under denaturing (loading dye containing β-mercaptoethanol was mixed with the protein sample and boiled before loading in the well). Purity of the purified proteins was also confirmed by resolving the protein in SDS-PAGE (15%), denaturing conditions. Protein confirmation was done by MALDI-TOF-TOF analysis of gel excised protein.

Localization of Sll1252 by Western blotting analysis:

Western blotting analysis was performed as described previously with some modifications (48). Polyclonal antibodies raised in rabbit against His-Sll1252 protein were used as the primary antibody, and alkaline phosphatase-linked antibody raised in goat against rabbit IgG was used as the secondary antibody. After SDS-PAGE separation, proteins were blotted onto polyvinylidene fluoride membrane (Immobilon-P; Millipore) in a semidry transfer apparatus (TE77-PWR semi dry transfer unit, GE health care). Levels of Sll1252 were determined immunologically with NBT-BCIP chromogenic detection system according to the manufacturer's instructions (Sigma fast BCIP/NBT, Cat No: B5655, Sigma-Aldrich).

Complementation of the *sll1252* mutation in Δ*sll1252*^{ins} cells:

We complimented Δ*sll1252* cells with a derivative of the cyanobacterial autonomously replicating plasmids pVZ321 harboring the *sll1252* gene. A DNA fragment containing the *sll1252* gene and its upstream was amplified, using the genomic DNA as template, from wild-type *Synechocystis* cells, by PCR with the primers,

F P : with ClaI site 5'TGC <u>ATCGAT</u> TTG CTA CCT GGA TGG TGA AAA TCA TG-3'and

R P: with XhoI site 5' – CGA <u>CTCGAG</u> GAA CCA CCA GTC AAG ACA ATG CGA C-3'

The PCR amplified product was digested with ClaI and XhoI and cloned into pVZ321 which digested with the similar enzymes. The recombinant plasmid was transformed into Δ*sll1252*^{ins} cells by triparental mating (93). Transformed colonies were selected with antibiotic selection pressure of 25 µg of chloramphenicol / ml on BG-11 agar medium. The complimented strain was designated *sll1252*$^{+}$.

Triparental mating:

Triparental mating is carried out by three strains, donor strain, helper strain and the recipient strain. We used *E. coli* DH5α cells containing pVZ321 (with *sll1252* gene) as donor strain, *E. coli* R591 cells as the helper strain and Δ*sll1252*^{ins} *Synechocystis* cells as recipient strain. Active cultures of the Donor, helper (grown to stationary phase) and recipient cell (grown to a turbidity (D_{730}) of 0.8) suspensions were mixed in 1:1:10 (by volume; total volume 1.2 ml) proportions and centrifuged at 1000 g for 1 min, after discarding the supernatant, the cell pellet was rinsed with 40 µl BG-11 medium and transferred on to a sterile Durapore™ membrane filter (13 mm diameter, 22 µm pore size; Millipore, Billerica, MA, U.S.A.) placed on BG-11 and 5% (v/v) LB medium agar-plates and incubated in light at 900 lux overnight at

34 °C. The membrane was placed in a micro-centrifuge tube, which contained 200µl of BG-11 medium and vortexed to separate the cells from the membrane. The membrane was removed and the cells were centrifuged at 1000 *g* for 5 min. The supernatant was discarded and the cells were suspended in fresh BG-11 medium and spread on BG-11 agar plate that contained 10 µg/ml chloramphenicol and 25 µg/ml kanamycin for isolation of pVZ321/PCC 6803 transformants. The plates were incubated at 34 °C in light at 350 lux. Actively grown cells were transferred to BG11 agar plates containing increasing concentrations of chloramphenicol (15 µg/ml, 25 µg/ml, 35 µg/ml).

Screening for spontaneous suppressor mutants of Δ*sll1252*^{ins}:

Suppressor mutant colonies were isolated from the Δ*sll1252*^{ins} mutant, which was streaked on the BG-11 agar plates supplemented with 5 mM glucose and kanamycin (25 µg per ml) under prolonged continuous illumination of 70 µmol photons m^{-2} s^{-1}. Selected colonies which were developed after 2 to 3 weeks of incubation were grown in the liquid BG-11 medium and then genomic DNA was isolated. Amplified the DNA with the primers designed at 146 bp and 49 bp, upstream and downstream regions respectively of the *sll1252* open reading frame. The primers used for PCR amplification were, SF: AGA TCT GCC AAG ATA ATT GAT TG and SR: AGA TCT GTC GAC ATT CCA CTG GCA AAA. The resulted PCR amplified product was sequenced using the kanamycin specific primers, FP1: ACC TAC AAC AAA GCT CTC ATC AAC C and RP1: GCA ATG TAA CAT CAG AGA TTT TGA G. Sequencing was done by using the detection method, Big Dye terminator fluorescence. (Applied Biosystems, Foster City, CA, USA).

Deletional mutagenesis of the *sll1252* gene (Δ*sll1252*^{del}):

A 500-bp upstream and 500-bp downstream flanking regions of ORF *sll1252* were amplified from the genomic DNA using primer sets UF (5'GCA TCA ATT TGT TCT GTC AC 3') and UR (5'AGA TCT CGA GCA ACG GCA TTA GCT 3'); DF (5'CGT TGC TCG AGA TCT CCA GTT TCA AGG CTT GCC 3') and DR (5'CCA CAA TTA AAG TTG TAC TG 3') respectively. A BglII site (underlined) was created in UR and DF primers, during primer synthesis. The PCR fragments amplified using UF-UR and DF-DR primer sets were used to setup a third fusion PCR with UF-DR primer set. The fusion PCR amplified product thus generated was cloned onto T-Vector pMD19 (simple) cloning vector (Takara-Bio. Ohtsu, Japan). The resultant construct was named pT-*sll1252*^{del}. The Kanamycin resistance gene was amplified with the primers Kan2SalI-F: 5' TCG TCG ACC AAC CAT CAT CGA TGA ATT 3' and Kan2SalI-R: 5' TCG TCG ACA AAG CCG CCG TCC CGT CAA 3'. A SalI *site* (underlined) was created in Kan2SalI-F and Kan2SalI-R primers, during primer synthesis. SalI digested Kanamycin gene was cloned onto the BglII site of pT-*sll1252*^{del} construct by blunting and ligation. The final construct in which the *sll1252* ORF was replaced by the Kanamycin was transformed to wild-type cells of *Synechocystis*. Genomic DNA isolated from mutant cells was amplified by PCR with UF and DR primers to examine, the extent of replacement of the wild-type copy of the chromosome by the mutated copy of the chromosome.

Construction of *sll1252* N-terminal truncated mutant (Δ*sll1252*-N^{trn}):

A 500-bp upstream flanking region of *sll1252* ORF and a 327-bp *sll1252* downstream region of ORF covering S4-domain were amplified from the genomic DNA primer sets UF (5'GCA TCA ATT TGT TCT GTC AC 3') and *sll1252-trn*-UR (5'CGA GCA ACG GCA TTA GCT

AA 3'); *sll1252*-N^{trn}-F (5'**TAA TGC CGT TGC TCG ATG** GTG CGT ACT GTA 3') and *sll1252*-N^{trn}-*R* (5'CCC GGG TTA AAG ATA TCG GGT 3') respectively. A 15 bp 5' nucleotide sequence is an overlap of the *sll1252-trn-UR* primer followed by ATG were created during synthesis of *sll1252*-N^{trn}-*F* primer. The overlap and the start site are written in bold letters. A smaI site (underlined) was created in *sll1252*-N^{trn}-R primer. The PCR fragments amplified using UF & *sll1252-trn*-UR and *sll1252*-N^{trn}-F & *sll1252*-N^{trn}-R primer sets were used to setup a third fusion PCR with UF and *sll1252*-N^{trn}-R primer set. A second fusion PCR was performed using *sll1252*-N^{trn}-DF: 5' TAT CTT TAA CCC GGG CCA GTT TCA AGG CTT 3' and DR primer set. The fusion PCR amplified product thus generated was cloned onto T-Vector pMD19 (simple) cloning vector (Takara Inc. Kyoto, Japan). The resultant construct was named *sll1252*-N^{trn}. The Kanamycin resistant gene which was generated using the primers Kan2SalI-F and Kan2SalI-R as mentioned above was cloned onto the smaI site of *sll125*-N^{trn} construct by blunt end ligation. The final construct in which 456 first half of the *sll1252* open reading frame had been deleted transformed into wild-type cells of *Synechocystis*.

Construction of *sll1252* C-terminal truncated mutant (Δ*sll1252*-C^{trn}):

A 953-bp DNA fragment including 500-bp upstream flanking region and a 453-bp *sll1252* ORF and a 500-bp downstream flanking region of *sll1252* ORF were amplified from the genomic DNA primer sets UF (5'GCA TCA ATT TGT TCT GTC AC 3') and *sll1252-trn*-DR (5'CCC GGG TTA CTG GGT **TAA** ATG AAG ACT 3'); *sll1252-C^{trn}*-F (5'**TAA CCC AGT AAC CCG GG**C CAG TTT CAA GGC TT 3') and DR respectively. A 14 bp 5' nucleotide sequence is an overlap of the *sll1252-trn-DR* followed by stop codon, TAA were created during synthesis of *sll1252-C*^{trn}-*F* primer. The overlap and the start site are written in bold letters. A smaI site (underlined) was created in *sll1252*-trn-*DR* and *sll1252*-C^{trn}-*F* primers. The PCR fragments amplified using UF & *sll1252*-trn-DR and *sll1252*-C^{trn}-*F* & DR primer sets were used to setup a third fusion PCR with UF and DR primer set. The fusion PCR amplified product thus generated was cloned onto T-Vector pMD19 (simple) cloning vector (Takara-Bio). The resultant construct was named *sll1252*-C^{trn}. The Kanamycin resistant gene was cloned onto the smaI site of *sll1252*-C^{trn} construct by blunt end ligation as mentioned above. Thus, the final construct, in which 327-bp second half of the *sll1252* open reading frame had been deleted, was transformed to the wild-type cells of *Synechocystis*.

Transmission Electron Microscopy:

Cell suspensions of wild type, Δ*sll1252*-N^{trn} and Δ*sll1252*-C^{trn} were mixed with 1:1 volume of 1% glutaraldehyde in sodium cacodylate buffer (0.2 M, pH 7.2) and incubated for 2h at 4^{o}C. After incubation the cells were washed with cacodylate buffer, and fixed by incubating for 2h in 1% osmium tetroxide solution at 4^{o}C. After fixation, the buffer was washed and the cells were dehydrated. Dehydration was carried through increasing concentrations of ethanol: 50% ethanol for 1h, then followed by 75%, 90%, 95% and 99.5% ethanol for 30 min each. Later the cells were treated with equal volumes of 99.5% ethanol and propylene oxide two times for 10 min each , and then with 99.5% propylene oxide twice for 10 min each. AGAR Low viscosity resin (Product code: R1370, Agar Scientific Ltd. Stansted, England) was used to replace propylene oxide and the cells were treated with 1:1 mixture of propylene oxide and resin, and finally treated with the resin and allowed to polymerize for 12h at 70˚C. Ultramicrotome (EM-Ultracuts, Reichert, Germany) was used to cut thin sections (50-nm thickness). The sections were stained with 2% uranyl acetate and lead citrate and observed under a transmission electron microscope (H-7650, Hitachi, Tokyo, Japan) (150).

4. RESULTS

Functional characterization of Sll1252:

In the cyanobacterium *Synechocystis,* among 1624 hypothetical proteins, Sll1252 is one such hypothetical protein with calculated mass of 28.4 kDa. Computational domain prediction tools, indicated that Sll1252 has S4 domain (RNA binding domain) in the C-terminal half suggesting it as a, probable RNA binding protein. There are several S4-like RNA binding domain proteins identified in various organisms, however physiological function of S4-domain is yet to be elucidated. Sll1252 was also reported to be associated with PSII (53). Therefore, in this study we generated a mutant of the *sll1252* gene by insertional inactivation and subsequently characterized the mutant (Δ*sll1252*$^{\text{ins}}$) to assess its role in PSII structure and function.

Sll1252 is a conserved hypothetical protein:

In *Synechocystis,* the ORF of *sll1252* encodes a hypothetical protein (92). Figure 4.1 shows the alignment of top 10 Blast P hits of Sll1252 protein. Orthologs of the protein were detected in chloroplasts of *A.thaliana* (At1g53120) and *O.sativa* (Os01g0747700) (105). This protein is assumed to have important physiological function, since it is conserved in cyanobacteria, and also in higher plants. Hence this protein is presumed to play a crucial role in the process of photosynthesis. Kashino *et al.,* suggested that it is required for balancing energy levels in PET in *Synechocystis.*

Figure 4.1: *In silico* analysis of the Sll1252 protein

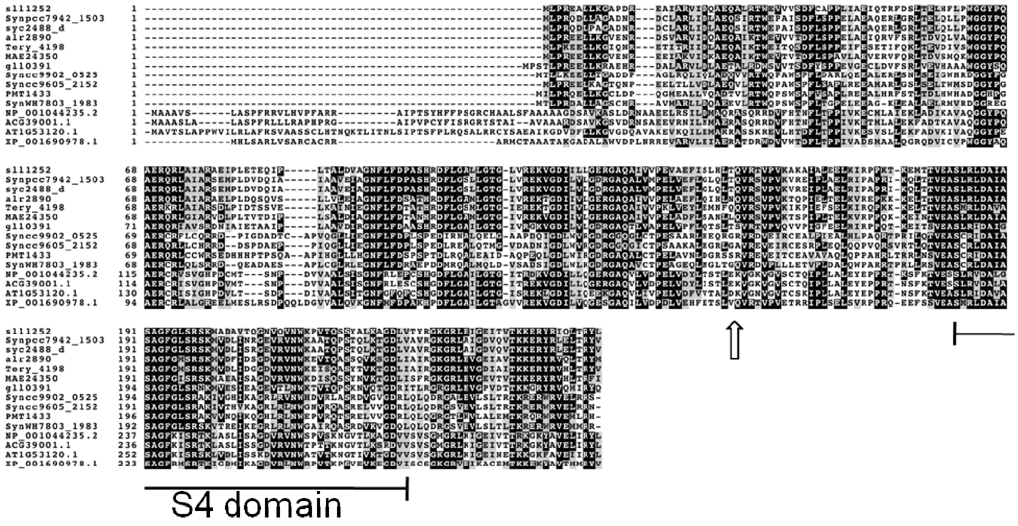

Figure 4.1: Multiple sequence alignment of the Sll1252 from *Synechocystis* and its homologues proteins encoded in other cyanobacterial genomes and higher plants. The sequences were aligned by Clustal W algorithm. Identical amino acids are shown in black and conservatively exchanged amino acids are in gray. *NP_001044235.2, Orizae sativa; ACG39001.1, Zea mays; AT1G53120.1, Arabidopsis thaliana; XP_001690978.1, Chlamydomonas reinhardtii; Synpcc7942_1503, Synechococcus elongates PCC7942; syc2488_d, Synechococcus elongates PCC6301; alr2890, Anabaena sp.PCC7120; Tery_4198, Trichodesmium erythraeum IMS101; MAE24350, Microcystis aeruginosa NIES-843; sll1252, Synechocystis sp. PCC6803; gll0391, Gloeobacter violaceus PCC7421; Syncc9902_0525, Synechococcus sp. CC9902; Syncc9605_2152, Synechococcus sp. CC9605; PMT1433, Prochlorococcus marinus MIT9313; SynWH7803_1983, Synechococcus sp. WH 7803*. S4-domain is indicated by a horizontal line. The insertion site of kanamycin gene in the Δ*sll1252*^{ins} is indicated with an open arrow.

Mutagenesis of *sll1252* in *Synechocystis*:

To elucidate the function of Sll1252, the *sll1252* gene was disrupted by inserting kanamycin-resistance gene using *in vitro* transposon mutagenesis. The kanamycin gene was inserted within the *sll1252* open reading frame as shown in the schematic representation of construct made for generating Δ*sll1252*^{ins} (Figure 4.2A). As *Synechocystis* contains multiple copies of the identical genomes, a mutant without functional *Sll1252* can be obtained only after replacement of all copies of the *sll1252* gene by the inactivated version of *sll1252.* After culturing the mutant cells for, several rounds in the presence of increasing concentrations of kanamycin, the extent of replacement of wild-type copies of *sll1252*, (complete segregation) in the Δ*sll1252*, was analyzed by PCR amplification. In this mutant, all copies of the *sll1252* gene were replaced by the disrupted copies of *sll1252* genes as confirmed by the fact that when genomic DNA of wild-type cells was used as a template with specific primers (*sll1252*-FP and *sll1252*-RP), a PCR product of 957 bp corresponding to the *sll1252* ORF and its upstream and downstream flanking regions was amplified (Figure 4.2B). In contrast, when the genomic DNA of *sll1252* cells was used as the template with the same set of primers, a 2157 bp DNA fragment corresponding to the wild-type fragment (957 bp) plus the inserted kanamycin gene (1200 bp) was amplified (Figure 2B). These observations suggest that the *sll1252* ORF's in all genomes were completely disrupted by kanamycin gene in *Synechocystis.*

Figure 4.2: Mutation of *sll1252* and PCR based confirmation of mutation

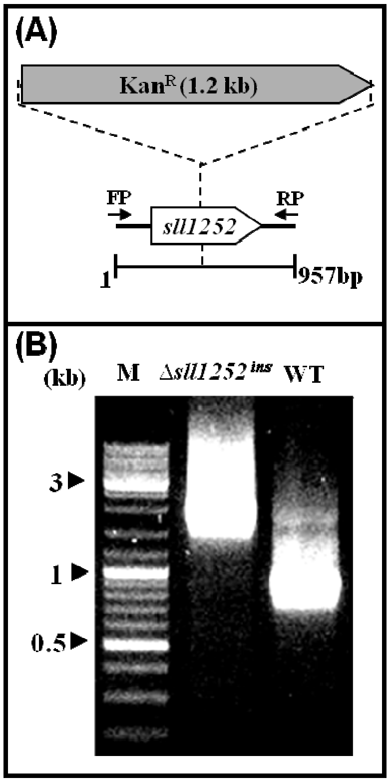

+-

Figure 4.2: Strategy for disruption of *sll1252* gene in the genome of *Synechocystis*. The wild-type copy of the *sll1252* gene was completely replaced by the mutated copy of the gene in Δ*sll1252*$^{\text{ins}}$ mutant cells. A 957 bp DNA fragment representing *sll1252* gene was insertionally inactivated with a kanamycin resistance cassette (1200bp). (A). Schematic representation of the genotype of the Δ*sll1252*$^{\text{ins}}$ mutant. The sll1252 gene and the Kan^{R} cassette are shown in the open and filled arrows respectively. Thick arrows indicate sll1252 -F (FP) and sll1252-R (RP), the two primers that were used for PCR amplification of the wild-type copy of the sll1252 gene and that of the Kan ^{R} cassette. (B). Genomic PCR analysis with the primers indicated in the construct map. M represents 1-kb DNA ladder. WT, PCR product with wild-type DNA as template; Δ*sll1252*$^{\text{ins}}$, PCR product with Δ*sll1252*$^{\text{ins}}$ DNA as template.

Insertional inactivation of *sll1252* influences growth at 70 *μmol photons* $m^{-2}s^{-1}$ light:

In order to analyze whether the disruption of *sll1252* would influence the physiological activities of *Synechocystis* cells, we compared wild type and Δ*sll1252*^{ins} growth profile at optimal growth conditions (70 μmol photons m^{-2} s^{-1}, 1.5% CO_2 in air and 34°C (Figure. 4.3A). As shown in figure 4.3A, growth of Δ*sll1252*^{ins} culture was much slower than that of WT culture. Insertional inactivation and slow growth phenotype of Δ*sll1252*^{ins} demonstrated that Sll1252 plays a key role in the physiology of *Synechocystis* cells. Since Sll1252 seems to be associated with PSII, it is likely that the mutation in *sll1252* might have influenced the photosynthetic efficiency and, thereby, resulted in the phenotype of slow growth. Hence, we observed the growth of wild type and Δ*sll1252*^{ins} strains at low light (5 μmol photons m^{-2} s^{-1}, 1.5% CO_2 in air and 34°C), under photo-heterotrophic and mixotrophic conditions (Figure 4.3B). As can be seen in Figure 4.3B, Δ*sll1252*^{ins} mutant exhibited growth only when it was grown at 5 μmol photons m^{-2} s^{-1} light. In the presence of 5 mM glucose (photo-heterotrophic and mixotrophic conditions), growth was not observed in Δ*sll1252*^{ins} culture. Collectively, growth analysis of Δ*sll1252*^{ins} clearly suggests that the insertional inactivation of *sll1252* leads to a light sensitive and glucose sensitive phenotype. This suggests that the presence of *Sll1252* may be essential for the cell when respiratory or photosynthetic electron transport is more active.

Figure 4.3: Growth profile of WT *Synechocystis* cells and Δ*sll1252*^{ins} mutant

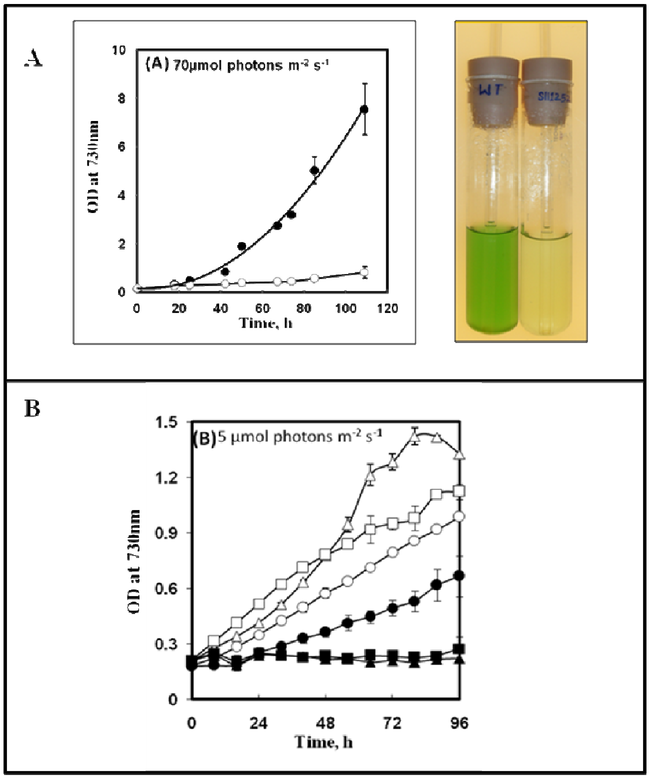

Figure 4.3: Growth profile of WT *Synechocystis* cells and Δ*sll1252*^{ins} mutant. (A). Effect of light intensity on the photoautotrophic growth of WT cells (open circles) and Δ*sll1252*^{ins} cells (closed circles) under 70 µmol photons m^{-2} s^{-1} and (B) at 5 µmol photons m^{-2} s^{-1}. In panel B, photo-heterotrophic growth in the presence of 5mM glucose and 10 µM of DCMU of wild type (open triangle) and Δ*sll1252*^{ins} (closed triangle). Growth under mixotrophic conditions (5 mM glucose and 5µmol photons m^{-2} s^{-1}), of WT (Open squares) and Δ*sll1252*^{ins} (closed squares). Standard deviations are shown in vertical bars. h, hours.

Insertional inactivation of *sll1252* alters the rate of WCE and the effect is beyond PSII:

The rate of PSII and WCE was measured in the WT and Δ*sll1252*^{ins} to elucidate the effect of mutation on photosynthesis. The WCE rate of the Δ*sll1252*^{ins} mutant cells was found to be reduced by about 40% in comparision with the WT cells, when measured with $NaHCO_3$ as the final electron acceptor. To test whether this effect was caused by a decreased PSII content, oxygen evolution of PSII was measured with PBQ as electron acceptor, but there was no reduction of oxygen evolution in mutant strain (Figure 4.4) suggesting Sll1252 may not be required for the structural and functional integrity of PSII.

Figure 4.4: Measurement of PSII and WCE activity of wild type and Δ*sll1252*^{ins}

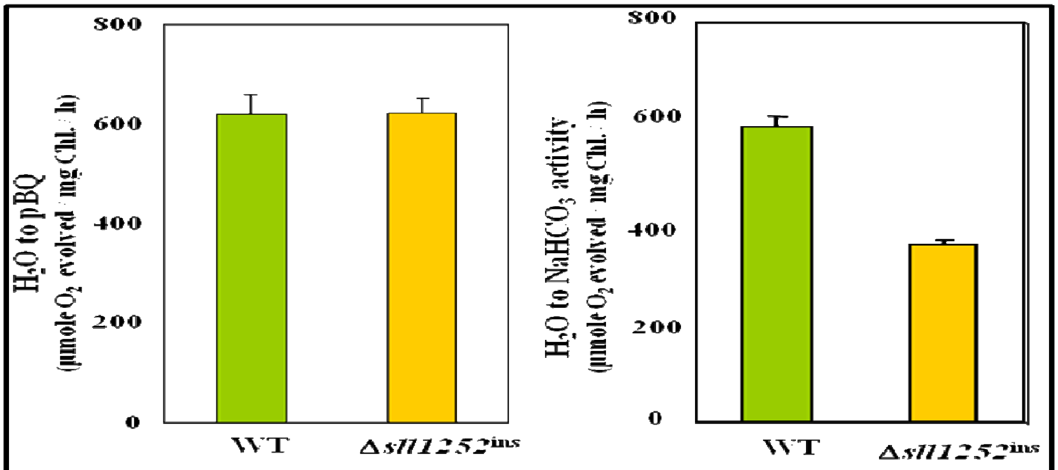

	PSII activity (Water to pBQ)	WCE transport activity (Water to $NaHCO_3$)
Wild type	618.5±40	519.3±17
Δ*sll1252*^{ins}	622±28	310±10

Figure 4.4: Comparison of PSII activity and WCE activities of wild type and Δ*sll1252*^{ins} mutant strains. PSII and WCE activities of wild type and Δ*sll1252* mutant strains grown at 34°C, aerated with 1.5 % CO_2 and 70 μmol photon $m^{-2}s^{-1}$. Rate of PET and WCE was measured in terms of μmol oxygen evolution / mg Chl / h. Mean values ±SE were calculated from three independent experiments.

Mutation in *sll1252* and addition of DBMIB induced similar effects on the global expression of genes:

Since the Δ*sll1252*^{ins} exhibited slow growth phenotype under optimal light conditions (70 µmol photons m^{-2} s^{-1}), and as this protein seems to be essentially required when the cell remains photosynthetically active, lead us to infer its role in electron transport chain. In order to identify the probable site of its action in the linear electron transport, we performed DNA microarrays of this mutant with low, (5 µmol photons m^{-2} s^{-1}) and optimal light (70 µmol photons m^{-2} s^{-1}) conditions.

Since the photosynthetic transfer of electrons and/or the redox status of electron-transport components are supposed to be a primary signal for the expression of a set of genes, we examined the effect of *sll1252* insertional inactivation on the genome-wide expression of genes with Δ*sll1252*$^{\text{ins}}$ cells that were grown under low 5 µmol photons m^{-2} s^{-1} (Fig 4.5A). Our previous studies of the expression of genes with DNA microarrays have suggested that the genes with expression ratios above 2.0 are distinctly induced and those below 0.5 are distinctly down-regulated due to mutation of a gene or upon changes in environmental conditions. Microarray analysis results in the present study proved that the mutation in Δ*sll1252*$^{\text{ins}}$ cells had no effect on the genome-wide expression of genes when the cells were grown in light at 5 µmol photons m^{-2} s^{-1} (Figure 4.5A). We examined the effect of mutation in Δ*sll1252*$^{\text{ins}}$ cells that had been grown in light at 70 µmol photons m^{-2} s^{-1} on the genome-wide expression of genes with comparison to that in WT cells that had been grown under the same conditions. We observed that expression of 37 genes were up-regulated with >2.5 times in the Δ*sll1252*$^{\text{ins}}$ cells (Figure 4.5B). Genes that were upregulated due to Δ*sll1252*$^{\text{ins}}$ are listed in Table 4.1.

Figure 4.5 Genome wide expression of genes due to mutation in *sll1252* gene

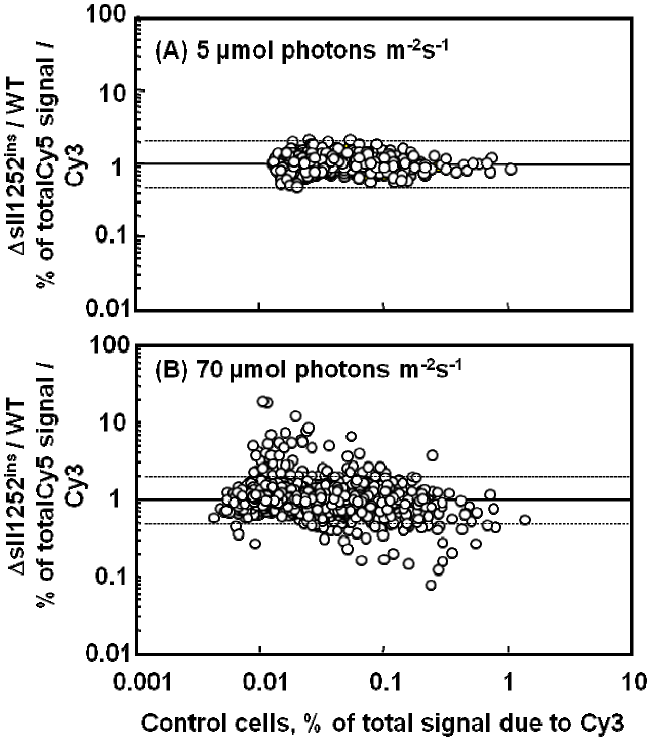

Figure 4.5: DNA microarray analysis to compare the gene expression in Δ*sll1252*$^{\text{ins}}$ mutant cells with that in WT cells, both grown for 48 h, at 5 µmol photons m^{-2} s^{-1} (A) and at 70 µmol photons m^{-2} s^{-1} (B). RNA extracted from WT and the mutant cells were used for synthesis of Cy3- and Cy-5 labeled cDNAs, respectively. In (A) Cy5 / Cy3 ratio of almost all the genes was between 2 and 0.5 (indicated by dashed lines), suggesting that the mutation in *sll1252* gene had no effect on gene expression when both types of cells were grown at 5 µmol photons m^{-2} s^{-1} light. In (B) Cy5 / Cy3 ratio of several genes altered due to the growth of Δ*sll1252*^{ins} at 70 µmol photons m^{-2} s^{-1}, suggesting that the mutation in *sll1252* affects the gene expression at 70 µmol photons m^{-2} s^{-1} light. Similar results were obtained in two independent experiments, and the figure shows the result of one of these experiments.

Sll1252 assists electron transfer between PQ pool and Cyt b$_6$/f complex

The profile of gene expression in Δ*sll1252*$^{\text{ins}}$ cells was compared with that of wild-type cells upon treatment with inhibitors of electron transport, such as DBMIB or DCMU (149). Interestingly 22 out of 37 up-regulated genes by Δ*sll1252*$^{\text{ins}}$ were reported to be induced by inhibition of cells with DBMIB in wild-type. But, none of the genes upregulated due to mutation in Δ*sll1252*^{ins}, was exclusively induced by DCMU inhibition (Table 4.1) 7 out of 37 genes induced by Δ*sll1252*, at 70 µmol photons m^{-2} s^{-1} were commonly up-regulated due to the inhibition of wild-type cells with DCMU and DBMIB. As 60% of the genes upregulated by Δ*sll1252*^{ins} were inducible due to inhibitory action of DBMIB and none of them were inducible by DCMU inhibitory effect, it is quite likely that the effect of lack of functional Sll1252 protein (due to mutation in Δ*sll1252*^{ins}) is similar to the effect caused due to inhibition by DBMIB on global gene expression profile (Figure 4.6). This may indicate that Sll1252 functions to sustain the electron transfer from reduced PQ pool to Cyt b_6/f complex. With this probable function, as a protein component being required for regulation of election transfer between PQ pool to Cyt b_6/f complex, we analyzed relative sensitivity of inhibition by DCMU on Q_A to Q_B site of election transfer and sensitivity to DBMIB on PQH_2 to Cyt b_6/f electron transfer site between WT and Δ*sll1252*^{ins} mutant cells to establish the involvement of *Sll1252* in the regulation of electron transport.

Table 4.1: Effect of *sll1252* mutation on genome-wide expression of genes

ORF and description	(Δ*sll1252*^{ins} / WT) Fold increase in expression in Δ*sll1252*^{ins}		Effect of inhibitor on expression^{a}	
	5 µmol/ m^{-2} s^{-1}	**70 µmol/ m^{-2} s^{-1}**	**DBMIB**	**DCMU**
sll0330, Sepiapterine reductase	1.3 ± 0.4	18.7 ± 5.5		
slr1544	1.1 ± 0.1	17.8 ± 1.7	I	
slr1704	1.3 ± 0.1	11.9 ± 0.2		
slr1674	1.1 ± 0.1	8.3 ± 0.6	I	
sll0528	1.1 ± 0.1	7.6 ± 0.2	I	
sll1483, Periplasmic protein	1.1 ± 0.0	7.2 ± 0.7	I	I
sll1652	1.2 ± 0.1	6.6 ± 3.6		
sll0306, *sigB, rpoD,* RNA polymerase group 2 sigma factor	1.5 ± 0.1	6.5 ± 0.4	I	
sll1862	1.2 ± 0.1	5.8 ± 0.8		
sll1515, *gifB,* glutamine synthetase inactivating factor IF17	1.2 ± 0.1	5.6 ± 1.0	I	I
sll1653 menG, probable phylloquinone biosynthesis methyl transferase	0.9 ± 0.1	5.5 ± 0.9		

sll1514, *hspA*, *hsp1,* 16.6 kDa small heat shock protein	1.1 ± 0.1	5.5 ± 1.3	I	
ssr2194	1.1 ± 0.1	5.2 ± 0.1		
slr1516, *sodB*, superoxide dismutase	0.8 ± 0.1	4.9 ± 0.4		
sll1236	1.0 ± 0.1	4.9 ± 0.0		
slr1738	1.1 ± 0.1	4.7 ± 0.2	I	
slr0581	1.0 ± 0.1	4.5 ± 0.5	I	I
ssr2016	1.1 ± 0.0	4.1 ± 0.2		
slr2075, *groES, 10 kDa chaperonin, GroES* protein	0.7 ± 0.0	3.9 ± 0.5	I	
ssr2595, *hilB, scpD,* high light inducible protein	1.1 ± 0.1	3.9 ± 0.2	I	I
sll1598, *mntC,* ABC-type manganese transport system substrate binding protein	1.1 ± 0.2	3.7 ± 0.8		
slr1675, *hypA1*, putative hydrogenase expression/formation protein HypA1	0.7 ± 0.1	3.7 ± 0.5	I	
slr2076, *groEL1, cpn60,* 60 kDa chaperonin 1, GroEL1, molecular chaperone	0.9 ± 0.0	3.7 ± 0.1	I	R
slr0967	0.8 ± 0.2	3.6 ± 0.4	I	I

ssl3044, hydorgenase component	1.0 ± 0.1	3.5 ± 0.4		
sl0416, *groEL2, cpn60,* 60 kDa chaperonin 2, *GroEL2,*	1.1 ± 0.0	3.5 ± 1.1		R
sll0846	1.0 ± 0.0	3.2 ± 0.3	I	
sll1863	1.0 ± 0.1	3.2 ± 1.3		
slr0093, *dnaJ, DnaJ* protein, heat shock protein 40, molecular chaperone	1.1 ± 0.0	3.1 ± 0.2	I	
ssl1911, *gifA*, glutamine synthetase inactivating factor IF7	1.3 ± 0.1	2.9 ± 0.5	I	I
slr1687	1.1 ± 0.2	2.8 ± 0.1	I	I
sll1620	1.2 ± 0.0	2.8 ± 0.6	I	
slr1204, *htrA,* serine protease Htra	1.1 ± 0.2	2.8 ± 1.2		
sll1621, membrane protein	0.8 ± 0.1	2.7 ± 0.4	I	
slr1963, water soluble carotenoid protein	1.1 ± 0.1	2.6 ± 0.8	I	R
ssl3364, *cp12*	1.3 ± 0.0	2.6 ± 0.7		
ssl2542, *hliA, scpC,* Highlight inducible protein	0.8 ± 0.1	2.6 ± 0.5	I	

Table 4.1 Genes whose expression was significantly affected due to the mutation in $\Delta sll1252^{ins}$: WT and $\Delta sll1252^{ins}$ cells were grown at 34 ^{o}C for 48 h, 70µmol photons m^{-2} s^{-1} light or grown at 5 µmol photons m^{-2} s^{-1}. Each value indicates the ratio of levels of the mRNA from $\Delta sll1252^{ins}$ cells to those from wild-type cells. The values shown are the means ± range of two independent experiments. The numbering of ORFs corresponds to that of Kaneko *et al.,* (1996).[a] DBMIB, effect of DBMIB and DCMU, on the expression of genes according to (149).

Figure4.6: Venn diagram showing the common genes induced by *sll1252* mutation, DCMU and DBMIB.

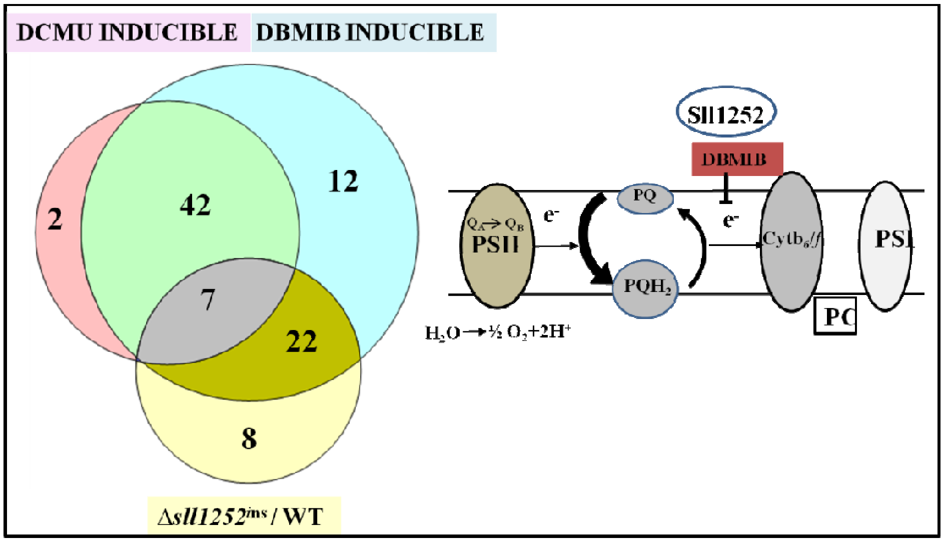

Figure 4.6: **Common genes induced by *sll1252* mutation, DCMU and DBMIB inhibitors**. Same set of genes were up regulated due to mutation in *sll1252* and due to DBMIB inhibition of electron transport. Site of action of Sll1252 and DBMIB is similar i.e, between PQ pool to Cyt b$_6$/f complex.

Δ*sll1252*^{ins} mutant cells were more sensitive to inhibition by DBMIB than WT cells

Reduced rate of WCE activity together with DNA microarray gene expression profiling, suggest that the *Sll1252* is required to transfer electrons from PQ pool to Cyt b$_6$/*f* complex. Differential degree of sensitivity to specific inhibitors, DCMU and DBMIB, by WT and Δ*sll1252*^{ins} mutant cells was examined by measuring PET rates in the presence of various concentrations of inhibitors (Figure 4.7). DCMU inhibits electron flow at the acceptor side of PSII (151). The oxygen-evolving activity under the rate-saturating irradiance showed a gradual decrease in PSII activity with increase in concentration of DCMU in both the WT and Δ*sll1252*^{ins} mutant cells with PPBQ as the electron acceptor. Figure 4.7A shows that the ratio of uninhibited (V$_0$) / inhibited (V$_i$) PPBQ-mediated PSII activities *versus* DCMU concentration. DCMU required for 50% inhibition of the original activity was about the same (80 nM) in WT and Δ*sll1252*$^{\text{ins}}$ mutant cells. These results suggested that mutation in *sll1252* had no effect on the site of DCMU action and confirms that the *Sll1252* does not involve in the PSII catalyzed electron transport activity**.**

We analyzed the effect of various concentrations of DBMIB on WCE activity in the WT and *Δsll1252*^{ins} mutant cells. The pattern of inhibition was similar to that induced by DCMU. However, the inhibitor required for 50% inhibition of the WCE activity was 140 nM and 300 nM in the wild type and Δ*sll1252*^{ins} mutant cells respectively (Figure 4.7B). This suggests that the Δ*sll1252*^{ins} cells are more sensitive to DBMIB, and points the site of action of Sll1252.

Figure 4.7: Measurement of PET rates with DCMU and DBMIB

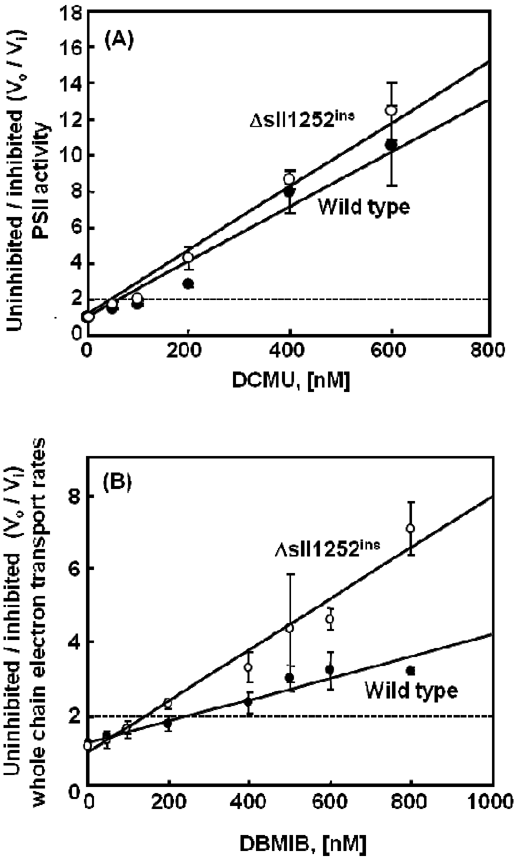

Figure 4.7: Effect of varying concentrations of DCMU (A) and DBMIB (B) on PSII and WCE activity. Rates of uninhibited / inhibited (Vo/Vi) activities plotted as a function of DCMU (A) and DBMIB (B) concentrations. Three independent experiments were performed and the data are represented as means ± SD. WT cells (filled circles) and Δ*sll1252*^{ins} cells (open circles). Standard deviations are shown as vertical bars.

Enhancement in the reduced PQ pool as a result of reduced electron transfer from PQ pool to Cyt b_6/f complex

In support of the experiments demonstrating the site of action of Sll1252, mutation in *sll1252* impairs electron transfer from reduced PQ pool to Cyt b_6/*f* complex. Consequence of this impaired rate of electron transfer would lead to the relatively higher level of plastoquinones in reduced state in Δ*sll1252*^{ins} cells grown at 70 μmol photons $m^{-2}s^{-1}$, when compared to WT cells that had been grown in light at the same intensity. Hence, the rate of PQ reduction was estimated. As shown in (Figure 4.8) enhancement in the rate of PQ pool reduction was observed in Δ*sll1252*^{ins} mutant, when compared to WT cells that had been grown in light at 70 μmol photons m^{-2} s^{-1}. Relatively, about 4 fold increase in the PQ reduction rate was observed in Δ*sll1252*^{ins} compared to WT *Synechocystis* cells. In WT cells, inhibition of electron transport by DBMIB also resulted in enhanced rate of PQ reduction.

Figure 4.8: Rate of reduction of PQ pool in wild type, *sll1252* mutant and wild type+DBMIB

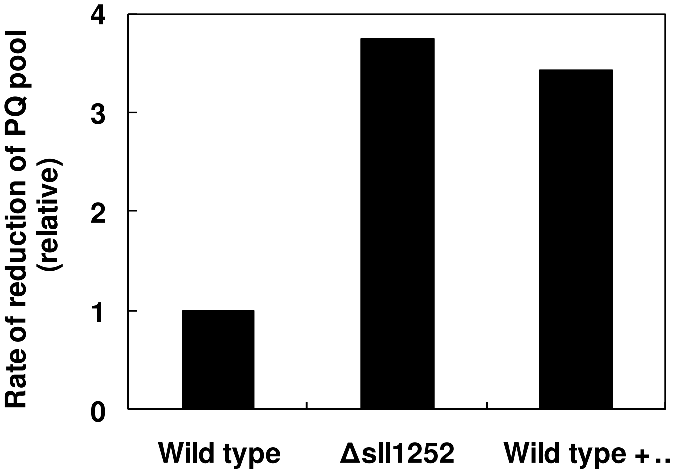

Figure 4.8: **Rate of reduction of the PQ pool was monitored in the DBMIB treated and untreated wild type cells and Δ*sll1252*^{ins} mutant cells.** The rate of reduced plastoquinones were monitored spectroscopically by measuring OD at 260 nm. Cells were incubated for one minute in dark and then exposed to actinic light (600 nm) continuously for 1 minute. During the dark and light incubation OD at 260 nm was monitored.

Complementation of the mutation in Δ*sll1252*^{ins} cells

Δ*sll1252*^{ins} cells showed slow growth phenotype at optimal light conditions (70 μE photons m^{-2} s^{-1}) compared to the wild type cells. Therefore to check whether the phenotype observed was due to mutation or not, we have complemented Δ*sll1252*^{ins} cells. An extra copy of the *sll1252* gene was expressed in Δ*sll1252*^{ins} cells using a cyanobacterial expression vector pVZ321. DNA region 149 bp covering *sll1252* gene and its upstream sequence was PCR amplified (Figure. 4.9A) and cloned into pVZ321 vector at ClaI and XhoI sites (Figure. 4.9B) and transformed to *E.coli* DH5α. pVZ321 vector, and the colonies were screened by colony PCR, a 1349bp DNA fragment representing *sll1252* gene was amplified in lanes 3,4,7, (Figure. 4.9C). The positive construct was transformed to *Synechocystis* by triparental mating (186) and screened under kanamycin and chloromphenicol antibiotic selection pressure. So formed strain was named as *sll1252*+.

Figure 4.9: Complementation of Δ*sll1252*^{ins} and PCR based confirmation of cloning

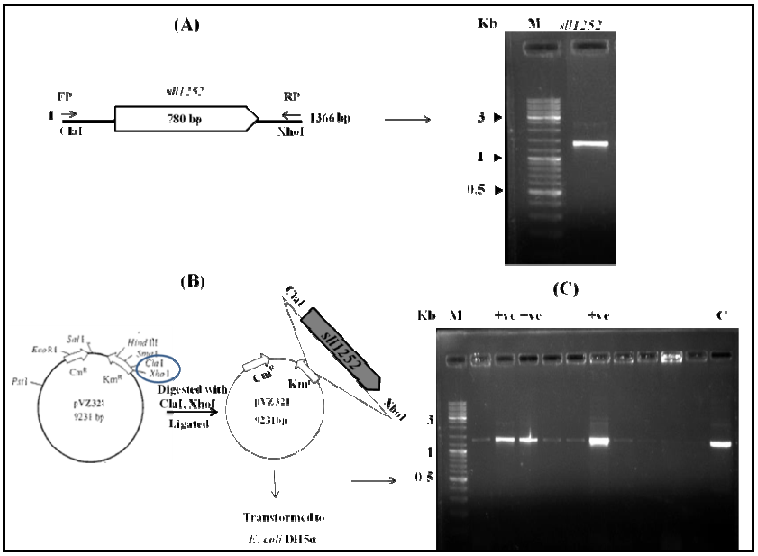

Figure 4.9: Strategy for complementation of *sll1252* gene in Δ*sll1252*^{ins} cells. (A) A 1349 bp DNA fragment representing *sll1252* gene was amplified with wild type DNA as template. Thick arrows indicate *sll1252-F* (FP) and *sll1252-R* (RP) primers used for PCR amplification of the wild-type copy of the *sll1252* gene. M represents 1-kb DNA ladder (B) Schematic representation of cloning of *sll1252* gene in pVZ321vector. The *sll1252* gene is shown in light gray arrows. (C) Colony PCR - A 1349 bp DNA fragment representing *sll1252* gene was amplified in 3rd 4th and 7th lane, C represents control *sll1252* DNA, M represents 1-kb DNA ladder.

sll1252$^+$ Complement grows similar to wild type :

Growth profile of wild type, *Δsll1252* and *sll1252*$^+$ were compared at optimal growth conditions, growth of *sll1252*$^+$ cells was similar to the growth of wild type cells (Figure 4.10) which confirms that the phenotype observed by Δ*sll1252*^{ins} cells was due to the effect of mutation of *sll1252* gene in wild type. Growth of the cultures at 34°C and 70 μmol photons/m^2/s was measured as the cell density in terms of OD at 730nm.

Figure 4.10: Growth profile of WT, Δ*sll1252*^{ins}, and *sll1252*$^+$

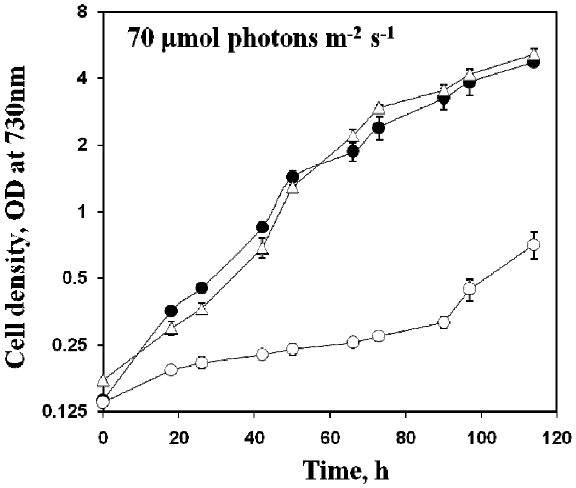

Figure 4.10: Growth profiles wild type (-●-), *sll1252*$^+$(-Δ-) and Δ*sll1252*^{ins} mutant cells(○-) *Synechocystis* cells at optimal growth temperature (34°C). Similar results were obtained in three independent experiments, and the data are represented as means ± S.D.

Over expression and purification of Sll1252

To study the biochemical properties of purified protein, Sll1252 was over expressed using pET28a(+) in *E. coli* BL-21 (DE3) pLysS. 780bp fragment corresponding to the ORF *sll1252* was amplified, from the genomic DNA as template (Figure 4.11A) and ligated into the pET28a vector (5.3Kb) Figure 4.11B) and transformed to *E.coli* BL21 cells to generate pET-Sll1252 plasmid, restriction digestion of pET28a isolated from BL21 with BamH1 resulted in approx 6Kb band (Figure 4.11C) which confirmed the presence of *sll1252* gene (780bp) in pET (5.3Kb). The expression of the protein was monitored by SDS PAGE. Protein expression was induced with 0.4 mM IPTG and the expressed protein was purified using Ni-NTA column by His-affinity chromatography. Whereas, purified (N-terminal His tag) His-Sll1252 protein elutes exhibited ~3-4 kDa larger size (32 kDa) due to his tag than expected (28kDa) which corresponds to expected size on SDS-PAGE (15%) (Figure 4.12).

Figure 4.11: PCR based amplification of *sll1252* gene and confirmation of cloned gene in Pet28(+) vector

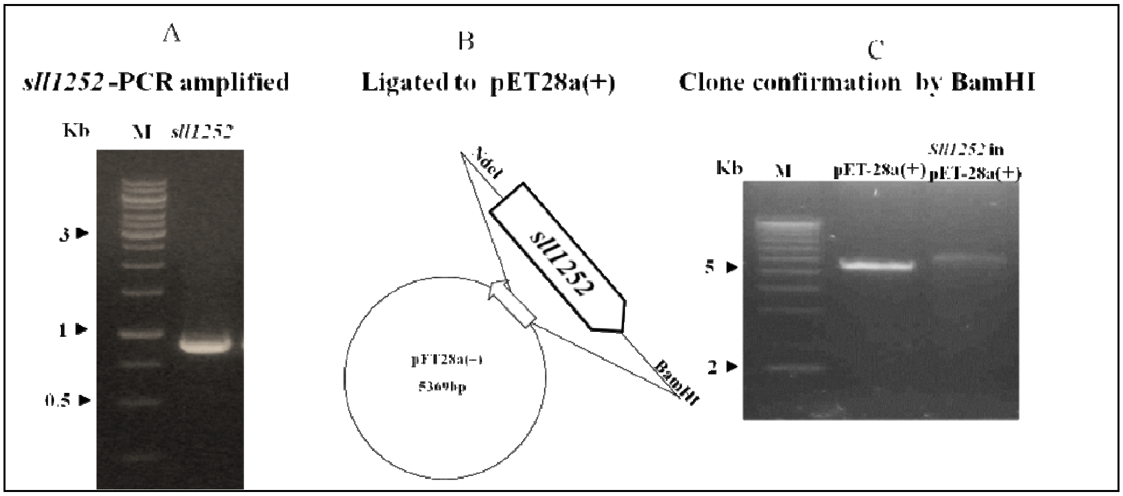

Figure 4.11: PCR amplification and cloning of *sll1252* gene in pET28a. (A). *sll1252* PCR amplified product, lane 1-M represents 1-kb marker, lane 2, A 780 bp DNA fragment representing *sll1252* gene with wild type DNA as template. (B). Schematic representation of cloning of *sll1252* gene in pET28a(+) vector. The *sll1252* gene is shown in open arrow. (C). Clone confirmation by digestion of the vector with BamHI. Lane 1-M represents 1-kb Marker, lane 2-pET vector, band observed at 5 kb, lane-3 recombinant pET vector containing *sll1252* gene, band size observed was 5780bp which corresponds to gene (780bp) + pET vector (5kb).

Fig 4.12: SDS PAGE analysis of over expressed and purified Sll1252 protein

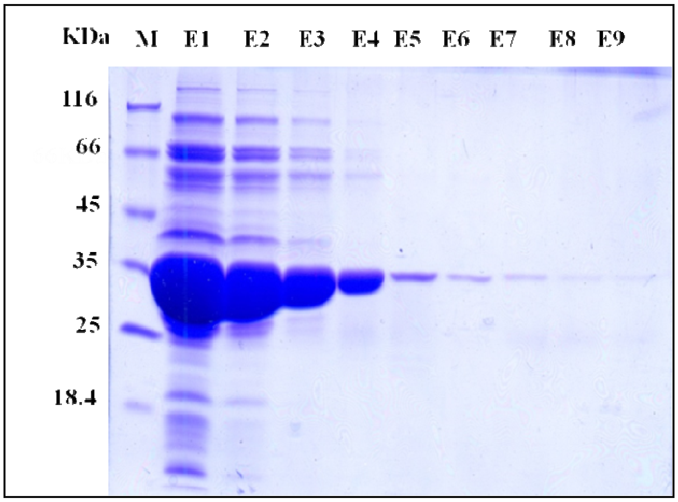

Figure 4.12: Purification of Sll1252 using Ni-NTA from sll1252 expressing *E. coli***.** Ni-NTA purified protein elutes of His-Sll1252 resolved on 15%SDS-PAGE. M-marker, E1 to E9- Elutes, KDa-kilodaltons.

Sll1252 is a soluble protein

As the Sll1252 protein was reported to be associated with PSII by kashino *et al.,* we wanted to localize the protein by western blotting analysis. Western blotting analysis was carried out using anti-Sll1252 polyclonal antibody raised against purified His-Sll1252 in Rabbit. Figure 4.13, shows the immuno-detection of Sll1252 in the soluble fractions and insoluble fractions of WT and *sll1252*$^+$ and Δ*sll1252*^{ins} mutant cells. The anti-Sll1252 antibody detected Sll1252 in the soluble fraction of only wild type cells and *sll1252*$^+$. Sll1252 protein was not detected in the insoluble/membrane fraction of the cells (Figure 4.13). Thus, it is clear that the Sll1252 is a soluble protein and was absent in the insoluble membrane fraction (Figure 4.13). This also confirms that the Sll1252 is not associated with PSII. Sll1252 protein was detected neither in the soluble nor insoluble fractions of Δ*sll1252*^{ins}, suggesting absence of Sll1252 functional protein in the mutant and its complete inactivation. Detection of Sll1252 in cultures grown in optimal conditions confirms that it is a constitutively expressing protein.

Figure 4.13: Localization of the Sll1252 protein by western blotting analysis

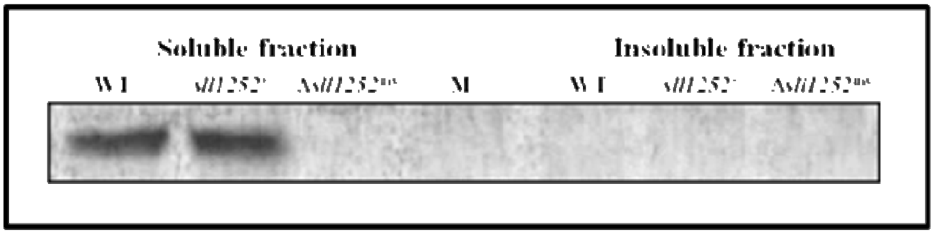

Figure 4.13: Immuno detection of Sll1252 protein in the soluble (S) and insoluble. membrane (I) fractions extracted from wild type, Δ*sll1252*^{ins} and *sll1252*$^{+}$ *Synechocystis* cells; Sll1252 was detected by anti-Sll1252 antibody. WT- wild type, M–marker, *sll1252*$^{+}$ - complement.

Suppression of insertionally inactivated Δsll1252^{ins} mutation effect (Δ*sll1252*^{ins} Rev):

In the BG-11 agar plates, we observed some colonies which were relatively growing faster than the Δ*sll1252*^{ins} with different colony morphology. Hence we cross-checked these colonies by PCR amplification and DNA sequencing to locate the presence of the kanamycin gene, inserted in the *sll1252* gene of these colonies. To our surprise, we have identified presence of another naturally occurring cyanobacterial transposable element (ISY523) along with the kanamycin gene used for inactivation of *sll1252* gene, at the insertion site (Figure. 4.14A). It is interesting to note that *Synechocystis* cells used a natural transposable element for suppressing the mutations if they are lethal to the cells. The mechanism by which

Synechocystis cells place the transposon (ISY523) at insertion site to suppress the mutation is yet to be elucidated. It may be also interesting to study, whether the placement of the transposon, by *Synechocystis* cells for suppressing lethal effect of mutation, is by selective insertion or random transposition.

Deletional and truncational mutants of *sll1252* (Δ*sll1252*^{del}, Δ*sll1252*N^{trn} and Δ*sll1252*C^{trn}):

Kashino et al., reported that no significant growth phenotype, when *sll1252* ORF was completely deleted in *Synechocystis* cells (54). Hence we generated a deletion mutant of *sll1252*. figure 4.14B corresponds to a 1780 bp DNA fragment representing *sll1252* gene replaced with a kanamycin resistance cassette (1200 bp). We performed growth analysis of the deletional mutant and observed that the deletional mutant Δ*sll1252*^{del} did not show any phenotype change. The mean generation time calculated for this mutant is 9.8 with no effect on PSII and whole chain electron transport activities (Table 4.2). However, we observed that the insertionally inactivated Δ*sll1252*^{ins} mutant exhibited a severe slow growth phenotype. As the Δ*sll1252*^{ins} exhibited a slow growth phenotype and inhibition of electron transfer between PQ pool to Cyt b_6/f complex, but not the deletional mutant, Δ*sll1252*^{del} we further characterized the functional roles of N-terminal and C-terminal halves of the *sll1252* by generating truncated mutants, for selective expression of them in *Synechocystis*. We assumed that in the Δ*sll1252*^{ins}, the insertion of kanamycin gene cassette might have resulted in expression of either N-terminal or C-terminal half of the *sll1252* ORF (sll1252-N or sll1252-C), leading to the severe slow growth phenotype. The natural transposon has been placed by *Synechocystis* cells, between the kanamycin and C-terminal half of the *sll1252,* perhaps to inhibit the expression of either sll1252-N or sll1252-C, thereby suppressing the mutation effect. If this assumption is correct then the expression of sll1252-N or sll1252-C may be lethal to the cells. In order to examine whether expression of only C-terminal half of *sll1252* is lethal to the cells, we generated two truncated mutants. We made the truncational mutants in such a way that only N-terminal half consisting of 453 bp from start of *sll1252* ORF (in Δ*sll1252*-N^{trn}) and only C-terminal upstream covering 454 bp onwards to end of *sll1252* ORF (Δ*sll1252*-C^{trn}) has been expressing in Δsll1252N^{trn} and Δ*sll1252*C^{trn} respectively. (Figure 4.14 C, D). The constructs thus generated were transformed to wild type *Synechocystis* cells. The extent of replacement of wild-type copies of *sll1252*, thereby complete segregation of the Δ*sll1252*-N^{trn} and Δ*sll1252*-C^{trn}, was analyzed by PCR amplification using UF and DR primers. As shown in Fig 4.14C and D, the *sll1252* ORF in all genomes were completely replaced by truncated copies of *sll1252* gene in the truncated mutants.

Figure 4.14: Schematic representation of the genotype of suppressor mutant and PCR based confirmation of Δ*sll1252*^{del,} Δ*sll1252*N^{ter} and Δ*sll1252*C^{ter} truncated mutants.

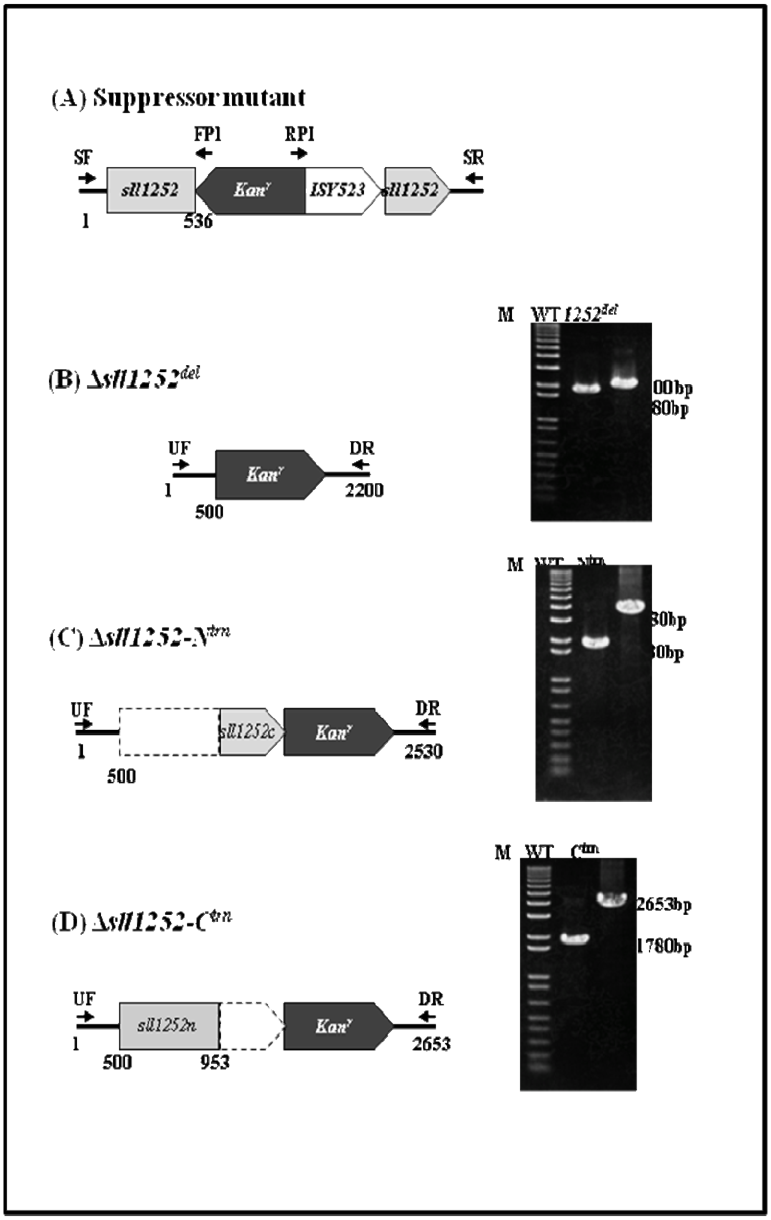

Figure 4.14: Schematic representation of the genotypes of the suppressor mutant deletional mutant, N terminal, and C terminal truncated mutants. (A). Schematic representation of the genotype of the Δ*sll1252*$^{ins-}$*Rev*. The *sll1252*^{ins} mutation effect was

suppressed by spontaneous insertion of naturally occurring transposon, ISY523. ISY523 is indicated by open arrow. SF and SR are the primers used for amplification of DNA fragment covering the *sll1252* open reading frame. FP1 and RP1 kanamycin specific primers were used for sequencing to locate the position of sponstaneous insertion of ISY523. Genomic PCR analysis with the primers indicated in the construct map M represents 1-kb DNA ladder. WT, PCR product with wild-type DNA as template; *1252*$^{\mathrm{ins}}$-*Rev*, PCR product with Δ*sll1252*$^{\mathrm{ins}}$-*Rev* DNA as template. Strategies for generation of deletional mutant Δ*sll1252*$^{\mathrm{del}}$, N-terminal truncational mutant expressing only C-terminal half of the *sll1252* ORF, Δ*sll1252* N$^{\mathrm{trn}}$ and C-terminal truncational mutant in which only N-terminal half of the *sll1252* ORF is expressing, Δ*sll1252* C$^{\mathrm{trn}}$. The wild-type copy of the *sll1252* gene was completely replaced by the mutated copy of the gene in Δ*sll1252*$^{\mathrm{del}}$, Δ*sll1252* N$^{\mathrm{trn}}$ and Δ*sll1252* C$^{\mathrm{trn}}$ mutant cells. (B) Schematic representation of the genotype of the Δ*sll1252*$^{\mathrm{del}}$ cells. A 1780 bp DNA fragment representing *sll1252* gene was replaced with a kanamycin resistance cassette (1200 bp). Genomic PCR analysis with the primers indicated in the construct map M represents 1-kb DNA ladder. WT, PCR product with wild-type DNA as template; *1252*$^{\mathrm{del}}$, PCR product with Δ*sll1252* DNA as template. (C) Schematic representation of the genotype of the Δ*sll1252*-N$^{\mathrm{trn}}$ mutant. A 453 bp DNA fragment representing 5'-half of the *sll1252* gene was deleted using fusion PCR as described in materials and methods. Genomic PCR analysis with the primers indicated in the construct map M represents 1-kb DNA ladder. WT, PCR product with wild-type DNA as template; N$^{\mathrm{trn}}$, PCR product with Δ*sll1252*-N$^{\mathrm{trn}}$ DNA as template. (D) Schematic representation of the genotype of the Δ*sll1252*-C$^{\mathrm{trn}}$ mutant. A 327 bp DNA fragment representing 3'-half of the *sll1252* gene was deleted using fusion PCR as described in materials and methods. Schematic representation of the genotype of the Δ*sll1252*-C$^{\mathrm{trn}}$ mutant. Thick arrows in panels B, C and D indicate *UF* and *DR* primers used for PCR amplification of the WT copy of the *sll1252* gene and that of the mutated copy of *sll1252* gene together with kanamycin gene. Genomic PCR analysis with the primers indicated in the construct map M represents 1-kb DNA ladder. WT, PCR product with wild-type DNA as template; C$^{\mathrm{trn}}$, PCR product with Δ*sll1252*-C$^{\mathrm{trn}}$ DNA as template. The *sll1252* gene and the kanamycin-resistance gene (*kan*$^{\mathrm{R}}$) are shown in light gray and dark gray arrows, respectively. Deleted part of the *sll1252* gene is shown in open rectangles with dotted outline in the Δ*sll1252*-N$^{\mathrm{trn}}$ and *Δsll1252*-C$^{\mathrm{trn}}$ construct maps. Other details are described in METHODS.

Expression of only C-terminal half of *sll1252* influences growth of *Synechocystis* cells:

As expected we observed no significant loss in the photosynthetic oxygen evolution in Δ*sll1252*$^{\mathrm{ins}}$Rev, Δ*sll1252*$^{\mathrm{del}}$, and Δ*sll1252*C$^{\mathrm{trn}}$. In Δ*sll1252*N$^{\mathrm{trn}}$ cells there was a 50□ decrease in the whole chain electron transport rate (Table 4.2). A slight decrease in PSII catalyzed oxygen evolution was observed in all strains of *sll1252* mutants, except for Δ*sll1252*C$^{\mathrm{trn}}$ in which about 40% loss in the PSII activity was observed (Table 4.2). The mean generation time calculated for wild type *Synechocystis* cells was ~ 8 h. As mentioned before the Δ*sll1252*^{ins} exhibited a severe slow growth phenotype. The mean generation time of Δ*sll1252*-N^{trn} was 22 h. The growth was much slower than the wild type cells (~ 8 h) and Δ*sll1252*^{del}. Since, only Δ*sll1252*-N^{trn} exhibited slow growth phenotype like Δ*sll1252*^{ins} and reduction in whole chain electron transport suggests that expression of C-terminal half of *sll1252* is deteriorative to the cell (Table 4.2). Perhaps, both C-terminal and N-terminal halves of Sll1252 are involved in regulation of rate of electron transport between PQ pool to Cyt b$_6$/*f* complex. C-terminal half of Sll1252, consisting of S4- domain may act as inhibitor of electron flow. Probably interaction of N-terminal half with C-terminal half masks the inhibitory effect, thereby regulating the electron flow. Thus depending on requirement, rate of electron transport may be regulated by *Sll1252* using both its N-terminal and C-terminal halves. Thus, expression of only C-terminal half of *sll1252* down regulates the electron transfer from PQ pool to Cyt b$_6$/*f* complex, leading to slow growth phenotype.

Table 4.2: Measurement of growth, PSII ativity and WCE activity of wild type and truncated mutants

Strain	Mean generation time (h)	PSII activity (H_2O to PPBQ)	WCE activity (H_2O to MV)
Wild type	8.3 ± 0.3	1 ± 0.11	1 ± 0.13
Δ*sll1252*^{ins}	Not detected	0.8 ± 0.11	0.59 ± 0.06
Δ*sll1252*^{del}	9.8 ± 0.2	0.78 ± 0.23	0.82 ± 0.06
Δ*sll1252*^{inv}*-Rev*	8.1 ± 0.2	0.89 ± 0.16	0.91 ± 0.09
Δ*sll1252-N*^{trn}	22.0 ± 2.5	0.75 ± 0.04	0.51 ± 0.06
Δ*sll1252-C*^{trn}	11.5 ± 0.7	0.59 ± 0.03	0.91 ± 0.06

Table 4.2: Comparison of PSII, WCE activity and growth of Δ*sll1252* mutant strains with the wild type *Synechocystis* sp. PCC6803. PS II and WCE activities of WT and Δ*sll1252* mutant strains grown at 34^{o}C, aerated with 1.5 % CO_2 and 70 µmol photon m^{-2}s^{-1}. Rate of PET was measured in terms of oxygen evolution. Mean values ±SE were calculated from three independent experiments.

Thylakoid membrane is disorganized in Δ*sll1252N*^{trn}:

Since we observed slow growth phenotype, only when C-terminal half is expressed (i.e., Δ*sll1252-N*^{trn}), but no phenotype in the Δ*sll1252-C*^{trn}, we further examined the ultrastructural changes caused in *Synechocystis* cells due to expression of truncated forms of *sll1252.* As can be seen in (Figure. 4.15), Wild type and Δ*sll1252-C*^{trn} looked alike. A well organized thylakoid membranes are visible, when examined under transmission electron micrograph. Layers of thylakoid membranes were arranged in rows. In contrast to wild type *Synechocystis* cells and Δ*sll1252-C*^{trn} cells, thylakoid membranes were disorganized in Δ*sll1252-N*^{trn}. Only a few polyphosphate granules were observed in wild type and Δ*sll1252-C*^{trn} cells, indicating actively growing and dividing cells in these cultures, which might be using the stored phosphate for their active growth. In contrast more number of polyphosphates in Δ*sll1252*-N^{trn} is the indication of slow growth phenotype. In Δ*sll1252*-N^{trn} we found spherical dense bodies, probably contain the degraded thylakoid membrane lipids. Thus it is clear from the transmission electron microscopic observations that expression of only C-terminal half of Sll1252 leads to the ultrastructural changes, especially the disorganization of thylakoid membranes. This supports important physiological role of Sll1252 in photosynthetic electron transport.

Figure 4.15: TEM Images of the thylakoid membrane of wild type and truncated mutants.

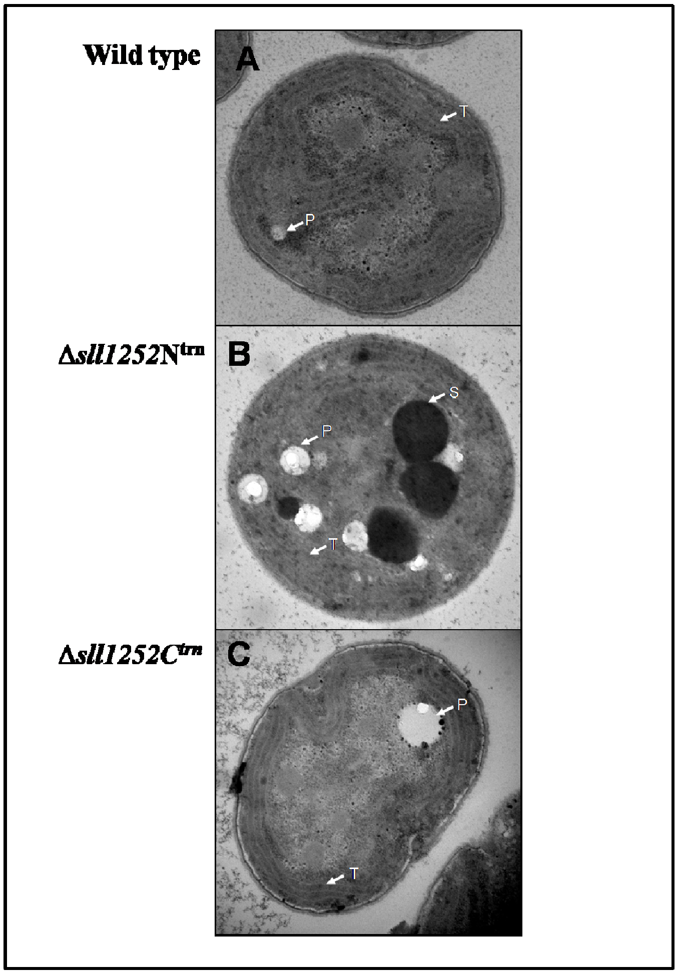

Figure 4.15. **Changes in cell morphology due to truncation of 5’ half and 3’ half of the *sll1252* open reading frame.** (A) Representative electron micrograph of (A) wild type cells (B) Δ*sll1252*-N^{trn} cells and (C) Δ*sll1252*-C^{trn} cells. The cells were grown at 70 µmol photons m^{-2} s^{-1} for 24 h and then fixed for transmission electron microscopic observations. Carboxysomes (C), thylakoid membrane (T), and polyphosphate bodies (P) are indicated by arrows. Block spherical bodies (B) are seen only in the *Δsll1252*-N^{trn} mutant. Scale bar = 500 nm.

5. DISCUSSION AND CONCLUSIONS

Functional characterization of Sll1252 in *Synechocystis*

In most of the genomes nearly 50% of the proteins belong to (HPs), which are of utmost importance to better understand molecular mechanisms and to discover the unknown cellular biochemical reactions, thus getting insights into complete genomic and proteomic information of living organisms. In bacteria, 30-40% of the proteins encoded by their genomes do not have an assigned function (23). Even in a well studied organism such as *Synechocystis* 46.3% of the proteins are functionally unknown. Sll1252 is a hypothetical protein and is assumed to have important physiological function since it is conserved in cyanobacteria and higher plants. Assigning a functional role to such hypothetical protein is a matter of utmost importance to decode the role played by it. Using reverse genetic approach, we found that this protein is essentially required for regulation of electron flow between PQ pool to cytochrome b_6/f complex in the linear electron transport (Table 4.1 and Figure 4.5).

Sll11252 is a soluble protein but not PSII associated protein

Kashino *et al.,* indicated that Sll1252 is associated with the PSII, we started verifying the role of Sll1252 in PSII structure and function. Complete mutation of *sll1252* in *Synechocystis* has affected growth. Slow growth phenotype of Δ*sll1252*^{ins} clearly demonstrated that Sll1252 plays an important role in the physiology of *Synechocystis* cells. Since Sll1252 seems to be associated with PSII it is likely that the mutation in *sll1252* might have influenced the photosynthetic efficiency and, thereby, resulted in the phenotype of slow growth. Being associated with purified PSII complexes this protein is assumed to have transmembrane domain in it. However, computational analysis of the protein indicated, it had no predicted transmembrane domains. Several proteins including GroEL were shown to be associated with thylakoid membranes, even though they are not part of multi-protein complexes of thylakoids, without having any known transmembrane domains (152). Sll1252 being the member of PSII complex, a membrane protein complex, Sll1252 was expected to be found in membrane fraction of *Synechocystis* cells. Detection of Sll1252 in the soluble fraction of *Synechocystis* but not in insoluble fraction by anti-Sll1252 antibody (Figure 4.13), further confirms that the Sll1252 protein is not associated with PSII complex but is a soluble protein. The rate of photosystem II-mediated electron transport and the rate of whole chain electron transport activity were compared in the WT and Δ*sll1252*$^{\text{ins}}$ cells, the rate of WCE activity in Δ*sll1252*$^{\text{ins}}$ mutant cells was reduced by about 40% in comparison with that in WT cells (Table 4.2) With these observations we report that Sll1252 is soluble protein with no role in PSII structure, function.

Sll1252 assists electron transfer beyond PSII

Since the Δ*sll1252*^{ins} cells exhibited slow growth phenotype, Sll1252 protein seems to be essentially required when the cell remains photosynthetically active, in order to identify the probable site of its action in the linear electron transport, we performed DNA microarray analysis of this mutant. Since the photosynthetic transfer of electrons and/or the redox status of electron-transport components are supposed to be a primary signal for the expression of a set of genes, we examined the effect of *sll1252* insertional inactivation on the genome-wide expression of genes with Δ*sll1252*$^{\text{ins}}$ cells (Fig 4.5). The profile of gene expression in Δ*sll1252*$^{\text{ins}}$ cells was compared with that of WT cells upon treatment with inhibitors of electron transport, such as DBMIB or DCMU (149). Interestingly 22 out of 37 up-regulated genes by Δ*sll1252*^{ins} were reported to be induced by inhibition of cells with DBMIB in WT (Table 4.1). As 60% of the genes upregulated by Δ*sll1252*^{ins} were inducible due to inhibitory action of DBMIB and none of them were inducible by DCMU inhibitory effect, it is quite likely that the effect of lack of functional Sll1252 protein (due to mutation in Δ*sll1252*^{ins}) is similar to the effect caused due to inhibition by DBMIB on global gene expression profile. This may indicate that Sll1252 functions to sustain the electron transfer from reduced PQ pool to Cyt b_6/f complex (Figure 4.6).

Sll1252 assists electron transfer between PQ pool to Cyt b_6/f complex

Reduced rate of whole chain electron transport activity together with DNA micro array gene expression profiling, suggest that the *Sll1252* is required for electron transfer from PQ pool to Cyt b_6/f complex. Differential degree of sensitivity to specific inhibitors, DCMU and DBMIB, by WT and Δ*sll1252*^{ins} mutant cells was examined by measuring PET rates in the presence of various concentrations of inhibitors. DCMU required for 50% inhibition of the original activity was about the same in WT and Δ*sll1252*^{ins} mutant cells (Figure 4.7A). However, the inhibitor required for 50% inhibition of the WCE activity was 140 nM and 300 nM in the Δ*sll1252*^{ins} mutant and WT cells respectively. This suggests that the Δ*sll1252*^{ins} cells are more sensitive to DBMIB, and points the site of action of Sll1252. To further confirm the site of action of Sll1252, the rate of PQ pool was estimated, if the site of action of Sll1252 is between PQ pool to Cyt b_6/f complex, then mutation in *sll1252* impairs the transfer of electrons from reduced PQ pool to Cyt b_6/f complex. Consequence of this impaired rate of electron transfer would lead to the relatively higher level of plastoquinones in reduced state in Δ*sll1252*^{ins} cells when compared to wild-type cells that had been grown in light at the same intensity. Relatively, about 4 fold increase in the PQ reduction rate was observed in Δ*sll1252*$^{\mathrm{ins}}$ when compared to wild type *Synechocystis* cells (Figure 4.8). In WT cells, inhibition of electron transport by DBMIB also resulted in enhanced rate of PQ reduction (Figure 4.8) which further confirms the site of action of Sll1252.

Complementation of the Δ*sll1252*^{ins} resulted in recovery of the WT phenotype.

To determine whether the phenotypical outcomes of Δ*sll1252*$^{\mathrm{ins}}$ mutation are due to gene inactivation itself or rather due to polar effects (by interruption of the regulatory integrity of an operon) the wild type copy of *sll1252* gene was reintroduced into the Δ*sll1252*$^{\mathrm{ins}}$ by expressing it on a self-replicating plasmid. Growth profile of wild type, *Δsll1252* and *sll1252*$^{+}$ were compared at optimal growth conditions, growth of *sll1252*$^{+}$ cells was similar to the growth of wild type cells (Figure 4.9) which confirms that the phenotype observed by *Δsll1252*$^{\mathrm{ins}}$ cells was due to the effect of mutation of *sll1252* gene in wild type.

C-terminal of Sll1252 plays an important role

Kashino *et al*., reported that no significant growth phenotype was observed, when *sll1252* ORF was completely deleted in *Synechocystis* cells (54). We also observed the roles of N terminal and C terminal halves of the *sll1252* by generating truncated mutants, by selective expression of them in *Synechocystis*. Since, only Δ*sll1252*-N$^{\mathrm{trn}}$ exhibited slow growth phenotype like Δ*sll1252*$^{\mathrm{ins}}$ and reduction in whole chain electron transport suggests that expression of C-terminal half of *sll1252* is deteriorative to the cell (Table 4.2). Perhaps, both C-terminal and N-terminal halves of Sll1252 are involved in regulation of rate of electron transport between PQ pool to Cyt b_6/f complex. C-terminal half of Sll1252, consisting of S4-domain may act as inhibitor of electron flow. Probably interaction of N-terminal half with C-terminal half masks the inhibitory effect, thereby regulating the electron flow. Thus depending on requirement, rate of electron transport may be regulated by *Sll1252* using both its N-terminal and C-terminal halves. Thus, expression of only C-terminal half of *sll1252* down regulates the electron transfer from PQ pool to Cyt b_6/f complex, leading to slow growth phenotype. Since we observed slow growth phenotype, only when C-terminal half is expressed (i.e., Δ*sll1252*-N^{trn}), but no phenotype in the Δ*sll1252*-C^{trn}, we further examined the ultrastructural changes caused in *Synechocystis* cells due to expression of truncated forms of *sll1252.* Wild type and Δ*sll1252*-C^{trn} looked alike. Well organized thylakoid membranes are visible, when examined under transmission electron micrograph. Layers of thylakoid membranes were arranged in rows. In contrast to wild type *Synechocystis* cells and Δ*sll1252-C*^{trn} cells, thylakoid membranes were disorganized in *Δsll1252*-N^{trn} (Figure 4.15). Thus it is clear from the transmission electron microscopic observations that expression of only C-terminal half of Sll1252 leads to the ultrastructural changes, especially the disorganization of thylakoid membranes. This supports important physiological role of Sll1252 in photosynthetic electron transport.

Proposed model for explaining the function of Sll1252

We present a model to show the various experimental results as the basis for drawing a conclusion about the function of Sll1252 in the thylakoids membrane (Figure 4.16). As the PQ pool is a common electron carrier and receives electrons from NDH complex and PSII, the size of the PQH_2 is represented with relatively bigger oval shape than the oxidized PQ. Sll1252 is probably associated with Cyt b_6/f complex. Electron transfer is regulated by Sll1252 N and C-terminal halves depending on the efficiency of electron transport chain and balances functional co-ordination between PSII and PSI. For simplification, cyclic electron transport, terminal oxidases, and ATP synthase complexes were not shown. In figure 4.16B electron transfer from PQ pool to Cyt b_6/*f* complex is inhibited due to expression of C-terminal half of Sll1252. This leads to further increase in reduced PQH_2 level where as the expression of N-terminal half of Sll1252 has no effect on electron transfer between PQ pool Cyt b_6/*f* complex (Figure 4.16C).

Figure 4.16: Proposed model to explain the function of Sll1252

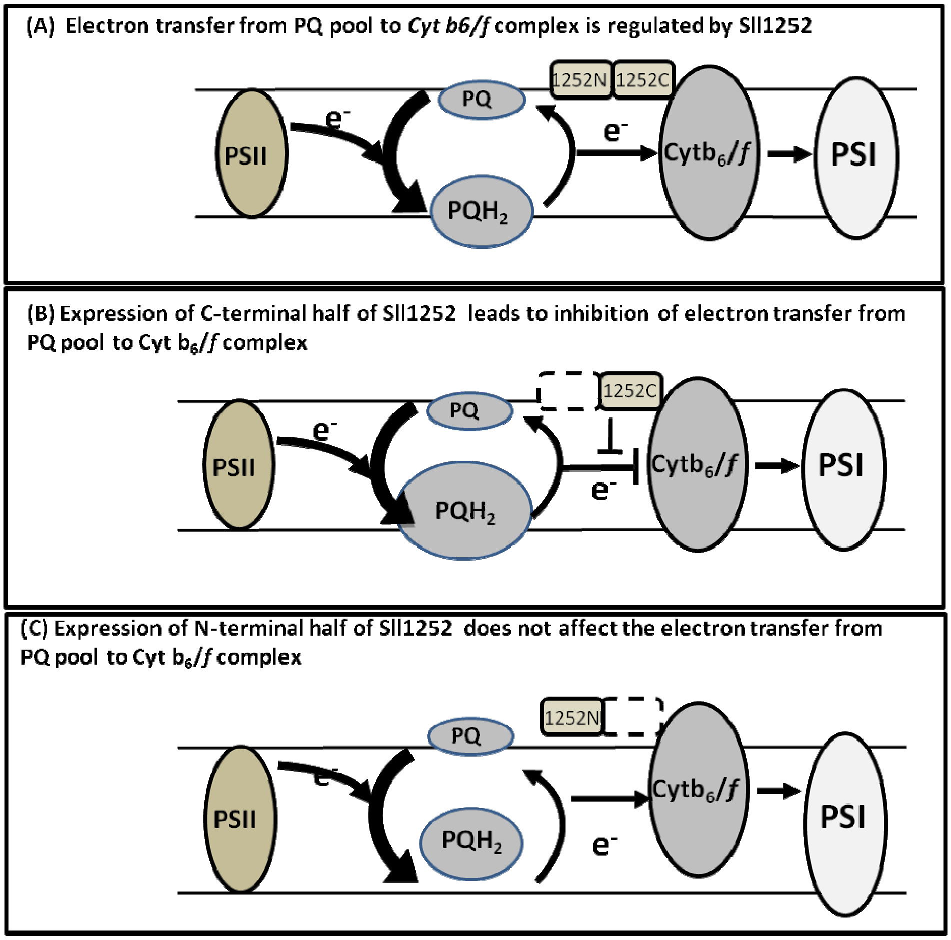

Figure 4.16: Proposed model to explain the function of Sll1252. (A). shows the usual linear photosynthetic electron transport chain. (B). Inhibition of electron transfer from PQ pool to Cyt b_6/*f* complex due to expression of C-terminal half of Sll1252. (C). Expression of c N-terminal half of Sll1252 has no effect on electron transfer between PQ pool Cyt b_6/*f* complex.

CONCLUSIONS

Sll11252 is a soluble proteins, expressing constitutively in the *Synechocystis* cell. Sll1252 is a conserved protein with S4 domain. Slow growth phenotype due to mutation clearly demonstrates that Sll1252 plays a crucial role in the physiology of *Synechocystis* cells. Microarrays has shown that 60% of the genes upregulated by mutation were inducible due to inhibitory action of DBMIB suggesting that the effect of lack of functional Sll1252 protein (due to mutation in Δ*sll1252*^{ins}) is similar to the effect caused due to inhibition by DBMIB on global gene expression profile. Reduced rate of whole chain electron transport activity together with DNA micro array gene expression profiling, suggest that the Sll1252 is required for electron transfer from PQ pool to Cyt b_6/f complex. Relatively, about 4 fold increase in the PQ reduction rate in Δ*sll1252*^{ins} when compared to wild type *Synechocystis* cells further confirms the site of action of Sll1252. Similar Growth of *sll1252*$^{+}$ cells and wild type cells confirms that the phenotype observed by Δ*sll1252*^{ins} cells was due to the effect of mutation of *sll1252* gene in wild type and not polar effect. Perhaps, both C-terminal and N-terminal halves of Sll1252 are involved in regulation of rate of electron transport between plastoquinone pool to Cyt b_6/f complex. C-terminal half of Sll1252, consisting of S4- domain act as inhibitor of electron flow. Probably interaction of N-terminal half with C-terminal half masks the inhibitory effect, thereby regulating the electron flow. Thus depending on requirement, rate of electron transport may be regulated by Sll1252 using both its N-terminal and C-terminal halves.

6. PRIMER SEQUENCES

Primers used for the expression of *sll1252*

Name	Primer sequence 5’-3’	RE sites
sll1252-Ex-F	ACT CAT ATG TTA CCA AGA GAA GCT TTG TTA AAG	*NdeI*
sll1252-Ex-R	CCC GGA TCC TTA AAG ATA TCG GGT TAA TTG GAT GC	*BamHI*

Primers used for complementation of *sll1252*

Name	Primer sequence 5’-3’	R.E. sites
sll1252-Com-F	TGC ATCGAT TTG CTA CCT GGA TGG TGA AAA TCA TG	ClaI
sll1252-Com-R	CGA CTCGAG GAA CCA CCA GTC AAG ACA ATG CGA C-3’	XhoI

Primers used for PCR amplification of Δ*sll1252*^{ins} mutant during mutagenesis

Name	Primer sequence 5’-3’	R.E. sites
sll1252-F	AACCATAGGCGCATTGTAGCTCCTTG	- -
sll1252-R	GATATCAACATTATCCTT TGCCTCGAACG	- -

Primers used for amplification of *sll1252* in suppressor mutants of Δ*sll1252*^{ins}

Name	Primer sequence 5'-3'	R.E sites
S F	AGA TCT GCC AAG ATA ATT GAT TG	--
S R	AGA TCT GTC GAC ATT CCA CTG GCA AAA	--
FP1	ACC TAC AAC AAA GCT CTC ATC AAC C	--
RP1	GCA ATG TAA CAT CAG AGA TTT TGA G	--

Primers used for generating (Δ*sll1252*^{del})

Name	Primer sequence 5'-3'	RE sites
UF	UF GCA TCA ATT TGT TCT GTC AC	--
UR	AGA TCT CGA GCA ACG GCA TTA GCT	BglII
DF	CGT TGC TCG AGA TCT CCA GTT TCA AGG CTTGCC	BglII
DR	CCA CAA TTA AAG TTG TAC TG	--
Kan2-F	TCG TCG ACC AAC CAT CAT CGA TGA ATT	SalI
Kan2-R	TCG TCG ACA AAG CCG CCG TCC CGT CAA	SalI

Primers used for generating (Δ*sll1252*-N^{trn})

Gene	Primer sequence (5' -3')	RE sites
UF	GCA TCA ATT TGT TCT GTC AC	--
UR	CGA GCA ACG GCA TTA GCT AA	--
Ntrn-F	**TAA TGC CGT TGC TCG ATG** GTG CGT ACT GTA	--
Ntrn-R	CCC GGG TTA AAG ATA TCG GGT	SmaI
sll1252 Ntrn DF	5’ TAT CTT TAA CCC GGG CCA GTT TCA AGG CTT	SmaI
DR	CCA CAA TTA AAG TTG TAC TG	--

Primers used for generating (Δ*sll1252*-C^{trn})

Gene	Primer Sequence (5' -3')	RE sites
UF	GCA TCA ATT TGT TCT GTC AC	--
sll1252-trn-DR	CCC GGG TTA CTG GGT **TAA** ATG AAG ACT	SmaI
Ctrn-F	**TAACCCAGTAACCCG GG**CCAGTTTCAAGGCTT	SmaI
DR	CCA CAA TTA AAG TTG TAC TG	--

REFERENCES

1. *Nachimuthu Saraswathy, Ponnusamy Ramalingam, in* Concepts and Techniques in Genomics and Proteomics*, 2011.*
2. F. Sanger, S. Nicklen, and A. R. Coulson, DNA sequencing with chain-terminating inhibitors. PNAS December 1, 1977 74 (12) 5463-5467.
3. A M Maxam, W Gilbert Proceedings of the National Academy of Sciences Feb 1977, 74 (2) 560-564; DOI: 10.1073/*pnas*.74.2.560.
4. Smith, L. M. et al. Fluorescence detection in automated DNA sequence analysis. *Nature* 321, 674±679 (1986).
5. Fleischmann RD, Adams MD, White O, R A Clayton, E F Kirkness, A R Kerlavage, C J Bult, J F Tomb, B A Dougherty, J M Merrick et al. Whole-genome random sequencing and assembly of Haemophilus influenzae Rd. *Science*. 1995;269(5223):496-512. doi:10.1126/science.7542800.
6. Venter, J. C., Adams, M. D., Myers, E. W., Li, P. W., Mural, R. J., Sutton, G.G.,Smith, H. O., Yandell, M., Evans, C. A., Holt, R. A., *et al.* (2001) *Science* 291, 1304–1351.
7. Venter, J. C., Levy, S., Stockwell, T., Remington, K. & Halpern, A. (2003) *Nat.Genet.* 33, Suppl., 219–227.
8. Metzker, M. Sequencing technologies — the next generation. *Nat Rev Genet* 11, 31–46 (2010).
9. F. Ozsolak, P.M. Milos RNA sequencing: Advances, challenges and opportunities Nat. Rev. Genet., 12 (2011), pp. 87-98.
10. Qiao J, Shao M, Chen L, Wang J, Wu G, Tian X, Liu J, Huang S, Zhang W. Systematic characterization of hypothetical proteins in Synechocystis sp. PCC 6803 reveals proteins functionally relevant to stress responses. Gene. 2013 Jan 1;512(1):6-15. doi: 10.1016/j.gene.2012.10.004. Epub 2012 Oct.
11. Brenner, S. E. Errors in genome annotation. *Trends Genet.* 15, 132–133 (1999).
12. Ijaq, J., Malik, G., Kumar, A. et al. A model to predict the function of hypothetical proteins through a nine-point classification scoring schema. BMC Bioinformatics 20, 14 (2019).
13. Bork,P.(2000)Powers and pitfalls in sequence analysis: the70%hurdle. Genome Res., 10, 398–400.
14. Huynen M.A., Snel B., von Mering C., Bork P. Function prediction and protein networks, Curr. Opin. Struct. Biol., 2003, vol. 15(pg. 191-198).
15. Sankha Ghatak, Zachary A King, Anand Sastry, Bernhard O Palsson, The y-ome defines the 35% of *Escherichia coli* genes that lack experimental evidence of function, *Nucleic Acids Research*, Volume 47, Issue 5, 18 March 2019, Pages 2446–2454.
16. Hanson AD, Pribat A, Waller JC, de Crécy-Lagard V. 'Unknown' proteins and 'orphan' enzymes: the missing half of the engineering parts list--and how to find it. Biochem J. 2009;425(1):1-11. Published 2009 Dec 14. doi:10.1042/BJ20091328
17. Loewenstein, Y., Raimondo, D., Redfern, O.C. et al. Protein function annotation by homology-based inference. Genome Biol 10, 207 (2009).
18. Nimrod G, et al. Detection of functionally important regions in “hypothetical proteins” of known structure. Structure. 2008;16(12):1755–63.
19. Mohan R, Venugopal S. Computational structures and functional analysis of hypothetical proteins of Staphylococcus aureus. Bioinformation. 2012;8(15):722–8.
20. Lubec G, Afjehi-Sadat L, Yang JW, John JP (2005) Searching for hypothetical proteins: theory and practice based upon original data and literature. Prog Neurobiol 77: 90–127.

21. Cui J.J., Tran-Dubé M., Shen H., Nambu M., Kung P.-P., Pairish M., Jia L., Meng J., Funk L., Botrous I., et al. Structure Based Drug Design of Crizotinib (PF-02341066), a Potent and Selective Dual Inhibitor of Mesenchymal–Epithelial Transition Factor (c-MET) Kinase and Anaplastic Lymphoma Kinase (ALK) J. Med. Chem. 2011;54:6342–6363. doi: 10.1021/jm2007613.
22. Da Fonsêca M.M., Zaha A., Caffarena E.R., Vasconcelos A.T. Structure-based functional inference of hypothetical proteins from Mycoplasma hyopneumoniae. J. Mol. Model. 2011;18:1917–1925. doi: 10.1007/s00894-011-1212-3.
23. Galperin, M., Y. and Koonin, E., V. (2004) 'Conserved hypothetical' proteins: prioritization of targets for experimental study. Nucleic Acids Res. 32, 5452–5463.
24. Tatusov, R., L., Natale, D., A., Garkavtsev, I., V., Tatusova, T., A., Shankavaram, U., T., Rao, B., S., Kiryutin, B., Galperin, M., Y., Fedorova, N., D. and Koonin, E., V. (2001) The COG database: new developments in phylogenetic classification of proteins from complete genomes. Nucleic Acids Res. 29, 22–28.
25. T. I. Zarembinski, *et al*., *Proc. Natl. Acad. Sci.*, 95:15189 (1998) [PMID:9860944].
26. Kufryk, G., I. and Vermaas, W., F., J. (2001) A novel protein involved in the functional assembly of the oxygen-evolving complex of photosystem II in *Synechocystis* sp. PCC 6803. Biochemistry 40:9247-9255.
27. W. R. Pearson, *et al., Proc Natl Acad Sci.*, 85:2444 (1998) [PMID:3162770]
28. S. F. Altschul & E. V. Koonin, *Trends Biochem Sci.,*23:444 (1998) [PMID:9852764]
29. Larkin MA, Blackshields G, Brown NP, Chenna R, McGettigan PA, McWilliam H, Valentin F, Wallace IM, Wilm A, Lopez R, Thompson JD, Gibson TJ, Higgins DG (2007) Clustal W and Clustal X version 2.0. *Bioinformatics* 23: 2947–2948
30. Notredame C, et al. T-coffee: a novel method for fast and accurate multiple sequence alignment, J. Mol. Biol., 2000, vol. 302(pg. 205-217).
31. Letunic I, Doerks T, Bork P (2012) SMART 7: recent updates to the protein domain annotation resource. Nucleic Acids Res 40: D302–305
32. Punta M, Coggill PC, Eberhardt RY, Mistry J, Tate J, et al. (2012) The Pfam protein families database. Nucleic Acids Res 40: D290–301.
33. Marchler-Bauer A., Anderson J.B., Cherukuri P.F., DeWeese-Scott C., Geer L.Y., Gwadz M., He S., Hurwitz D.I., Jackson J.D., Ke Z., et al. CDD: a Conserved Domain Database for protein classification. Nucleic Acids Res. 2005;33:D192–D196.
34. Sigrist CJ, Cerutti L, de Castro E, Langendijk Genevaux PS, Bulliard V, et al. (2010) PROSITE, a protein domain database for functional characterization and annotation. Nucleic Acids Res 38: D161–166.
35. Hunter S, Jones P, Mitchell A, Apweiler R, Attwood TK, et al. (2011) InterPro in 2011: new developments in the family and domain prediction database. Nucleic Acids Res 40: D306–312.
36. *Pellegrini, M., Marcotte, E.M., Thompson, M.J., Eisenberg, D., and Yeates, T.O. 1999. Assigning protein functions by comparative genome analysis: Protein phylogenetic profiles. Proc. Natl. Acad. Sci. 96: 4285-4288.*
37. Angela M. Thornton and Ethan M. Shevach. Suppressor Effector Function of $CD4^{+}CD25^{+}$ Immunoregulatory T Cells Is Antigen Nonspecific J Immunol January 1, 2000, 164 (1) 183-190; DOI: https://doi.org/10.4049/jimmunol.164.1.183
38. Stark, A., Sunyaev, S. & Russel, R. B. (2003). A model for statistical significance of local similarities in structure. J. Mol. Biol. 326, 1307–1316.
39. Aloy P, Russell RB. InterPreTS: protein interaction prediction through tertiary structure, Bioinformatics, 2003, vol. 19(pg.161).
40. Barton, G. J. (1993). OC - a cluster analysis program.
41. Waterhouse A, Bertoni M, Bienert S, et al. SWISS-MODEL: homology modelling of protein structures and complexes. *Nucleic Acids Res* 2018; 46: W296–303.
42. Lawrence A. Kelley, Robert M. Mac Callum and Michael J. E. SternbergEnhanced Genome Annotation Using Structural Profiles in the Program 3D-PSSM. Journal of molecular biology, 2000 – Elsevier. Volume 299, Issue 2, 2 June 2000, Pages 501-522
43. Zhang, S., S. M. Laborde, L. K. Frankel, and T. M. Bricker. 2004. Identification of four novel genes required for efficient photoautotrophic growth of the cyanobacterium Synechocystis sp. PCC 6803 by in vitro transposon mutagenesis. J. Bacteriol. 186 : 875-879.

44. J. Yu *et al.*, Suppressor mutations in the study of photosystem I biogenesis: sll0088 is a previously unidentified gene involved in reaction center accumulation in Synechocystis sp. strain PCC 6803. *J. Bacteriol.* 185, 3878 (2003).
45. G. I. Kufryk, W. F. Vermaas, Sll1717 affects the redox state of the plastoquinone pool by modulating quinol oxidase activity in thylakoids. *J. Bacteriol.* 188, 1286 (2006).
46. T. Volkmer *et al.*, Ssr2998 of Synechocystis sp. PCC 6803 is involved in regulation of cyanobacterial electron transport and associated with the cytochrome b6f complex. *The Journal of biological chemistry* 282, 3730 (2007).
47. A. Kamei, T. Yuasa, K. Orikawa, X. X. Geng, M. Ikeuchi, A eukaryotic-type protein kinase, SpkA, is required for normal motility of the unicellular Cyanobacterium synechocystis sp. strain PCC 6803. *J. Bacteriol.* 183, 1505 (2001).
48. J. S. Prakash *et al.*, An RNA helicase, CrhR, regulates the low-temperature-inducible expression of heat-shock genes groES, groEL1 and groEL2 in Synechocystis sp. PCC 6803. *Microbiology* 156, 442 (2010).
49. Gerdes, S., Edwards, R., Kubal, M., Fonstein, M., Stevens, R. and Osterman, A. (2006) Essential genes on metabolic maps. Curr. Opin. Biotechnol. 17, 448–456.
50. Tzafrir, I., Dickerman, A., Brazhnik, O., Nguyen, Q., McElver, J., Frye, C., Patton, D., and Meinke, D. (2003). The Arabidopsis Seed Genes project. Nucleic Acids Res. 31, 90–93.
51. Masamoto, K., Misawa, N., Kaneko, T., Kikuno, R. and Toh, H. (1998) β-Carotene hydroxylase gene from the cyanobacterium *Synechocystis* sp.PCC6803. Plant Cell Physiol. 39, 560–564.
52. Okuda, K., Hayashi, H. and Nishiyama, Y. (2005) Systematic characterization of the ADP-ribose pyrophosphatase family in the Cyanobacterium *Synechocystis* sp. strain PCC 6803. J Bacteriol. 187, 4984-4991.
53. Y. Kashino *et al.*, Proteomic analysis of a highly active photosystem II preparation from the cyanobacterium Synechocystis sp. PCC 6803 reveals the presence of novel polypeptides. *Biochemistry (Mosc.)* 41, 8004 (2002).
54. N. Inoue-Kashino *et al.*, S4 Protein Sll1252 Is Necessary for Energy Balancing in Photosynthetic Electron Transport in Synechocystis sp. PCC 6803. *Biochemistry (Mosc.)*, (2010).
55. Thornton, L., E., Ohkawa, H., Roose, J., L., Kashino, Y., Keren, N., and Pakrasi, H., B. (2004) Homologs of plant PsbP and PsbQ proteins are necessary for regulation of photosystem II activity in the cyanobacterium, *Synechocystis* 6803. Plant Cell. 16, 2164–2175.
56. Beckova´ M, Yu J, Krynicka´ V, Kozlo A, Shao S, Konı´k P, Komenda J, Murray JW, Nixon PJ. 2017 Structure of Psb29/Thf1 and its association with the FtsH protease complex involved in photosystem II repair in cyanobacteria. Phil. Trans. R. Soc. B 372, 20160394. (doi:10.1098/rstb.2016.0394).
57. Keren, N., Ohkawa, H., Welsh, E., A., Liberton, M., and Pakrasi, H., B. (2005) Psb29, a conserved 22-kD protein, functions in the biogenesis of Photosystem II complexes inSynechocystisandArabidopsis. Plant Cell. 17, 2768–2781.
58. DeRisi JL, Iyer VR, Brown PO. Exploring the metabolic and genetic control of gene expression on a genomic scale. Science. 1997;278:680–686. doi: 10.1126/science.278.5338.680.
59. Victor E. Velculescu, Lin Zhang, Bert Vogelstein, Kenneth W. Kinzler. Serial Analysis of Gene Expression. *Science* 20 Oct 1995: Vol. 270, Issue 5235, pp. 484-487, DOI:10.1126/science.270.5235.484.
60. de Cr´ecy-Lagard, V. (2007) Identification of genes encoding tRNA modification enzymes by comparative genomics. Methods Enzymol. 425, 153–183.
61. Gollub, J., Ball, C., A. and Sherlock, G. (2006) The Stanford Microarray Database: a user's guide. Methods Mol. Biol. 338, 191–208.
62. Laule, O., Hirsch-Hoffmann, M., Hruz, T., Gruissem, W. and Zimmermann, P. (2006) Web-based analysis of the mouse transcriptome using Genevestigator. BMC Bioinformatics 7, 311.
63. Obayashi, T., Kinoshita, K., Nakai, K., Shibaoka, M., Hayashi, S., Saeki, M., Shibata, D., Saito, K. and Ohta, H. (2007) ATTED-II: a database of co-expressed genes and cis

elements for identifying co-regulated gene groups in Arabidopsis. Nucleic Acids Res. 35, 863–869.

64. Y. Kanesaki, I. Suzuki, S. I. Allakhverdiev, K. Mikami, N. Murata, Salt stress and hyperosmotic stress regulate the expression of different sets of genes in Synechocystis sp. PCC 6803. *Biochem. Biophys. Res. Commun.* 290, 339 (2002).
65. Y. Hihara, A. Kamei, M. Kanehisa, A. Kaplan, M. Ikeuchi, DNA microarray analysis of cyanobacterial gene expression during acclimation to high light. *The Plant cell* 13, 793 (2001).
66. Mikami, K., Kanesaki, Y., Suzuki, I., and Murata, N. (2002). The histidine kinase Hik33 perceives osmotic stress and cold stress in *Synechocystis* sp. PCC 6803. Mol. Microbiol. 46, 905–915.
67. Shingo Suzuki, Ali Ferjani, Iwane Suzuki, and Norio Murata. The SphS-SphR Two Component System Is the Exclusive Sensor for the Induction of Gene Expression in Response to Phosphate Limitation in *Synechocystis.* doi: 10.1074/jbc.M313358200 *March 26, 2004 The Journal of Biological Chemistry 279, 13234-13240.*
68. Herrero, A. and Flores, F. G. (2008) The Cyanobacteria: Molecular Biology, Genomics, and Evolution, Caister Academic Press, Norfolk,
69. Whitton B.A., Potts M. (2012) Introduction to the Cyanobacteria. In: Whitton B. (eds) Ecology of Cyanobacteria II. Springer, Dordrecht. https://doi.org/10.1007/978-94-007-3855-3_1.
70. Raven, J.A., Allen, J.F. Genomics and chloroplast evolution: what did cyanobacteria do for plants?. *Genome Biol* 4, 209 (2003).
71. Keeling P. J. (2010). The endosymbiotic origin, diversification and fate of plastids. *Philosophical transactions of the Royal Society of London. Series B, Biological sciences*, *365*(1541), 729–748. https://doi.org/10.1098/rstb.2009.0103.
72. Horsten Heidorn, Daniel Camsund, Hsin-Ho Huang, Pia Lindberg, Paulo Oliveira, Karin Stensjö, Peter Lindblad, Chapter Twenty-Four - Synthetic Biology in Cyanobacteria: Engineering and Analyzing Novel Functions, Editor(s): Chris Voigt,Methods in Enzymology,Academic Press,Volume 497,2011.
73. Dvornyk, V. and Nevo, E . (2003). Genetic polymorphism of cyanobacteria under permanent natural stress: a lesson from the "Evolution Canyons". *Res Microbiol.* 154, (2),79-84.
74. Ferjani, A., Mustardy, L., Sulpice, R., Marin, K., Suzuki, I., Hagemann, M. and Murata, N. (2003). Glucosylglycerol, a compatible solute, sustains cell division under salt stress. *Plant Physiol.* 131, (4), 1628-1637.
75. Kobayashi, M., Ishizuka, T., Katayama, M., Kanehisa, M., Bhattacharyya-Pakrasi, M., Pakrasi, H. B. and Ikeuchi, M. (2004). Response to oxidative stress involves a novel peroxiredoxin gene in the unicellular cyanobacterium Synechocystis sp. PCC 6803. *Plant Cell Physiol.* 45, (3), 290-299.
76. Suzuki, I., Los, D. A. and Murata, N. (2000b). Perception and transduction of low temperature signals to induce desaturation of fatty acids. *Biochem Soc Trans.* 28, (6), 628-630.
77. Dilley, R. A., Nishiyama, Y., Gombos, Z. and Murata, N. (2001). Bioenergetic responses of Synechocystis 6803 fatty acid desaturase mutants at low temperatures. *J Bioenerg Biomembr.* 33, (2), 135-141.
78. Rajaram, H. and Kumar Apte, S. (2003). Heat-shock response and its contribution to thermotolerance of the nitrogen-fixing cyanobacterium Anabaena sp. strain L-31. *Arch Microbiol.* 179, (6), 423-429.
79. Allakhverdiev, S. I. and Murata, N. (2004). Environmental stress inhibits the synthesis de novo of proteins involved in the photo damage-repair cycle of P.S II in Synechocystis sp. PCC 6803. *Biochim BiophysActa.* 1657, (1), 23-32.
80. Baier, K., Lehmann, H., Stephan, D. P. and Lockau, W. (2004). NblA is essential for phycobilisome degradation in Anabaena sp. strain PCC 7120 but not for development of functional heterocysts. *Microbiology.* 150, (Pt 8), 2739-2749.
81. Muramatsu, M. and Hihara, Y. (2003). Transcriptional regulation of genes encoding subunits of photosystem I during acclimation to high-light conditions in Synechocystissp. PCC 6803. *Planta.* 216, (3), 446-453.

82. Kimura, A., Eaton-Rye, J. J., Morita, E. H., Nishiyama, Y. and Hayashi, H. (2002).Protection of the oxygen-evolving machinery by the extrinsic proteins of photosystem II is essential for development of cellular thermo tolerance in Synechocystis sp. PCC 6803.*Plant Cell Physiol.* 43, (8), 932-938.

83. Garcia-Dominguez, M., Muro-Pastor, M. I., Reyes, J. C. and Florencio, F. J. (2000). Light-dependent regulation of cyanobacterial phytochrome expression. J 5ac/eno/. 182, (1), 38-44.

84. Park, C. M., Kim, J . I., Yang, S. S., Kang, J . G., Kang, J . H., Shim, J . Y., Chung, Y. H., Park, Y. M. and Song, P. S. (2000). A second photochromic bacterio phytochrome from Synechocystis sp. PCC 6803: spectral analysis and down-regulation by light. *Biochemistry.* 39, (35), 10840-10847.

85. Hirani, T. A., Suzuki, I., Murata, N., Hayashi, H. and Eaton-Rye, J. J. (2001). Characterization of a two-component signal transduction system involved in the induction of alkaline phosphatase under phosphate-limiting conditions in Synechocystissp. PCC 6803. *Plant Mol Biol.* 45, (2), 133-144.

86. Suzuki, S., Ferjani, A., Suzuki, I. and Murata, N. (2004). The SphS-SphR two component system is the exclusive sensor for the induction of gene expression in response to phosphate limitation in synechocystis. J5/o/ *Chem.* 279, (13), 13234-13240.

87. Yamaguchi, K., Suzuki, I., Yamamoto, H., Lyukevich, A., Bodrova, I., Los, D. A.,Piven, L, Zinchenko, V., Kanehisa, M. and Murata, N. (2002). A two-component Mn2+-sensing system negatively regulates expression of the mntCAB operon in Synechocystis. *Plant Cell.* 14, (11), 2901-2913.

88. Ogawa, T., Bao, D. H., Katoh, H., Shibata, M., Pakrasi, H. B. and Bhattacharyya-Pakrasi, M. (2002). A two-component signal transduction pathway regulate manganese homeostasis in Synechocystis 6803, a photosynthetic organism. J Biol 277, (32), 28981-28986.

89. Mikami, K., Dulai, S., Suplice, R., Takahashi, S., Ferjani, A., Suzuki, I . and Murata, N. (2003). Histidine kinases, Hik2, Hik6 and Hik33, in Synechocystis sp. PCC 6803 are involved in the Tolerance of photosystem I I to environmental stress. *Plant Cell Physiol.*43 Suppl, S82-S82.

90. Rippka, R., Deruelles, J. , Waterbury, J . B., Herdman, M. and Stanier, R. Y. (1979). Generic assignments, strain histories and properties of pure strains of cyanobacteria. *J.Gen. Microbiol.* I1l, 1-61.

91. Grigorieva, G., and S. Shestakov. 1982. transformation in the cyanobacterium Synechocystis sp. 6803. FEMS Microbiol. Lett. 13:367-370.

92. T. Kaneko *et al.*, Sequence analysis of the genome of the unicellular cyanobacterium *Synechocystis* sp. strain PCC6803. II. Sequence determination of the entire genome and assignment of potential protein-coding regions. *DNA Res.* 3, 109 (1996).

93. Zinchenko, V., V., Piven, I., V., Melnik, V., A. and Shestakov, S., V. (1999). Vectors for the complementation analysis of cyanobacterial mutants.Russ J Genet. 35, 228–232.

94. https://www.genome.jp/kegg/. http://genome.microbedb.jp/cyanobase.

95. Takatomo Fujisawa, Rei Narikawa, Shin-ichi Maeda, Satoru Watanabe, Yu Kanesaki, Koichi Kobayashi, Jiro Nomata, Mitsumasa Hanaoka, Mai Watanabe, Shigeki Ehira, Eiji Suzuki, Koichiro Awai, Yasukazu Nakamura, CyanoBase: a large-scale update on its 20th anniversary, *Nucleic Acids Research*, Volume 45, Issue D1, January 2017, Pages D551–D554.

96. I. Suzuki, Y. Kanesaki, K. Mikami, M. Kanehisa, N. Murata, Cold-regulated genes under control of the cold sensor Hik33 in Synechocystis. *Mol. Microbiol.* 40, 235 (2001).

97. K. Marin *et al.*, Identification of histidine kinases that act as sensors in the perception of salt stress in Synechocystis sp. PCC 6803. *Proc. Natl. Acad. Sci. U. S. A.* 100, 9061 (2003).

98. H. Ohta *et al.*, Identification of genes expressed in response to acid stress in Synechocystis sp. PCC 6803 using DNA microarrays. *Photosynth. Res.* 84, 225 (2005).

99. I. Suzuki, W. J. Simon, A. R. Slabas, The heat shock response of Synechocystis sp. PCC 6803 analysed by transcriptomics and proteomics. J. Exp. Bot. 57, 1573 (2006).
100. Y. Kanesaki *et al.*, Histidine kinases play important roles in the perception and signal transduction of hydrogen peroxide in the cyanobacterium, Synechocystis sp. PCC 6803. *Plant J.* 49, 313 (2007).
101. Aravind, L., and Koonin, E. V. (1999) Novel predicted RNA-binding domains associated with the translation machinery. J. Mol. Evol. 48, 291–302.
102. Davies, C., Gerstner, R. B., Draper, D. E., Ramakrishnan, V., and White, S. W. (1998) The crystal structure of ribosomal protein S4 reveals a two-domain molecule with an extensive RNA-binding surface: One domain shows structural homology to the ETS DNA-binding motif. EMBO J. 17, 4545–4558.
103. Fadda, D., Pischedda, C., Caldara, F.,Whalen, M. B., Anderluzzi, D., Domenici, E., and Massidda, O. (2003) Characterization of divIVA and other genes located in the chromosomal region downstream of the dcw cluster in Streptococcus pneumoniae. J. Bacteriol. 185, 6209–6214.
104. Emanuelsson, O., Brunak, S., von Heijne, G., and Nielsen, H. (2007) Locating proteins in the cell using TargetP, SignalP and related tools. Nat. Protoc. 2, 953–971.
105. Zybailov, B., Rutschow, H., Friso, G., Rudella, A., Emanuelsson, O.,Sun, Q., and van Wijk, K. J. (2008) Sorting signals, N-terminal modifications and abundance of the chloroplast proteome. PLoS One 3, e1994.
106. Y. Kashino *et al.*, Proteomic analysis of a highly active photosystem II preparation from the cyanobacterium Synechocystis sp. PCC 6803 reveals the presence of novel polypeptides. *Biochemistry (Mosc.)* 41, 8004 (2002).
107. N. Inoue-Kashino *et al.*, S4 Protein Sll1252 Is Necessary for Energy Balancing in Photosynthetic Electron Transport in Synechocystis sp. PCC 6803. *Biochemistry (Mosc.)*, (2010).
108. *S. Yamanaka, ... K. Yamaguchi, in Advances in Quantum Chemistry, 2012.*
109. Guskov, A., Kern, J., Gabdulkhakov, A., Broser, M., Zouni, A. and Saenger, W. (2009). "Cyanobacterial photosystem II at 2.9 Ao resolution and the role of quinones, lipids, channels and chloride". Nat. Struct. Mol. Biol. 16, 334–42.
110. Bricker, T.M. (1990), The structure and function of Cpa-1 and Cpa-2 in photosystem II, Photosynthesis Res. 24, 1-13.
111. M.M. Najafpour, M.Z. Ghobadi, A.W. Larkum, J.R. Shen, S.I. AllakhverdievThe biological water-oxidizing complex at the nano-bio interface Trends Plant Sci. (2015)
112. Shipton, C., A. and Barber, J. (1991) Photoinduced degradation of the D1 polypeptide in isolated reaction centers of photosystem II: evidence for an autoproteolytic process triggered by the oxidizing side of the photosystem. Proc. Natl. Acad. Sci. USA. 88, 6691-6695.
113. Salter, A., H., Virgin, I., Hagman, A. and Andersson, B. (1992) On the molecular mechanism of light-induced D1 protein degradation in photosystem II core particles. Biochemistry. 31, 3990-3998.
114. Steffen Heinz, Pasqual Liauw, Jörg Nickelsen, Marc Nowaczyk, Analysis of photosystem II biogenesis in cyanobacteria, Biochimica et Biophysica Acta (BBA) - Bioenergetics, Volume 1857, Issue 3, 2016,
115. E. Miskiewicz, A.G. Ivanov, N.P. HunerStoichiometry of the photosynthetic apparatus and phycobilisome structure of the cyanobacterium *Plectonema boryanum* UTEX 485 are regulated by both light and temperature. Plant Physiol., 130 (2002), pp. 1414-1425.
116. Y. Yang, D.A. Jiang, H.X. Xu, C.Q. Yan, S.R. HaoCyclic electron flow around photosystem 1 is required for adaptation to salt stress in wild soybean species *Glycine cyrtoloba* ACC 547 Biol. Plant., 50 (2006), pp. 586-590.
117. K.E. Wilson, A.G. Ivanov, G. Öquist, B. Grodzinski, F. Sarhan, N.P.A. HunerEnergy balance, organellar redox status, and acclimation to environmental stress Can. J. Bot., 84 (2006), pp. 1355-1370.
118. N. Murata, S. Takahashi, Y. Nishiyama, S.I. Allakhverdiev Photoinhibition of photosystem II under environmental stress Biochim. Biophys. Acta, 1767 (2007), pp. 414-421.

119. J.F. Allen, T. Pfannschmidt Balancing the two photosystems: photosynthetic electron transfer governs transcription of reaction center genes in chloroplastsPhilos. Trans. R. Soc. Lond., B Biol. Sci., 355 (2000), pp. 1351-1359.
120. A.K. Singh, B.M. Pakrasi, T. Elvitigala, B. Ghosh, R. Aurora, H.B. Pakrasi. A systems-level analysis of the effects of light quality on the metabolism of a cyanobacterium Plant Physiol., 151 (2009), pp. 1596-1608
121. N. Murata. Control of excitation transfer in photosynthesis. I. Light-induced change of chlorophyll *a* fluorescence in *Porphyridium cruentum.* Biochim. Biophys. Acta, 172 (1969), pp. 242-251.
122. C.W. Mullineaux, J.F. AllenState 1–state 2 transitions in the cyanobacterium *Synechococcus* 6301 are controlled by the redox state of the electron carriers between photosystem I and II Photosynth. Res., 23 (1990), pp. 297-311.
123. M.D. McConnell, R. Koop, S. Vasilev, D. Bruce. Regulation of the distribution of chlorophyll and phycobilin-absorbed excitation energy in cyanobacteria. A structure-based model for the light state transition. Plant Physiol., 130 (2002), pp. 1201-1212 .
124. C.W. Mullineaux, D. Emlyn-Jones. State transitions — an example of acclimation to low-light stress J. Exp. Bot., 56 (2005), pp. 389-393.
125. A.N. Glazer, C. Chan, R.C. Williams, S.W. Yeh, J.H. Clark. Kinetics of energy flow in the phycobilisome core. Science, 230 (1985), pp. 1051-1053
126. J. Zhao, J. Zhou, D.A. Bryant. Energy transfer processes in phycobilisomes as deduced from analyses of mutants of *Synechococcus* sp. PCC 7002. N. Murata (Ed.), Research in Photosynthesis, vol. 1, Kluwer Academic Publishers, Dordrecht, The Netherlands (1992), pp. 25-32
127. G.C. Papageorgiou. The photosynthesis of cyanobacteria (blue bacteria) from the perspective of signal analysis of chlorophyll *a* fluorescence. J. Sci. Ind. Res., 55 (1996), pp. 596-617
128. C.W. Mullineaux, M.J. Tobin, G.R. Jones. Mobility of photosynthetic complexes in thylakoid membranes. Nature, 390 (1997), pp. 421-424.
129. M. Sarcina, M.J. Tobin, C.W. Mullineaux. Diffusion of phycobilisomes on the thylakoid membranes of the cyanobacterium *Synechococcus* 7942. Effects of phycobilisome size, temperature, and membrane lipid composition. J. Biol. Chem., 276 (2001), pp. 46830-46834.
130. A. Murakami, Y. Fujita. Regulation of photosystem stoichiometry in the photosynthetic system of the cyanophyte *Synechocystis* PCC 6714 in response to light intensity. Plant Cell Physiol., 32 (1991), pp. 223-230.
131. A. Murakami, S.-J. Kim, Y. Fujita. Changes in photosystem stoichiometry in response to environmental conditions for cell growth observed with the cyanophyte *Synechocystis* PCC6714. Plant Cell Physiol., 38 (1997), pp. 392-397.
132. K. Sonoike, Y. Hihara, M. Ikeuchi. Physiological significance of the regulation of photosystem stoichiometry upon high light acclimation of *Synechocystis* sp. PCC6803. Plant Cell Physiol., 42 (2001), pp. 379-384.
133. W.F.J. Vermaas. Photosynthesis and respiration in cyanobacteria Encycl. Life Sci. (2001), pp. 1-7.
134. J.F. Allen, C.A. Allen, S. Puthiyaveetil. Redox switches and evolutionary transitions, J.F. Allen, E. Gantt, J.H. Golbeck, B. Osmond (Eds.), Photosynthesis Energy from the Sun. Proceedings of the 14th International Congress on Photosynthesis, Springer, Heidelberg (2008), pp. 1155-1160.
135. T. Pfannschmidt, A. Nilsson, J.F. Allen. Photosynthetic control of chloroplast gene expression, Nature, 397 (1999), pp. 625-628.

136. M. Herranen, T. Tyystjärvi, E.M. Aro. Regulation of photosystem I reaction center genes in *Synechocystis* sp. strain PCC 6803 during light acclimation Plant Cell Physiol., 46 (2005), pp. 1484-1493.
137. H.Y. Hsiao, Q. He, L.G.V. Waasbergen, A.R. Grossman. Control of photosynthetic and high-light-responsive genes by the histidine kinase DspA: negative and positive regulation and interactions between signal transduction pathways.
138. M. Muramatsu, Y. Hihara. Acclimation to high-light conditions in cyanobacteria: from gene expression to physiological responses. J. Plant Res., 125 (2012), pp. 11-39.
139. Arthur G. Roberts and David M. Kramer. Inhibitor "Double Occupancy" in the Qo Pocket of the Chloroplast Cytochrome b6f Complex. Biochemistry 2001 40 (45), 13407-13412 .DOI: 10.1021/bi015774.
140. Tova Trebitsh and Avihai Danon. Translation of chloroplast *psbA* mRNA is regulated by signals initiated by both photosystems II and I. PNAS October 9, 2001 98 (21) 12289-12294.kashino
141. J. G. K. Williams, Construction of specific mutations in photosystem II photosynthetic reaction center by genetic-engineering methods in *Synechocystis* 6803. *Methods Enzymol.*167, 766 (1988).
142. Stanier, R.Y., Kunisawa, R., Mandel, M. and Cohen-Bazire, G. (1971) Purification and properties of unicellular blue-green algae (order Chroococcales). Bacteriol. Rev. 35, 171–205.
143. Wada, H. and Murata, N. (1989) *Synechocystis* PCC 6803 mutants defective in desaturation of fatty acids. Plant Cell Physiol. 30, 971–978.
144. Sambrook, J., Fritsch, E., F. and Maniatis, T. (1989) Molecular Cloning: a laboratory manual. 2nd ed. NY, Cold Spring Harbor Laboratory, Cold Spring Harbor Laboratory Press.
145. Kaneko, T., Nakamura, Y., Sasamoto, S., Watanabe, A., Kohara, M., Matsumoto, M., Shimpo, S., Yamada, M. and Tabata, S. (2003) Structural Analysis of Four Large Plasmids Harboring in a Unicellular Cyanobacterium, *Synechocystis* sp. PCC 6803. DNA Research. 10, 221–228.
146. Los, D., A., Ray, M., K. and Murata, N. (1997) Differences in the control of the temperature-dependent expression of four genes for desaturases in Synechocystis sp. PCC 6803. Mol. Microbiol. 25, 1167–1175.
147. Arnon, D., I., McSWwain, B., D., Tsujimoto, H., Y. and Wada, K. (1974) Photochemical activity and components of membrane preparations from blue-green algae, Biochim. Biophys. Acta. 357, 231–245.
148. H. H. Stiehl, H. T. Witt, Quantitative treatment of the function of plastoquinone in photosynthesis. *Z. Naturforsch. B*24, 1588 (1969).
149. Y. Hihara, K. Sonoike, M. Kanehisa, M. Ikeuchi, DNA microarray analysis of redox-responsive genes in the genome of the cyanobacterium Synechocystis sp. strain PCC 6803. *J. Bacteriol.*185, 1719 (2003).
150. N. Yubuki, Y. Inagaki, T. Nakayama, I. Inouye, Ultrastructure and ribosomal RNA phylogeny of the free-living heterotrophic flagellate Dysnectes brevis n. gen., n. sp., a new member of the Fornicata. *The Journal of eukaryotic microbiology* 54, 191 (2007).
151. A. Trebst, in *Photosynthesis and Nitrogen Fixation - Part C,* A. S. Pietro, Ed. (Academic Press, Inc, 1980), vol. 69, pp. 675-715.
152. R. Agarwal, A. Matros, M. Melzer, H. P. Mock, J. K. Sainis, Heterogeneity in thylakoid membrane proteome of Synechocystis 6803. J Proteomics 73, 976 (2010).

Publications

Two publications in international journals as second author.

Impact factor 4.8

Biochim Biophys Acta
2012 Sep;1817(9):1525-36.
doi: 10.1016/j.bbabio.2012.04.016. Epub 2012 May 7.

RNA helicase, CrhR is indispensable for the energy redistribution and the regulation of photosystem stoichiometry at low temperature in Synechocystis sp. PCC6803

Kodru Sireesha[1], Balaga Radharani, Pilla Sankara Krishna, Nellaepalli Sreedhar, Rajagopal Subramanyam, Prasanna Mohanty, Jogadhenu S S Prakash.

- PMID: **22575444**
- DOI: 10.1016/j.bbabio.2012.04.016

Abstract

We investigated the role of a cold-inducible and redox-regulated RNA helicase, CrhR, in the energy redistribution and adjustment of stoichiometry between photosystem I (PSI) and photosystem II (PSII), at low temperature in Synechocystis sp. PCC 6803. The results suggest that during low temperature incubation, i.e., when cells are shifted from 34°C to 24°C, wild type cells exhibited light-induced state transitions, whereas the mutant deficient in CrhR failed to perform the same. At low temperature, wild type cells maintained the plastoquinone (PQ) pool in the reduced state due to enhanced respiratory electron flow to the PQ pool, whereas in ΔcrhR mutant cells the PQ pool was in the oxidized state. Wild type cells were in state 2 and ΔcrhR cells were locked in state 1 at low temperature. In both wild type and ΔcrhR cells, a fraction of PSI trimers were changed to PSI monomers. However, in ΔcrhR cells, the PSI trimer content was significantly decreased. Expression of photosystem I genes, especially the psaA and psaB, was strongly down-regulated due to oxidation of downstream components of PQ in ΔcrhR cells at low temperature. We demonstrated that changes in the low temperature-induced energy redistribution and regulation of photosystem stoichiometry are acclimatization responses exerted by Synechocystis cells, essentially regulated by the RNA helicase, CrhR, at low temperature.

Impact factor 4.89

Biochem J
2013 Feb 1;449(3):751-60.
doi: 10.1042/BJ20120928.

A novel transcriptional regulator, Sll1130, negatively regulates heat-responsive genes in Synechocystis sp. PCC6803

Pilla Sankara Krishna [1], Balaga Radha Rani, M Karthik Mohan, Iwane Suzuki, Sisinthy Shivaji, Jogadhenu S S Prakash

- PMID: **23088579**
- DOI: 10.1042/BJ20120928

Abstract

A conserved hypothetical protein, Sll1130, is a novel transcription factor that regulates the expression of major heat-responsive genes in Synechocystis sp. PCC6803. Synechocystis exhibited an increased thermotolerance due to disruption of sll1130. Δsll1130 cells recovered much faster than wild-type cells after they were subjected to heat shock (50°C) for 30 min followed by recovery at 34°C for 48 h. In Δsll1130 cultures, 70% of the cells were viable compared with the wild-type culture in which only 30% of the cells were viable. DNA microarray analysis revealed that in Δsll1130, expression of the heat-responsive genes such as htpG, hspA, isiA, isiB and several hypothetical genes were up-regulated. Sll1130 binds to a conserved inverted-repeat (GGCGATCGCC) located in the upstream region of the above genes. In addition, both the transcript and protein levels of sll1130 were immediately down-regulated upon shift of wild-type cells from 34 to 42°C. Collectively the results of the present study suggest that Sll1130 is a heat-responsive transcriptional regulator that represses the expression of certain heat-inducible genes at optimum growth temperatures. Upon heat shock, a quick drop in the Sll1130 levels leads to de-repression of the heat-shock genes and subsequent thermal acclimation. On the basis of the findings of the present study, we present a model which describes the heat-shock response involving Sll1130. followed by recovery at 34°C for 48 h. In Δsll1130 cultures, 70% of the cells were viable compared with the wild-type culture in which only 30% of the cells were viable. DNA microarray analysis revealed that in Δsll1130, expression of the heat-responsive genes such as htpG, hspA, isiA, isiB and several hypothetical genes were up-regulated. Sll1130 binds to a conserved inverted-repeat (GGCGATCGCC) located in the upstream region of the above genes. In addition, both the transcript and protein levels of sll1130 were immediately down-regulated upon shift of wild-type cells from 34 to 42°C. Collectively the results of the present study suggest that Sll1130 is a heat-responsive transcriptional regulator that represses the expression of certain heat-inducible genes at optimum growth temperatures. Upon heat shock, a quick drop in the Sll1130 levels leads to de-repression of the heat-shock genes and subsequent thermal acclimation. On the basis of the findings of the present study, we present a model which describes the heat-shock response involving Sll1130.

Have been acknowledged in a manuscript for helping in protein expression

P.V.P. Arun, K. B. Ranjith, M. Subhashini, P. Singh, N. P. Prabhu, I. Suzuki, J. S. S. Prakash. CyanoPhyChe: A database for physico-chemical properties, structure and biochemical pathway information of cyanobacterial proteins (In Press) *PLos One*. (2012).

A manuscript is under preparation

B.R. Rani, M. K. Mohan, Itoh, P. Mohanty, I. Suzuki, J. S. S. Prakash. Disruption of *sll1252* by targeted insertional mutagenesis impairs electron transport between plastoquinone to cytochrome b_6/f complex in *Synechocystis* sp. PCC 6803.

Presentations

1). **ORAL Presentation** in

UGC-SAP National Seminar, New Vistas in Plant Sciences,

Organized by Goa University on 15th March 2012.

2). ORAL Presentation in

Plant Sciences Colloquium,

Organized by University of Hyderabad on 4th March 2013.

3). **POSTER Presentation** in

Research Dialogue in the Life Sciences

Organized by University of Hyderabad on 22nd Feb 2012.

4). **POSTER Presentation** in

INDO-GERMAN symposium on Systems Biology

in University of Hyderabad on 27th Nov 2012.

5). Participated in the BioQuest 2010

The 3rd Annual Research Gala

in University of Hyderabad on 20th March 2010

Functional characterization of a hypothetical protein, Sll1252 in Synechocystis sp. PCC 6803

ORIGINALITY REPORT

16%	5%	15%	1%
SIMILARITY INDEX	INTERNET SOURCES	PUBLICATIONS	STUDENT PAPERS

PRIMARY SOURCES

1	Kodru Sireesha, Balaga Radharani, Pilla Sankara Krishna, Nellaepalli Sreedhar et al. "RNA helicase, CrhR is indispensable for the energy redistribution and the regulation of photosystem stoichiometry at low temperature in Synechocystis sp. PCC6803", Biochimica et Biophysica Acta (BBA) - Bioenergetics, 2012 Publication	4%
2	hdl.handle.net Internet Source	2%
3	"Photosynthesis: Mechanisms and Effects", Springer Science and Business Media LLC, 1998 Publication	1%
4	Deepak Kumar Singh, Bantu Lingaswamy, Tejaswi Naidu Koduru, Prakash Prabhu Nagu, Prakash Syama Sundar Jogadhenu. " A putative family transcription factor Slr0701 regulates mercury inducible expression of MerA in the cyanobacterium sp. PCC6803 ",	1%

Certified that This is part of her Papers

Prof. J.S.S. PRAKASH
Dept. of Biotechnology & Bioinformati
School of Life Sciences
University of Hyderabad
HYDERABAD-500 046. INDIA

Certified that This is part of her paper

Prof. J.S.S. PRAKASH
Dept. of Biotechnology & Bioinform
School of Life Sciences
University of Hyderabad
HYDERABAD-500 046. IN